INVESTIGATION OF EPITHELIAL CANONICAL AND NON-CANONICAL NF-κB SIGNALING IN LUNG ADENOCARCINOMA

By

Jamie Ausborn Saxon

Dissertation

Submitted to the Faculty of the

Graduate School of Vanderbilt University

in partial fulfillment of the requirements

for the degree of

DOCTOR OF PHILOSOPHY

in

CANCER BIOLOGY

May, 2016

Nashville, TN

Approved:

Timothy S. Blackwell, M.D.

Ann Richmond, Ph.D.

Stephen W. Fesik, Ph.D.

Barbara Fingleton, Ph.D.

For my husband James, my biggest cheerleader

In honor of my mom, an example of strength

In honor of my dad, a model of hard work and integrity

In memory of Roland and Patricia Ausborn and Armand and Mager DeSollar

ACKNOWLEDGEMENTS

I would first like to acknowledge my advisor, Tim Blackwell, for his guidance throughout my graduate school career and for giving me the space and support to develop into an independent scientist. In addition, I would like to thank my committee members, Ann Richmond, Stephen Fesik, Barbara Fingleton, and William Pao, for their invaluable advice and insights regarding both my project and my career. I am grateful for my colleagues in the Cancer Biology Department and the Pulmonary Division as well as the members of the Blackwell lab group, past and present, for their input and contributions to this work and my training. Particularly, I would like to acknowledge Dong-Sheng Cheng, Wei Han, Linda Gleaves, and Rasul Abdolrasulnia for always being available and willing to answer my questions or to help me search for the right answers, Jiqing Sai and Hui Yu for sharing their areas of expertise which truly enhanced this work, Dawn Newcomb Baker and Tammy Sobolik for helpful feedback on everything from qualifying exam proposals to presentations to experiments, and Fiona Yull and Whitney Barham for their enthusiasm and eagerness to contribute both ideas and resources. I am also especially grateful for Allyson McLoed Perry, my Blackwell lab partner in crime, who has been a great friend and colleague, and my graduate school classmates Hayley Clay, Christi French, Sudipta Chakraborty, David Cappel, Bobby Madamanchi, Clint Hasenour, Chris Muller, Scott Collier, Sarah Collier, and Seema Sinha, who have shared in the struggles and successes of graduate school alongside me.

Personally, I would like to acknowledge my parents, Chris and Pat Ausborn, for teaching me the value of education and always allowing me to pursue opportunity, and my brother Wyatt, who has supported and encouraged me in all of my endeavors. Last but not least, I am grateful for my husband James, who challenges me to always strive for more and with whom I am lucky to share this adventure.

This work was supported by the Department of Veterans Affairs Merit Review Award 1101BX002378 and NIH grants HL092870 and HL085317.

TABLE OF CONTENTS

LIST OF TABLES

LIST OF FIGURES

LIST OF ABBREVIATIONS

AAH	Atypical adenomatous hyperplasia
Ad-Luc	Luciferase adenovirus
Ad-RelB	RelB-His adenovirus
ARDS	Acute respiratory distress syndrome
BAL	Bronchoalveolar lavage
BrdU	5-bromo-2'-deoxyuridine
BSA	Bovine serum albumin
CBP	Cyclic-AMP response element binding protein
CCSP	Clara cell secretory protein
CCSP-p52	CCSP-rtTA CCSP-tTS/$(tet\text{-}O)_7$-FLAG-p52 mice
CDK	Cyclin-dependent kinase
CT	Computed tomography
DMEM	Dulbecco's Modified Eagle Medium
DN-IκB	Dominant negative IκBα
Dox	Doxycycline
EGFR	Epidermal growth factor receptor
$EGFR^{L/T}$	$EGFR^{L858R+T790M}$
ELISA	Enzyme-linked immunosorbent assay
EV	Empty vector
FBS	Fetal bovine serum
FVB	Friend leukemia virus B strain
FC	Fold change
FDR	False discovery rate

GAPDH	Glyceraldehyde-3-phosphate dehydrogenase
GO	Gene ontology
H&E	Hematoxylin and eosin
HAT	Histone acetyl transferases
HDAC	Histone deacetylase
IKK	Inhibitor of κB kinase
IP	Intraperitoneal
IT	Intratracheal
IκB	Inhibitor of κB
KRAS	Kirsten rat sarcoma viral oncogene homolog
LPS	Lipopolysaccharide
MIA	Minimally invasive adenocarcinoma
NAG	4-nitrophenyl 2-acetamido-2-deoxy-β-D-glucopyranoside
NEMO	NF-κB essential modulator
NF-κB	Nuclear factor κ-light chain enhancer of activated B cells
NIK	NF-κB-inducing kinase
NSCLC	Non-small cell lung cancer
PBS	Phosphate-buffered Saline
PCR	Polymerase chain reaction
RLE-EV	RLE-6TN cells stably transfected with cFLAG pcDNA3
RLE-p52	RLE-6TN cells stably transfected with p52 cFLAG pcDNA3
RLE-WT	RLE-6TN parental cells
ROS	Reactive oxygen species
RT-PCR	Reverse transcriptase polymerase chain reaction
rtTA	Reverse tetracycline-transactivator

SCLC	Small cell lung cancer
SDS-PAGE	Sodium dodecyl sulfate polyacrylamide gel electrophoresis
SEM	Standard error of the mean
SPC	Surfactant Protein C
TBP	TATA-binding protein
TCGA	The Cancer Genome Atlas
Tet	Tetracycline
TKI	Tyrosine kinase inhibitor
TMA	Tissue microarray
tTS	Tetracycline-controlled transcriptional silencer
TUNEL	Terminal deoxynucleotidyl transferase dUTP nick end labeling
VEGF	Vascular endothelial growth factor
WT	Wild-type

CHAPTER I:

INTRODUCTION

Lung Cancer

Lung cancer is the leading cause of cancer-related mortality in the U.S. In 2015, over 220,000 new diagnoses are expected as well as 155,000 lung cancer deaths, representing over a quarter of all deaths due to cancer (Siegel et al., 2015). The overall five-year-survival rate of a lung cancer diagnosis is 17.8% (Howlader et al., 2015), which is largely due to lack of early detection methods and lack of effective therapy for long-term survival. The majority of lung cancer patients present with locally advanced or metastatic disease at diagnosis (Howlader et al., 2015). Standard therapy for patients with advanced disease includes non-specific cytotoxic chemotherapy or, for patients with specific genetic alterations, targeted therapies. The five-year-survival rate of patients diagnosed with advanced disease is less than 5% (Howlader et al., 2015). Attempts to define methods and strategies for earlier lung cancer detection have demonstrated that low-dose spiral computed tomography (CT) screening can reduce lung cancer deaths by up to 20% in adults at high risk for developing lung cancer (The National Lung Screening Trial Research Team, 2011), showing promise for improving survival rates. However, the recurrence rate is high, even with early diagnosis. Currently, only about 15% of patients present with localized tumors at diagnosis. Standard therapy for patients diagnosed with a localized tumor is surgical resection with adjuvant chemotherapy, and the five-year-survival rate is 54% (Howlader et al., 2015).

The leading risk factor for developing lung cancer is smoking, and lung cancer risk increases with both smoking amount and duration. Globally, smoking accounts for 80% of the lung cancer burden in males and at least 50% of the burden in females (Ezzati and Lopez, 2003). In most Western countries, including many European countries, North America, and Australia, lung cancer death rates are declining due to increased awareness of smoking health hazards and reduced tobacco use (Bray and Weiderpass, 2009; Jemal et al., 2011, 2008; Siegel et al., 2015). In contrast, lung cancer rates are rising in countries in

Asia and Africa, where the tobacco epidemic emerged more recently and smoking prevalence continues to increase or remains stable. In the U.S., temporal differences in lung cancer incidence exist between men and women because of historical differences in tobacco use between sexes, with smoking becoming popular among women decades later than men, resulting in a delayed peak in lung cancer incidence in women (Jemal et al., 2008). Even though lung cancer is primarily thought of as a smoking-related disease, approximately 15% of lung cancers in the U.S. arise in never-smokers (Samet et al., 2009), and 50% of women and 20% of men worldwide who develop lung cancer are never-smokers (Ezzati and Lopez, 2003). Additional risk factors for developing lung cancer include secondhand smoke, which increases the risk of developing lung cancer by up to 25% (Stayner et al., 2007; Taylor et al., 2007), radon, asbestos, and other environmental exposures (Samet et al., 2009).

Histologically, lung cancer can be broadly divided into small-cell lung cancer (SCLC) and non-small-cell lung cancer (NSCLC). SCLC comprises about 15% of lung cancer diagnoses and is a very aggressive form of lung cancer, arising from neuroendocrine cells. NSCLC comprises approximately 85% of diagnosed lung cancers and can be further divided into three main histological subtypes--adenocarcinoma, squamous cell carcinoma, and large cell carcinoma (Howlader et al., 2015). Adenocarcinomas have glandular histology and are typically found in the periphery of the lung, arising from the bronchial, bronchiolar, or alveolar epithelium. In contrast, squamous cell carcinomas are characterized by squamous differentiation, arising from the pseudostratified columnar epithelium of the trachea and upper airways. Large cell carcinomas are diagnosed by exclusion if cells do not appear glandular or squamous (Davidson et al., 2013), although it is unclear if large cell carcinomas are genetically distinct from squamous cell carcinomas or adenocarcinomas.

Lung Adenocarcinoma

Lung adenocarcinoma is the most prevalent subtype of NSCLC, accounting for more than 40% of all lung cancers (Howlader et al., 2015). The earliest precursor of adenocarcinoma is thought to be an atypical adenomatous hyperplasia (AAH), a pre-invasive lesion that is characterized by proliferation of

mildly to moderately atypical type II pneumocytes and/or Clara cells lining alveolar walls or respiratory bronchioles (Kitamura et al., 1999; Mori et al., 2001). Adenocarcinoma *in situ* is a more advanced pre-invasive lesion defined as a localized small adenocarcinoma with growth restricted to neoplastic cells along pre-existing alveolar structures and lacking stromal, vascular, or pleural invasion (Travis et al., 2011). A minimally invasive adenocarcinoma (MIA) is a small adenocarcinoma with growth primarily along pre-existing alveolar structures and ≤5 mm invasion at any invasive focus. If the tumor invades lymphatics, blood vessels, or pleura or has an invasive protrusion >5 mm, the tumor is classified as an invasive adenocarcinoma (Travis et al., 2011).

The precursor cell for lung adenocarcinoma tumors remains a subject of controversy, with different studies implicating type II pneumocytes (Desai et al., 2014; Lin et al., 2012; Mainardi et al., 2014; Sutherland et al., 2014; Xu et al., 2012), Clara cells (Cho et al., 2011; Sutherland et al., 2014), and bronchoalveolar stem cells (Jackson et al., 2001; Kim et al., 2005) as the originating cell type. Alveolar type II cells are identified by expression of surfactant protein-C (SPC) and are able to repopulate the alveolar epithelium after injury (Adamson and Bowden, 1974; Evans et al., 1975). Clara cells are non-ciliated bronchial epithelial cells that similarly have the capacity to serve as progenitors for the bronchiolar epithelium in response to injury and are identified by expression of Clara cell secretory protein (CCSP) (Giangreco et al., 2002; Hong et al., 2001). In mice, bronchoalveolar stem cells have been described that express Clara (CCSP) and type II (SPC) cell markers and reside at the bronchoalveolar duct junction (Jackson et al., 2001; Kim et al., 2005). Early hyperplastic lesions expressing both CCSP and SPC have been observed (Jackson et al., 2001), suggesting that these lesions arose from bronchoalveolar stem cells. *In vivo* studies in which oncogenic mutations were expressed in individual lung epithelial cell types have indicated that hyperplasias and benign adenomas can originate in Clara cells and bronchoalveolar stem cells but only type II cells are capable of producing malignant adenocarcinomas (Desai et al., 2014; Lin et al., 2012; Mainardi et al., 2014; Xu et al., 2012). However, lineage tracing studies revealed that adenocarcinomas can arise from both type II cells as well as a subset of Clara cells and suggested that CCSP+SPC- cells can trans-differentiate to CCSP-SPC+ cells during the course of

tumorigenesis (Sutherland et al., 2014), potentially explaining the appearance of CCSP+SPC+ hyperplastic lesions.

In the past decade, researchers have moved beyond classifying tumors simply based on histology and have begun to further define lung adenocarcinoma subsets based on recurrent "driver mutations" in oncogenic genes. A "driver mutation" causes constitutive activation of the mutant signaling molecule, which initiates and sustains tumorigenesis. Multiple driver mutations are rarely found in the same tumor. The classification of tumors based on driver mutations enables a more precise identification of tumor subsets that respond to certain therapies and defines critical pathways in these tumors that can be targeted directly or indirectly to inhibit tumorigenesis.

The most common driver mutations in lung adenocarcinomas are Kirsten rat sarcoma viral oncogene homolog (KRAS) mutations, which are found in greater than 30% of lung adenocarcinoma tumors and are associated with poor prognosis and resistance to therapy (Herbst et al., 2008). KRAS is a small GTPase protein that cycles between a GDP-bound inactive state and a GTP-bound active state, linking extracellular signals transduced through membrane receptors to intracellular signaling pathways. Oncogenic mutations in KRAS most commonly occur in codons 12, 13, and 61. These mutations decrease the binding affinity of KRAS for its GTPase-activating protein (Trahey and McCormick, 1987), resulting in sustained KRAS activation and maintenance of signaling through downstream pathways involved in many processes known to promote tumorigenesis, including survival, proliferation, migration, and invasion. Even though KRAS is one of the most frequently mutated genes in a variety of cancers, no targeted therapies exist to treat patients with KRAS-mutant tumors.

While mutations in KRAS show a strong association with smoking, mutations in the epidermal growth factor receptor (EGFR) are more commonly found in non-smokers (Ahrendt et al., 2001; Husgafvel-Pursiainen et al., 1993; Rosell et al., 2009). EGFR is a receptor tyrosine kinase that signals through KRAS, resulting in activation of many of the same downstream pathways. EGFR mutations occur in approximately 15% of all lung adenocarcinomas (Rosell et al., 2009) and in about 50% of adenocarcinomas from patients of Asian descent (Shi et al., 2014), with the most common mutations

being exon 19 deletions and the exon 21 L858R point mutation (Li et al., 2008; Rosell et al., 2009). Mutations in EGFR destabilize the auto-inhibitory conformation of the kinase domain, resulting in constitutive kinase activation as well as constitutive activation of downstream signaling pathways (Yun et al., 2007), such as ERK, PI3K/Akt, and JAK/STAT. While targeted therapies have been developed to treat EGFR-mutant tumors, patient survival has only been modestly impacted because the tumors eventually become resistant, resulting in disease progression. The most common resistance mechanism to the first generation tyrosine kinase inhibitors (TKIs) erlotinib and gefitinib is a T790M mutation in the receptor's kinase domain, which increases its affinity for ATP (Pao et al., 2005; Yun et al., 2008). This finding has prompted the development of mutation-specific irreversible inhibitors, AZD9291 and rociletinib, which have shown therapeutic benefit in patients with T790M lung cancer (Jänne et al., 2015; Sequist et al., 2015). However, these patients also ultimately develop resistance.

Inflammation in Cancer

In the 19th century, Rudolf Virchow first proposed a connection between inflammation and cancer. A role for inflammation in tumorigenesis is now generally accepted, with inflammation thought to impact every step of tumorigenesis from tumor initiation to metastasis, modulating tumor progression through pro- or anti-tumorigenic effects. Early neoplastic lesions are hypothesized to undergo immunoediting during which transformed cells are "eliminated" by the immune system, but rare tumor cell variants may survive (Schreiber et al., 2011). These remaining cells enter into "equilibrium," where the immune system keeps them essentially dormant, but eventually these residual cells may "escape" by evading immune destruction or acquiring the capability to establish an immunosuppressive microenvironment. In tumors, anti-tumorigenic and pro-tumorigenic inflammatory signals coexist, competing for dominance throughout tumor development. Ultimately, the expression of various immune modulators and mediators as well as the presence and activation state of different inflammatory cell types dictate whether the inflammatory microenvironment is overall pro-tumorigenic or anti-tumorigenic (Grivennikov et al., 2010).

Current hypotheses suggest that inflammation and cancer can be linked through extrinsic or intrinsic inflammatory pathways (Figure 1) (Mantovani et al., 2008). The extrinsic inflammatory pathway is driven by a pre-existing chronic inflammatory condition that enhances cancer risk, and around 20% of cancers fall into this category of being related to chronic inflammation (Crusz and Balkwill, 2015). However, inflammatory cells and immune mediators are found in most, if not all, tumors, even those arising independently of a chronic inflammatory condition. In these tumors, intrinsic inflammation is driven by genetic alterations (such as an oncogenic mutation) that activate inflammatory signaling pathways resulting in production of extracellular mediators that recruit and/or polarize inflammatory cells (Mantovani et al., 2008). Thus, cancer can cause inflammation in the absence of a pre-existing inflammatory condition.

The intimate association between cancer and inflammation has led to further investigations of their relationships with the goal of developing new therapeutic approaches for cancer treatment that target immune cells and mediators. A variety of different inflammatory cells have been implicated in carcinogenesis, including macrophages, immature monocytes, myeloid-derived suppressor cells, T cells, B cells, neutrophils, dendritic cells, eosinophils, and natural killer cells, and within some of these different immune cell populations, phenotypic subsets exist that have distinct effects on tumor development and progression. Additionally, the impact of inflammatory cells on tumorigenesis can be dependent on the specific organ and even cell type in which a tumor arises. Macrophages, neutrophils, and T cells are the most studied inflammatory cell types in the context of cancer, and a variety of therapies have been developed to target these cells and their mediators.

Macrophages are the most abundant immune cell population in the lung and have been shown to promote both early and late stages of lung tumorigenesis (Zaynagetdinov et al., 2011a). Macrophages exist to phagocytose debris, pathogens, and dead/dying cells, as well as to release cytokines and chemokines regulating inflammation. Macrophages do not represent a single uniform cell type but, instead, are a heterogeneous population that can exhibit plasticity depending on microenvironmental cues. The two extremes of the macrophage phenotypic spectrum are the anti- tumorigenic M1 and the pro-

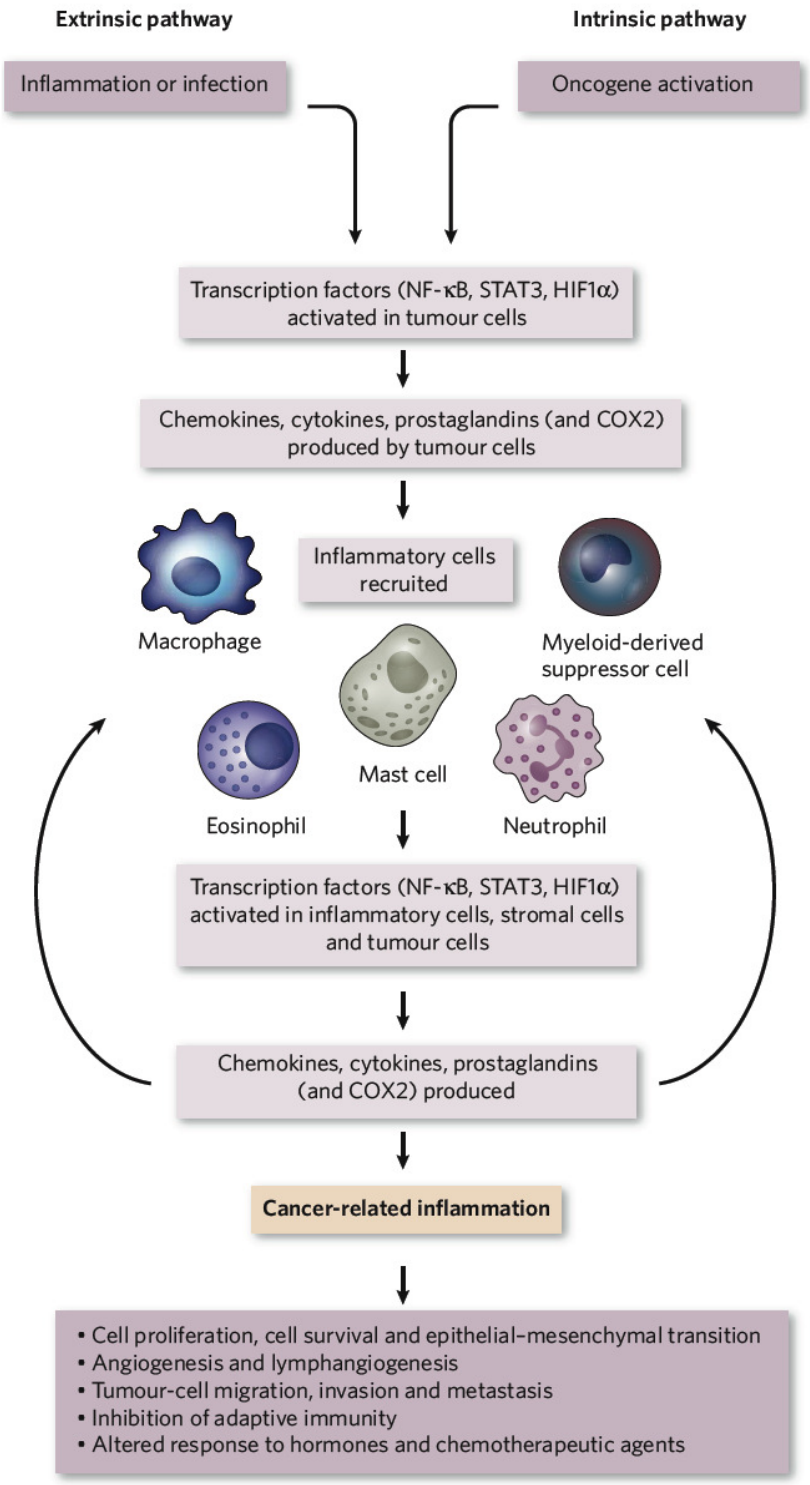

Figure 1: Inflammation and cancer can be linked through extrinsic or intrinsic inflammatory pathways.

Reprinted by permission from Macmillan Publishers Ltd: Nature (Mantovani, A., P. Allavena, A. Sica, and F. Balkwill. Cancer-related inflammation. 454(7203): 436–444), copyright (2008).

tumorigenic M2. M1 macrophages promote an anti-tumor response by presenting tumor-associated antigen to T cells and releasing pro-inflammatory cytokines, leading to tumor cell elimination. In contrast, M2 macrophages support tumorigenesis by suppressing anti-tumor immune responses, stimulating angiogenesis and lymphangiogenesis, and promoting tumor cell proliferation, invasion, and metastasis. *In vivo* studies have shown that a shift from an M1 to an M2 macrophage population occurs during the course of lung carcinogenesis (Redente et al., 2007). A number of factors produced by tumors such as extracellular matrix components, cytokines, and chemokines, including macrophage chemoattractants MCP-1/CCL2 and M-CSF/CSF1, can promote M2-skewing of the macrophage phenotype (Fridlender et al., 2011; Martinez et al., 2006; Roca et al., 2009; Sica and Mantovani, 2012). Current therapies in clinical trials that target macrophages or macrophage-associated factors include CSF1 receptor antagonists, anti-CCL2 monoclonal antibodies, and trabectedin, a chemotherapeutic agent that causes macrophage toxicity leading to reduced macrophages in tumor specimens (Crusz and Balkwill, 2015; Germano et al., 2013).

In lung cancer, neutrophil influx is associated with a poor prognosis (Bellocq et al., 1998). Neutrophils are the most common leukocyte in the bloodstream and function to protect the host from invading organisms by engulfing pathogens and, in instances of severe inflammation, secreting reactive oxygen species (ROS) and a variety of proteases. Neutrophils primarily exert their influence on tumors through production of ROS and proteases, although they can produce some cytokines and growth factors. Specifically in lung cancer, the neutrophil-derived protease neutrophil elastase promotes proliferation of tumors cells (Houghton et al., 2010), and in other cancers, neutrophils have been shown to enhance angiogenesis through production of matrix metalloproteinase-9 (Nozawa et al., 2006) and promote invasion and migration of tumor cells via hepatocyte growth factor and oncostatin M (Imai et al., 2005; Queen et al., 2005). ROS production by neutrophils can cause DNA damage, resulting in tumor promoting genotoxic effects (Sandhu et al., 2000), but ROS can also cause cytotoxic cell death of tumor cells (Dallegri et al., 1991). Similar to macrophages, some evidence suggests that neutrophils may exhibit phenotypic plasticity resulting in pro- and anti-tumorigenic N1 and N2 neutrophil populations (Fridlender

et al., 2009), although these phenotypes in neutrophils are not as well-described as in macrophages. Neutrophils are recruited by tumors and other cells in the tumor microenvironment primarily, but not exclusively, by CXC chemokines, including CXCL8/IL-8 or its murine homologs KC and MIP-2 (Ji et al., 2006). Reparixin, an inhibitor for the IL-8 receptors CXCR1/2 that reduces neutrophil chemotaxis (Zarbock et al., 2008), is currently being tested in clinical trials (Crusz and Balkwill, 2015).

Many different T cell subsets have been identified, but the T cell populations that have been best described in the context of cancer are CD4+ and CD8+ T cells and T regulatory cells. T cells function in the adaptive immune response, responding to specific antigens through T cell receptor-mediated recognition of peptides displayed by antigen presenting cells. Activation of T cells by antigen results in proliferation and migration to affected tissue. Cytotoxic CD8+ T cells are capable of direct lysis of malignant cells bearing the recognized antigen, while CD4+ helper T cells produce cytokines resulting in enhanced CD8+ T cell function and stimulation of other immune cell types. In contrast, T regulatory cells can suppress immune responses, hampering CD8+ T cell function by preventing activated T cell proliferation and maintaining T-cell tolerance to antigens (Woo et al., 2002). In lung tumors, increased T regulatory cell numbers have been observed (Woo et al., 2001). T cell-related treatments for cancer have mainly focused on re-activating T cell-mediated immunity through inhibition of PD-1/PD-L1 and CTLA-4 signaling. PD-1 expression on CD8+ effector T cells indicates T cell unresponsiveness or exhaustion, and increased expression of PD-1 has been observed on tumor-infiltrating CD8+ T cells in NSCLC (Zhang et al., 2010). The primary ligand for PD-1, PD-L1, is expressed on a variety of immune cells and can also be expressed by tumors, limiting the anti-tumor immune response. In lung cancer, high levels of PD-L1 expression is a poor prognostic factor (Mu et al., 2011). In 2015, clinical trials testing two PD-1 monoclonal antibodies, nivolumab and pembrolizumab (Borghaei et al., 2015; Garon et al., 2015), demonstrated therapeutic efficacy and received FDA approval for treatment of patients with NSCLC. Similarly, CTLA-4 is a negative regulator of T-cell-mediated immunity expressed on both CD4+ and CD8+ T cells, and ipilimumab, a monoclonal antibody targeting CTLA-4, led to increased progression free survival in a phase II clinical trial in NSCLC patients (Lynch et al., 2012).

NF-κB Signaling

Nuclear factor κ-light chain enhancer of activated B cells (NF-κB) is a central mediator of the inflammatory response, and, in tumors, is thought to be a key signaling pathway involved in intrinsic inflammation. The NF-κB transcription factor regulates genes involved in a variety of processes in addition to inflammation, including cytokines, chemokines, receptors, adhesion molecules, and enzymes, as well as cell cycle, apoptosis, and survival regulators. Recent studies have suggested that the NF-κB signaling pathway is critical for lung tumorigenesis, making investigations of the mechanisms and mediators of NF-κB's effect important for understanding lung tumor biology as well as for the identification of potential therapeutic targets.

The NF-κB transcription factor family contains 5 members (p105/p50, p100/p52, p65/RelA, RelB, c-Rel), which share an N-terminal Rel homology domain responsible for DNA binding and dimerization. In addition, all of the NF-κB family members except for p50 and p52 contain a transactivation domain, suggesting that p50 and p52 are poor transcription factors on their own. In resting cells, the NF-κB family members exist as homo- or heterodimers sequestered in the cytoplasm by inhibitory molecules or IκBs. Precursor proteins p105 and p100 also contain C-terminal IκB-like domains that must undergo proteasomal processing to liberate the active transcription factors p50 and p52, respectively. When NF-κB is activated, the IκBs are phosphorylated and degraded. The NF-κB homo- or heterodimers are then released to bind κB enhancer motifs found in promoters and introns of target genes and regulate transcription through the recruitment of co-activators and co-repressors. The consensus NF-κB binding sequence is 5'-GGGRN(Y)YYCC-3', where R is a purine, Y is a pyrimidine, and N is any nucleotide, but NF-κB dimers can also bind to DNA sequences that lack a κB consensus binding site (Hoffmann, 2006; Siggers et al., 2011; Wong et al., 2011; Zhao et al., 2014). NF-κB activation can occur through either the canonical (classical) or the non-canonical (alternative) pathway (Figure 2). The net effect of NF-κB activation, in terms of gene expression changes, is dependent upon the specific cell type, activating signals, and NF-κB dimer composition.

Canonical NF-κB signaling is highly dynamic and subject to tight regulation, as one of the targets

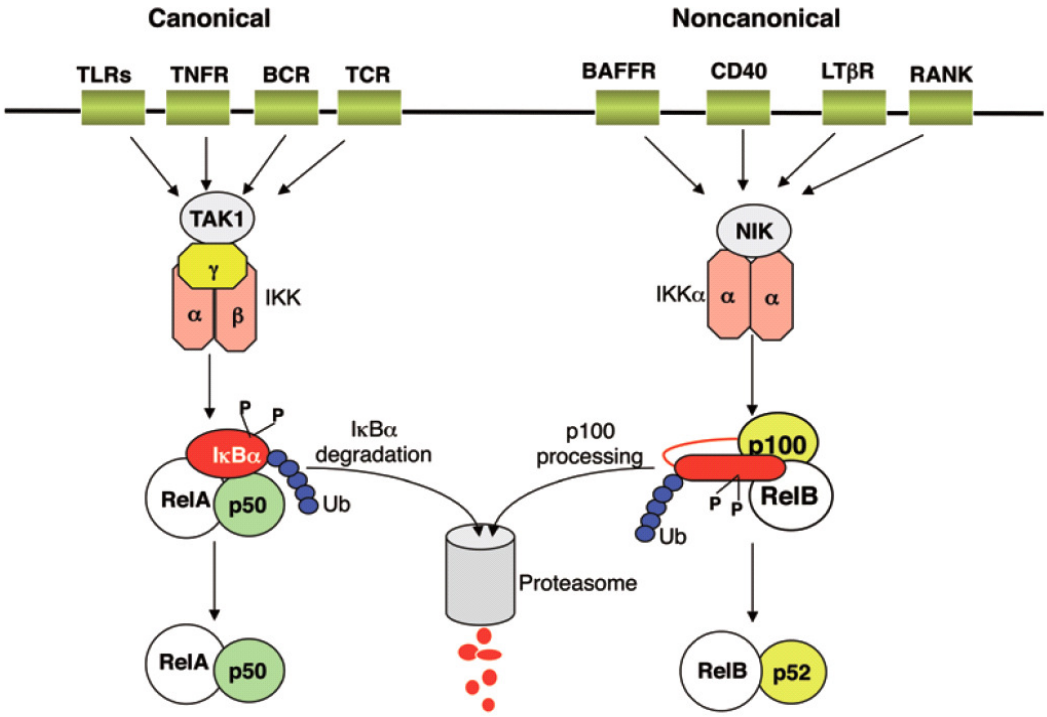

Figure 2: Schematic of canonical and non-canonical NF-κB signaling pathways.
Adapted by permission from Macmillan Publishers Ltd: Cell Research (Sun, S. Non-canonical NF-κB signaling pathway. 21(1): 71–85), copyright (2010).

of canonical pathway activation is its inhibitor, inhibitor of κBα (IκBα) (Brown et al., 1993). The canonical pathway is activated by a variety of stimuli including cytokine receptors, pattern-recognition receptors, and oncogenic mutations. When the canonical NF-κB signaling pathway is activated, a heterotrimeric IκB kinase (IKK) complex consisting of two kinases, IKKα and IKKβ, and a regulatory subunit, NF-κB essential modulator (NEMO)/IKKγ, becomes activated, with canonical pathway signaling being dependent on IKKβ and NEMO (Mercurio et al., 1997; Rothwarf et al., 1998; Woronicz et al., 1997; Yamaoka et al., 1998). IKKβ phosphorylates IκBα on N-terminal serines (Ser32/36) (Chen et al., 1996). This phosphorylation recruits the E3 ubiquitin ligase SCF/βTRCP, marking IκBα through K48-linked polyubiquitination for degradation via the 26S proteasome (Kanarek and Ben-Neriah, 2012). Ubiquitination and degradation of IκBα exposes a nuclear localization sequence on the NF-κB dimers, enabling them to translocate into the nucleus. Canonical pathway activation is associated with nuclear localization of the prototypic NF-κB heterodimer made up of RelA/p65, which contains a strong transcriptional activation region, and p50. Canonical pathway activation can also be associated with heterodimers containing c-Rel, although c-Rel is primarily expressed in B- and T-lymphocytes (Gilmore and Gerondakis, 2011).

In contrast, non-canonical pathway activation is significantly slower than canonical pathway activation and is long-lasting and steady, seemingly lacking strong negative feedback mechanisms and dynamic regulation (Hoffmann, 2006). The non-canonical pathway is activated by specific members of the TNF cytokine family, including lymphotoxin β (Dejardin et al., 2002) and CD40 ligand (Coope et al., 2002), but it can also be activated by other stimuli, such as ROS (Iannetti et al., 2014) and STAT3 (Nadiminty et al., 2006) signaling. Non-canonical pathway signaling is dependent on IKKα, which is activated by the upstream signaling kinase NF-κB-inducing kinase (NIK). When the non-canonical NF-κB signaling pathway is activated, NIK activates IKKα through phosphorylation on Ser176 and phosphorylates p100 at Ser866 and Ser870 (Senftleben et al., 2001; Xiao et al., 2001). The activated IKKα is then able to phosphorylate p100 at Ser99, Ser108, Ser115, Ser123, and Ser872. These phosphorylations provide a signal recognized by the SCF/βTRCP ubiquitin ligase complex, resulting in

proteolytic processing of p100 by the 26S proteasome to remove its inhibitory C-terminal domain, also known as IκBδ (Xiao et al., 2004). The remaining 52 kDa polypeptide (p52) translocates into the nucleus to regulate transcription, typically as a heterodimer consisting of p52 and RelB.

Canonical NF-κB Signaling in Cancer

Activation of canonical NF-κB signaling has been observed in a variety of solid tumors including lung, breast, pancreatic, prostate, colon, as well as head and neck squamous cell carcinoma and is often associated with poor prognosis (Kojima et al., 2004; Ondrey et al., 1999; Sovak et al., 1997; Sweeney et al., 2004; Tang et al., 2006; Wang et al., 1999; Zhang et al., 2006). Specifically in the lung, bronchial biopsies from patients display increased nuclear staining for p65 (an indicator of canonical NF-κB activation) in adenocarcinoma tumors as well as in areas of dysplasia when compared to normal airway epithelium (Tichelaar et al., 2005). Others have shown high levels of nuclear p65 in lung cancer specimens relative to normal tissue, with increasing levels of nuclear p65 in advanced stage adenocarcinomas compared to early stage (Zhang et al., 2006). This same study also showed increased p65 staining in adenocarcinoma precursor lesions that progressed with increasing histological severity, suggesting that NF-κB signaling is activated very early in tumor formation. In mice, we previously reported that expression of a dominant inhibitor of the canonical NF-κB pathway in airway epithelial cells reduced chemical carcinogen-induced lung tumorigenesis by greater than 50% (Stathopoulos et al., 2007), demonstrating a requirement for NF-κB signaling in lung tumorigenesis. Conversely, activation of canonical NF-κB signaling in the airway epithelium using transgenic mice expressing a constitutively active IKKβ enhanced chemical carcinogen-induced lung tumorigenesis (Zaynagetdinov et al., 2011b), suggesting that modulation of epithelial canonical NF-κB signaling can affect disease severity.

In lung cancer, canonical NF-κB activation has been shown to correlate with mutations in KRAS and EGFR (Tang et al., 2006). Studies in KRAS-mediated lung tumorigenesis as well as in mouse models of chemical carcinogen-induced lung cancer have demonstrated that NF-κB plays an important role in tumorigenesis (Bassères et al., 2010; Meylan et al., 2009; Stathopoulos et al., 2007; Zaynagetdinov et al.,

2011b). Additionally, inhibition of canonical NF-κB signaling slows growth of established KRAS-driven tumors (Bassères et al., 2014; Meylan et al., 2009; Xue et al., 2011). EGFR activation has been shown to lead to canonical NF-κB activation in a variety of different tumor types (Alberti et al., 2012; De et al., 2014; Sun and Carpenter, 1998), and in lung cancer, canonical NF-κB signaling has been shown to mediate resistance to both first generation and third generation EGFR TKIs (Bivona et al., 2011; Blakely et al., 2015; De et al., 2014; Galvani et al., 2015). However, the *de novo* importance of the NF-κB pathway during EGFR-driven lung tumorigenesis has not been investigated.

Activation of KRAS and EGFR increases production of inflammatory cytokines, such as CXCL1, CXCL2, IL-1α, IL-1β, IL-6, and IL-11 in mice (Ancrile et al., 2007; Sparmann and Bar-Sagi, 2004; Wislez et al., 2006). Transgenic mice expressing $KRAS^{G12D}$ specifically in the lung epithelium develop a profound inflammatory response characterized by increased macrophage and neutrophil infiltration (Ji et al., 2006). Similarly, in a different mouse model of KRAS-mediated lung tumorigenesis, macrophage infiltration was present even at the time of early hyperplastic lesion formation, and this infiltration increased with malignant progression (Wislez et al., 2005). Inflammatory cell infiltration has not previously been examined in mouse models of oncogenic EGFR expression in the lung, but in breast cancer, EGFR-positive tumors are associated with increased numbers of macrophages (Leek et al., 2000). Because of EGFR's role in cytokine production and known associations between KRAS and inflammatory cell populations, EGFR mutations likely lead to changes in the tumor-associated inflammatory milieu. Whether oncogenic EGFR signaling causes recruitment of inflammatory cells via activation of NF-κB and what these inflammatory cell subpopulations are remains unknown.

Non-Canonical NF-κB Signaling in Cancer

Studies of non-canonical NF-κB signaling have largely focused on its role in cells of the hematopoietic lineage where it is important for the maturation and function of immune cells and the development of secondary lymphoid organs. Mice with global knockout of *Nfkb2* (the gene for p100/p52) display defects in dendritic cell function, B-cell maturation, and T-cell responses and disorganization of

spleen and lymph node microarchitecture (Caamaño et al., 1998; Franzoso et al., 1998). Similarly, global knockout of the *Relb* gene leads to impaired cellular immunity, reduced dendritic cells, splenomegaly, and thymic atrophy (Weih et al., 1995). These effects are presumably due to the non-canonical pathway's role in regulating expression of chemokine genes important for normal lymphoid organogenesis (Dejardin et al., 2002; Weih et al., 2001).

In several hematopoietic malignancies including multiple myeloma, chronic lymphocytic leukemia, and B- and T-cell cutaneous lymphomas, chromosomal translocations in the *Nfkb2* gene have been identified that truncate the C-terminus, removing the inhibitory domain (Migliazza et al., 1994; Neri et al., 1995, 1991). These truncated proteins localize in the nucleus, essentially leading to constitutively active p52 (Migliazza et al., 1994). Mice with global truncation of the *Nfkb2* gene develop enlarged lymph nodes and hyperactive T cell responses, suggesting that p52 activation is playing a functional role in these diseases (Ishikawa et al., 1997).

Compared to normal lung, high levels of p100/p52 and RelB have been observed in NSCLC tumors (Dimitrakopoulos et al., 2012). Additionally, increased activation of p52 has been observed in breast (Cogswell et al., 2000), prostate (Lessard et al., 2005; Seo et al., 2009), and pancreatic cancer (Wharry et al., 2009). Despite these observations, our understanding of the role of non-canonical pathway signaling in non-hematopoietic cells is limited, and whether non-canonical NF-κB signaling contributes to the pathogenesis of solid tumors has not been studied.

Current evidence from *in vitro* and *in vivo* studies suggests that non-canonical NF-κB signaling may contribute to a number of critical factors affecting tumorigenesis. Tully, et al. demonstrated that lipopolysaccharide (LPS)-induced activation of inflammatory chemokines in airway epithelial cells is dependent upon non-canonical signaling components, supporting a role for non-canonical NF-κB signaling in paracrine signaling to inflammatory cells and implicating non-canonical NF-κB signaling as a regulator of inflammation in the lung (Tully et al., 2012). In fibroblasts, p52 and RelB protect against ROS-induced senescence *in vitro* by regulating cyclin-dependent kinase (CDK) 4 and CDK6 expression and antagonizing p53 function, suggesting that p52 may be important for promoting cell survival (Iannetti

et al., 2014). Several *in vitro* and *in vivo* studies have also implicated p52 in the regulation of proliferation. In androgen-dependent prostate cancer cells, p52 over-expression promotes proliferation in androgen-deprived conditions *in vitro*, protecting against cell cycle arrest and apoptosis through regulation of cyclin D1 (Nadiminty et al., 2008). *In vivo*, global p52 expression induced by deletion of the C-terminal inhibitory domain of p100 causes hyperplasia of the gastric epithelium (Ishikawa et al., 1997), although it is unclear whether this is a direct effect of p52 in the epithelium or the result of dysregulated immune responses. Transgenic mice that express p100 under the control of the β-lactoglobulin milk protein promoter develop ductal hyperplasia after multiple pregnancies (Connelly et al., 2007), again pointing toward a role for p52 in proliferation. Together these data suggest that non-canonical NF-κB signaling, and particularly p52, may be important in tumor development through regulation of chemokine genes and/or regulating cell proliferation/survival.

Summary and Dissertation Goals

The high mortality rate of a lung cancer diagnosis underscores the need for a comprehensive understanding of signaling pathways contributing to lung carcinogenesis that can be targeted in combination with current treatment methods. A significant amount of data implicates canonical and non-canonical NF-κB signaling as important factors in lung carcinogenesis. Several studies have demonstrated that canonical NF-κB signaling is a critical promoter of KRAS-driven lung tumors (Bassères et al., 2010; Meylan et al., 2009; Zaynagetdinov et al., 2011b). However, the mechanism(s) by which canonical NF-κB promotes lung tumors is not well understood, and whether canonical NF-κB signaling is also important in lung tumors with driver mutations other than KRAS remains unknown. Increased expression of non-canonical pathway components have been observed in lung cancer (Dimitrakopoulos et al., 2012), yet little is known about the role of non-canonical NF-κB signaling in solid tumors. Since both NF-κB signaling pathways are important regulators of cytokine and chemokine production, we hypothesized that both canonical and non-canonical NF-κB signaling promote lung cancer via paracrine signaling to the inflammatory microenvironment. Acknowledging that these pathways regulate a variety of genes with

different functions, the overarching goal of this dissertation was to elucidate the primary mechanism(s) by which canonical and non-canonical NF-κB signaling participate in carcinogenesis. By characterizing the function(s) of these pathways, we aimed to identify critical mediators that could potentially serve as therapeutic targets for lung cancer patients.

In Chapter 2, we examined the requirement for canonical NF-κB signaling in EGFR-mutant lung tumors, demonstrating that inhibition of canonical NF-κB signaling reduces EGFR-mediated tumor formation in *in vivo* models of TKI-sensitive and TKI-resistant lung cancer. Since previous studies suggest that canonical NF-κB signaling is primarily important in EGFR-mutant lung tumors for promoting TKI resistance, these findings indicate that canonical NF-κB signaling plays a broader role in EGFR-mediated lung cancer. Additionally, these studies suggest that the primary mechanism by which canonical NF-κB signaling promotes EGFR-mediated lung tumorigenesis is through macrophage recruitment.

To study non-canonical NF-κB signaling, we generated a novel transgenic mouse model with inducible expression of p52 in the lung epithelium. In Chapter 3, we used this model to investigate the role of non-canonical NF-κB signaling in lung cancer. Surprisingly, p52 over-expression had no effect on inflammatory signaling but enhanced carcinogen-induced lung cancer by promoting proliferation through the regulation of cell cycle-associated genes, providing the first evidence that non-canonical NF-κB signaling plays a functional role in promoting lung carcinogenesis. Since others have shown that non-canonical NF-κB signaling is activated by inflammatory stimuli and regulates cytokine genes, we examined the effect of *in vivo* p52 over-expression in the context of the inflammatory stimulus LPS in Chapter 4. In contrast to our findings in lung cancer, p52 over-expression in conjunction with LPS stimulation enhanced lung injury and epithelial cell apoptosis *in vivo*, and *in vitro* studies suggest that this apoptotic effect of p52 over-expression may be a more general response to acute cellular stress. Together, these studies demonstrate non-canonical NF-κB signaling as a regulator of proliferation/cell survival/apoptosis and implicate the non-canonical NF-κB pathway as a therapeutic target in the context of lung cancer and inflammatory diseases.

This thesis describes the functions of canonical and non-canonical NF-κB signaling in lung carcinogenesis and suggests that the primary mechanism by which these pathways promote lung cancer may be different. The findings presented here advance our understanding of the complexity of these signaling pathways in different contexts and provide important insights for targeting them therapeutically.

CHAPTER II:

EPITHELIAL CANONICAL NF-κB SIGNALING PROMOTES EGFR-DRIVEN LUNG CARCINOGENESIS VIA MACROPHAGE RECRUITMENT

Rationale

EGFR is a receptor tyrosine kinase that is mutated in approximately 15% of lung adenocarcinomas (Li et al., 2008; Rosell et al., 2009). Mutations in EGFR destabilize the auto-inhibitory conformation of the kinase domain (Yun et al., 2007), resulting in constitutive EGFR kinase activation as well as constitutive activation of downstream pathways, such as PI3K, MAPK, and JAK/STAT. Targeted therapies, such as TKIs, have been developed to treat lung cancer patients with EGFR-mutant tumors. However, these therapies have not significantly impacted overall patient survival because the tumors develop resistance, most commonly through the EGFR T790M mutation (Pao et al., 2005; Yun et al., 2008). This lack of effective therapy for long-term survival demonstrates the need for identification of new pathways that can be targeted alone or in combination with current treatment methods.

NF-κB is a transcription factor family that regulates genes involved in a variety of processes, including cytokines, chemokines, receptors, adhesion molecules, and enzymes, as well as cell cycle, apoptosis, and survival regulators. NF-κB family members exist as dimers sequestered in the cytoplasm by inhibitor molecules known as IκBs. When the pathway is activated, IκBs are phosphorylated and undergo rapid degradation by the proteasome, releasing NF-κB dimers to translocate into the nucleus and bind enhancer motifs found in the promoters and introns of target genes. NF-κB can be activated through either the canonical or non-canonical pathways. Canonical NF-κB signaling is associated with nuclear localization of a heterodimer consisting of p65 and p50, and non-canonical pathway signaling involves p52 and RelB.

In lung cancer, canonical NF-κB activation is associated with a poor prognosis (Zhang et al., 2006). High levels of nuclear p65 have been observed in lung cancer specimens relative to normal tissue,

with increasing levels of nuclear p65 in advanced stage adenocarcinomas (Tang et al., 2006). Lung adenocarcinoma precursor lesions also have increased nuclear p65 staining that progresses in intensity with increasing histological severity (Tang et al., 2006; Tichelaar et al., 2005), indicating that canonical NF-κB signaling is activated early in tumor formation. Canonical NF-κB activation in lung tumors is associated with mutations in common lung cancer driver genes, including KRAS and EGFR (Tang et al., 2006). In KRAS-mediated lung tumorigenesis, as well as in mouse models of chemical carcinogen-induced lung cancer, canonical NF-κB signaling plays an important role in tumor development (Bassères et al., 2010; Meylan et al., 2009; Stathopoulos et al., 2007; Zaynagetdinov et al., 2011b). EGFR signaling is known to activate canonical NF-κB in a variety of tumor types (Alberti et al., 2012; De et al., 2014), and canonical NF-κB signaling has been shown to facilitate resistance to EGFR inhibitor therapies in lung cancer (Bivona et al., 2011; Galvani et al., 2015). However, the importance of the canonical NF-κB signaling pathway during oncogenic EGFR-driven lung tumorigenesis has not been examined.

To investigate the role of canonical NF-κB signaling in EGFR-mutant lung tumors, we inhibited epithelial canonical NF-κB in mouse models of TKI-sensitive and TKI-resistant EGFR-driven lung tumorigenesis by inducible expression of a dominant negative IκB (DN-IκB). In the setting of canonical NF-κB inhibition, we observed a dramatic reduction in lung tumor formation and a decrease in lung inflammation without changes in EGFR-regulated downstream signaling pathways. Together, these studies demonstrate that canonical NF-κB-dependent signaling is important for generating a pro-tumorigenic inflammatory microenvironment in EGFR-mutant tumors.

Materials and Methods

Animal models

All animal care and experimental procedures were approved and conducted according to guidelines of the Vanderbilt University Institutional Animal Care and Use Committee. (tet-O)$_7$-EGFR^{L858R} mice (Politi et al., 2006), (tet-O)$_7$-EGFR$^{L858R+T790M}$ mice (Regales et al., 2007) (gifts from Dr. William

Pao, Vanderbilt University), (tet-O)$_7$-IκBα-DN mice (Cheng et al., 2007), and CCSP-rtTA (Tichelaar et al., 2000) mice and genotyping procedures have all been previously described. Double transgenic EGFR^{L858R} and EGFR$^{L/T}$ mice were generated by mating (tet-O)$_7$-EGFR^{L858R} or (tet-O)$_7$-EGFR$^{L858R+T790M}$ mice to homozygous CCSP-reverse tetracycline (tet) transactivator (rtTA) mice. Triple transgenic EGFR^{L858R} DN-IκB or EGFR$^{L/T}$ DN-IκB mice were generated by mating EGFR^{L858R} or EGFR$^{L/T}$ mice to homozygous (tet-O)$_7$-IκBα-DN mice. All mice were on a Friend leukemia virus B strain (FVB) background. Age- and sex-matched transgenic mice along with appropriate genotype-negative littermate controls (designated wild-type [WT]) were used in experiments. Transgene expression was activated by administering doxycycline (dox) at a concentration of 0.5 g/L for EGFR^{L858R} experiments or 1 g/L for EGFR$^{L/T}$ experiments in 2% sucrose drinking water, and water was replaced twice weekly.

For tissue harvest, lungs were lavaged as previously described (Zaynagetdinov et al., 2011b), and the left lung was tied off and frozen. The right lung was perfused and fixed by inflating with 10% neutral-buffered formalin. Total and differential bronchoalveolar lavage (BAL) cell counts were determined as previously described (Stathopoulos et al., 2007). For survival analysis, EGFR^{L858R} and EGFR^{L858R} DN-IκB mice were weighed on the day of dox initiation and at least twice weekly. Twenty percent weight loss was considered a mortality endpoint at which time mice were euthanized.

Tumor histological analysis

Hematoxylin and eosin (H&E) staining was performed on 5 μm sections for quantification of tumor burden. Three sections were analyzed per mouse, and each section was separated by 50 μm. For EGFR^{L858R} tumor analysis, twenty non-overlapping 20x fields were scored on each section based on lesion formation using a scale of 0 to 4 (0 = normal, 1 = <10% of alveoli have hyperplastic proliferative lesions, 2 = 10-50% of alveoli with proliferative lesions, 3 = <50% of alveoli with proliferative lesions, 4 = formation of tumor focus). For EGFR$^{L/T}$ tumor analysis, tumor area was measured and normalized to total lung area using Image-Pro Plus software (Media Cybernetics).

Immunostaining

For CD68 immunostaining, lung sections were stained with a CD68 antibody (ab125212; Abcam), and positive cells were enumerated on twenty 40x fields. Mean scores were calculated for each animal.

CT imaging

CT images were acquired using a Bioscan NanoSPECT/CT system. All imaging was performed by the Vanderbilt University Institute of Imaging Science.

RNA isolation, RT-PCR, and quantitative real-time PCR

Total mRNA was isolated from lung tissue using the RNeasy Mini kit (Qiagen) according to the manufacturer's instructions. Reverse transcriptase polymerase chain reaction (RT-PCR) was performed to measure $EGFR^{L858R}$ and $EGFR^{L/T}$ expression as previously described (Politi et al., 2006; Regales et al., 2007). RT-PCR was also performed for DN-IκB and Glyceraldehyde-3-phosphate dehydrogenase (GAPDH) using the following primers: DN-IκB (F: CCTGGCTGTTGTCGAATACC; R: GGTGATGGTGATGATGACCGG), GAPDH (F: CCTGCACCACCAACTGCTTAG; R: GTGGATGCAGGGATGATGTTC). Quantitative real-time polymerase chain reaction (PCR) was performed using Sybr Green PCR Master Mix (Applied Biosystems) and the following primer sets: CCL2 (F: TTAAAAACCTGGATCGGAACCAA; R: GCATTAGCTTCAGATTTACGGGT), M-CSF (F: GTGTCAGAACACTGTAGCCAC; R: TCAAAGGCAATCTGGCATGAAG) (PrimerBank ID: 166064045c1) (Spandidos et al., 2010, 2008; Wang and Seed, 2003), KC (F: CCGAAGTCATAGCCACACTCAA; R: GCAGTCTGTCTTCTTTCTCCGTTAC), MIP-2 (F: ACTCTCAAGGGCGGTCAAAA; R: GGCACATCAGGTACGATCCA), GAPDH (F: TGAGGACCAGGTTGTCTCCT; R: CCCTGTTGCTGTAGCCGTAT). For each sample, expression was normalized to GAPDH. Threshold values greater than 33 were considered below the limit of detection.

Cell lines

HBEC3-KT (WT) and HBEC3-KTGmSRZ ($EGFR^{L858R}$-mutant) immortalized human bronchial epithelial cells (Ramirez et al., 2004; Sato et al., 2006) (gifts from Dr. John Minna, The University of Texas Southwestern Medical Center) were maintained at 37ºC 5% CO_2 in Keratinocyte-SFM supplemented with epidermal growth factor 1-53 and bovine pituitary extract (Thermo Scientific). Cells were transfected with myc/His-IκB-DN pEF4 (Cheng et al., 2007) or empty vector (EV) pEF4 using Xfect transfection reagent (Clontech).

Western blot analysis

Whole lung lysates were prepared using RIPA buffer, separated by sodium dodecyl sulfate polyacrylamide gel electrophoresis (SDS-PAGE), transferred to nitrocellulose membranes, and probed with the following antibodies: p-Akt (Ser473) (4060; Cell Signaling), total Akt (9722; Cell Signaling), p-ERK (T202/Y204) (9101; Cell Signaling), total ERK (9102; Cell Signaling), p-STAT3 (Y705) (9131; Cell Signaling), total STAT3 (9132; Cell Signaling), or β-actin (SAB2100037, Sigma). Nuclear and cytoplasmic protein fractions were prepared from immortalized human bronchial epithelial cells using the NE-PER Nuclear and Cytoplasmic Extraction Reagents (Thermo Fisher). Western blots were probed using the following antibodies: myc (M4439; Sigma), caspase-3 (9622; Cell Signaling), β-actin (A2066, Sigma), p65 (C-20, Santa Cruz), or TATA-binding protein (TBP) (N-12, Santa Cruz). Jurkat cell lysates treated with cytochrome c were included as a positive control for cleaved caspase-3 (Cell Signaling; 9663). Immunodetection was performed using the corresponding AlexaFluor-conjugated antibodies and the Odyssey Infrared Imaging System (LI-COR Biosciences). All images were converted to grayscale.

Flow cytometry

Lung single-cell suspensions were generated and stained as previously described (Zaynagetdinov et al., 2011a, 2011b). To reduce non-specific staining, single-cell suspensions were incubated with Fc receptor block (BD Biosciences). For detection of T cell populations, cells were incubated with the

following antibodies: CD3-PE-Cy7 (145-2C11) and CD8a-AF700 (53-6.7) from BioLegend, CD4-FITC (RM 4-5) from eBioscience, and CD45-AP-Cy7 (30-F11) from BD Biosciences. For detection of neutrophil populations, cells were incubated with CD11b-A450 (M1/70) and Ly6G-PerCP-Cy5.5 (1A8) from BD Biosciences and CD45-AP-Cy7. Dead cells were excluded using a Live/Dead Fixable Blue Dead Cell Stain Kit (Life Technologies). Cells were analyzed using a LSR II flow cytometer (BD Biosciences), and data analysis was performed using FlowJo software (Tree Star, Inc.).

In vitro migration assays

Mouse bone marrow neutrophils were isolated from WT FVB mice as described by others. (Boxio et al., 2004) Neutrophil chemotaxis was assessed using a modified Boyden chamber MBA 96 (Neuroprobe) with a 3 μm pore size polycarbonate filter. (Sai et al., 2008) Cell-free BAL supernatant was diluted 1:1 with 0.2% bovine serum albumin (BSA)/RPMI serum-free and phenol red-free media (final BSA concentration of 0.1%) and placed in the bottom chamber as the chemoattractant. Each BAL sample was run in triplicate. $2x10^5$ neutrophils in 0.1% BSA/RPMI were loaded into the top chamber and incubated for one hour at 37ºC, 5% CO_2.

Mouse bone marrow-derived macrophages were isolated from WT FVB mice and matured as described by others (Munder et al., 1971). Macrophage chemotaxis was assessed as for neutrophils with a 5 μm pore size polycarbonate filter. 250 ug of whole lung lysates from 5 week dox $EGFR^{L858R}$ and $EGFR^{L858R}$ DN-IκB mice was diluted in Dulbecco's Modified Eagle Medium (DMEM) supplemented with 1% fetal bovine serum (FBS) and placed in the bottom chamber as the chemoattractant. Each lysate was run in triplicate. $1.5x10^5$ macrophages in DMEM supplemented with 1% FBS were loaded into the top chamber and incubated for 5.5 hours at 37ºC, 5% CO_2.

The trans-migrated cells were collected by centrifuging the 96 well plate, washed three times, and resuspended in 100 μL Hank's Balanced Salt Solution for neutrophils or 100 μL phosphate-buffered saline (PBS) for macrophages. 60 μL 4-nitrophenyl 2-acetamido-2-deoxy-β-D-glucopyranoside (NAG) solution (4mM NAG, 25mM citric acid, 25 mM sodium citrate, and 0.25% Triton X-100, pH 5.0) was

added to each well and incubated overnight at room temperature in the dark. 100 µL stop solution (50 mM glycine and 5 mM EDTA, pH 10.4) was added to each well, and the absorbance was measured at 405 nM.

Neutrophil depletion

For neutrophil depletion experiments, mice received either 100 µg of anti-Ly6G antibodies (Clone 1A8, BioLegend) or IgG2a isotype control antibodies (BioLegend) by intraperitoneal (IP) injection. Mice were injected on day 7, 9, 12, and 14 after dox initiation and twice weekly thereafter until they were sacrificed at day 35 of dox. Neutrophil depletion was confirmed by lung flow cytometry and Wright-Giemsa staining of peripheral blood smears at day 35 of dox, 2 days after the final antibody treatment.

Clodronate macrophage depletion

Clodronate (Sigma) or PBS-containing liposomes were prepared as previously described (Everhart et al., 2005). 100 µL of clodronate or control PBS lipsomes was delivered intratracheally (IT) 3 days prior to dox initiation, on the day of dox initiation, and weekly thereafter until mice were harvested at day 35 of dox. For liposome delivery, mice were anesthetized and intubated with a 1-mL syringe with a 6-mm-long, 22-gauge over-the-needle catheter (Abbocath-T; Venisystems). Macrophage depletion was confirmed by CD68 staining of lung sections at day 35 of dox, 3 days after the final liposome treatment.

Protein array

Whole lung lysates were prepared from $EGFR^{L858R}$ and $EGFR^{L858R}$ DN-IκB mice treated with dox for 2 weeks. To minimize the effects of mouse-to-mouse-variability, lysates were pooled from 3 mice for each sample, resulting in a total of 4 samples (2 $EGFR^{L858R}$ and 2 $EGFR^{L858R}$ DN-IκB). Cytokine expression was determined using the Mouse Inflammation Array (AAM-INF-G1; RayBiotech, Inc.), which measures 40 different inflammation-associated analytes, including BLC (CXCL13), CD30L

(TNFSF8), Eotaxin-1 (CCL11), Eotaxin-2 (CCL24), FasL (TNFSF6), Fractalkine (CX_3CL1), G-CSF, GM-CSF, IFNγ, IL-1α, IL-1β, IL-2, IL-3, IL-4, IL-6, IL-9, IL-10, IL-12 p40/p70, IL-12 p70, IL-13, IL-17A, I-TAC (CXCL11), KC, Leptin, LIX, Lymphotactin, MCP-1 (CCL2), M-CSF, MIG (CXCL9), MIP-1α (CCL3), MIP-1γ, RANTES (CCL5), SDF-1α (CXCL12α), I-309 (TCA-3/CCL1), TECK (CCL25), TIMP-1, TIMP-2, TNF-α, TNFRI (TNFRSF1A), and TNFRII (TNFRSF1B).

Enzyme-linked immunosorbent assays (ELISAs)

KC and MIP-2 (R&D Systems) were measured in cell-free BAL supernatants. ELISAs were performed according to manufacturer's instructions.

Statistics

Data were analyzed using GraphPad Prism 5.0 software (GraphPad Software, Inc.). Unpaired student t-tests were performed for comparisons between two groups. To analyze differences among more than two groups, one-way ANOVA followed by a Tukey's post-test was used. For the Kaplan-Meyer survival analysis, a log-rank test was employed. Values are presented as the mean ± standard error of the mean (SEM), and $p \leq 0.05$ was considered statistically significant.

Results

Inhibition of epithelial canonical NF-κB signaling reduces $EGFR^{L858R}$-mediated lung tumorigenesis

To investigate the requirement for epithelial canonical NF-κB signaling in EGFR-driven lung tumor formation, we developed a model in which canonical NF-κB signaling could be inhibited *in vivo* specifically in airway epithelial cells expressing oncogenic EGFR. In this model, transgenic mice harbor a dox-inducible human $EGFR^{L858R}$ construct and the CCSP promoter-driven reverse tetracycline transactivator (CCSP-rtTA; tet-O-$EGFR^{L858R}$) so that $EGFR^{L858R}$ is expressed specifically in the airway epithelium when given dox (designated $EGFR^{L858R}$ mice) (Politi et al., 2006). To inhibit epithelial

canonical NF-κB signaling in the lungs of these mice, $EGFR^{L858R}$ mice were mated to transgenic mice that express a dox-inducible dominant negative IκBα (DN-IκB) (Cheng et al., 2007). This DN-IκB is unable to be phosphorylated and degraded, thereby blocking translocation of the NF-κB heterodimers into the nucleus and preventing target gene transcription. Upon dox administration, these triple transgenic mice (designated $EGFR^{L858R}$ DN-IκB mice) express $EGFR^{L858R}$ with simultaneous inhibition of canonical NF-κB signaling in airway epithelial cells.

To assess the effect of canonical NF-κB inhibition on EGFR-mediated tumor formation, mice were administered dox for 5 weeks, and tumor burden was assessed by histological scoring of lung sections. After 5 weeks of dox treatment, $EGFR^{L858R}$ DN-IκB mice demonstrated a marked decrease in lung tumor burden compared to $EGFR^{L858R}$ mice (Figure 3A, B). In addition, fewer tumors were observed on CT scan images from $EGFR^{L858R}$ DN-IκB mice compared to $EGFR^{L858R}$ mice (Figure 3C). Transgene expression was validated in these mice using RT-PCR to measure expression of human $EGFR^{L858R}$ as well as DN-IκB in the lungs of mice administered dox for 5 weeks (Figure 3D). To further investigate the impact of reduced tumor formation in $EGFR^{L858R}$ DN-IκB mice, we performed a survival analysis, which revealed that $EGFR^{L858R}$ DN-IκB mice had significantly prolonged survival compared to $EGFR^{L858R}$ mice following dox treatment (Figure 3E). Together, these data show that epithelial canonical NF-κB inhibition can reduce tumor burden and prolong survival, implicating canonical NF-κB signaling in the epithelium as a critical factor for EGFR-mediated tumorigenesis.

Epithelial canonical NF-κB inhibition does not affect epithelial cell survival or activation of EGFR-regulated signaling pathways

To investigate the function of epithelial canonical NF-κB signaling in lung tumors, we tested whether canonical NF-κB inhibition results in apoptosis of lung epithelial cells expressing oncogenic EGFR. In *in vitro* studies, we transfected WT and $EGFR^{L858R}$-expressing immortalized human bronchial epithelial cells (Ramirez et al., 2004; Sato et al., 2006) with control EV or a myc-tagged DN-IκB expression vector and isolated nuclear and cytoplasmic protein extracts. Successful transfection was

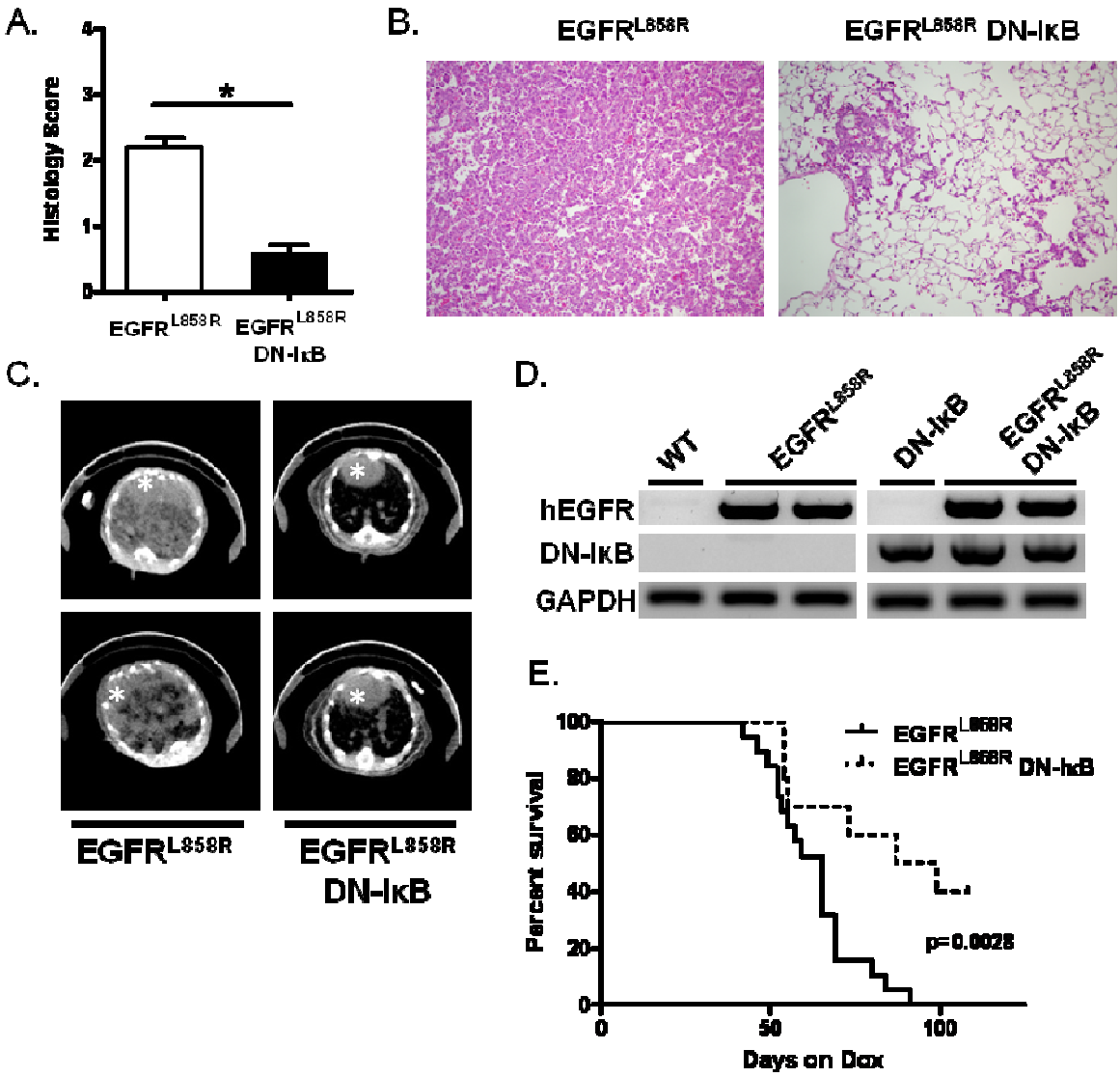

Figure 3: Epithelial canonical NF-κB inhibition reduces EGFR^{L858R}-mediated tumorigenesis.

Epithelial NF-κB inhibition reduces EGFR^{L858R}-mediated tumorigenesis. Histological analysis of tumor burden (A), representative photomicrographs of H&E-stained lung sections (20x magnification) (B), and representative CT images (C) from EGFR^{L858R} and EGFR^{L858R} DN-IκB mice administered dox for 5 weeks (n=13-14 mice/group; *p<0.0001). White asterisk designates the heart in CT images. (D) RT-PCR for EGFR^{L858R} (hEGFR) and DN-IκB transgenes using mRNA isolated from lungs of WT, DN-IκB, EGFR^{L858R}, and EGFR^{L858R} DN-IκB mice administered dox for 5 weeks. (E) Kaplan-Meier survival curve of EGFR^{L858R} and EGFR^{L858R} DN-IκB mice after dox administration (for EGFR^{L858R} n=19 mice, for EGFR^{L858R} DN-IκB n=10; log rank test p=0.0028).

verified by western blotting for myc-tagged transgene (Figure 4A). Reduced nuclear p65 was observed in DN-IκB-transfected cells, indicating reduced canonical NF-κB activation (Figure 4A). However, no increase in cleaved caspase-3 was observed as a result of NF-κB inhibition (Figure 4A), suggesting that canonical NF-κB activity is not required for survival of $EGFR^{L858R}$-expressing cells. To measure apoptosis *in vivo*, we performed terminal deoxynucleotidyl transferase dUTP nick end labeling (TUNEL) on lung sections from $EGFR^{L858R}$ and $EGFR^{L858R}$ DN-IκB mice treated with dox for 2 weeks (prior to appearance of tumors) and 5 weeks (when tumors were present). We observed no increase in TUNEL-positive cells in the lungs of $EGFR^{L858R}$ DN-IκB lungs compared to $EGFR^{L858R}$ at either time point (data not shown).

We also measured activation of key EGFR-regulated downstream signaling pathways on western blots from whole lung lysates obtained from mice treated with dox for 2 weeks. No changes in Akt, ERK, or STAT3 phosphorylation were observed (Figure 4B-E). In addition to examining whole lung lysates from mice administered dox for 2 weeks, western blotting was performed on lysates from an enriched lung epithelial cell population generated from lungs of mice administered dox for 5 weeks. Similarly, no changes in EGFR-regulated downstream signaling pathways were observed as a result of NF-κB inhibition in this enriched population (data not shown). Together, these data suggest that canonical NF-κB inhibition does not affect downstream EGFR pathway signaling in EGFR-mutant cells.

Canonical NF-κB inhibition reduces macrophage and neutrophil influx into the lungs of mice expressing mutant EGFR

Since NF-κB is a central mediator of the inflammatory response, we next evaluated the effects of canonical NF-κB inhibition on inflammatory cell recruitment in the lungs of mice expressing mutant EGFR. Total inflammatory cells were counted in BAL from $EGFR^{L858R}$, $EGFR^{L858R}$ DN-IκB, DN-IκB (CCSP-rtTA; tet-O-IκBα-DN), and WT mice treated with dox for 2 or 5 weeks. Prior to tumor formation, a ≥3-fold increase in BAL inflammatory cells was observed in $EGFR^{L858R}$ mice administered dox for 2 weeks compared to control groups, and this inflammatory cell influx was not present in $EGFR^{L858R}$ DN-

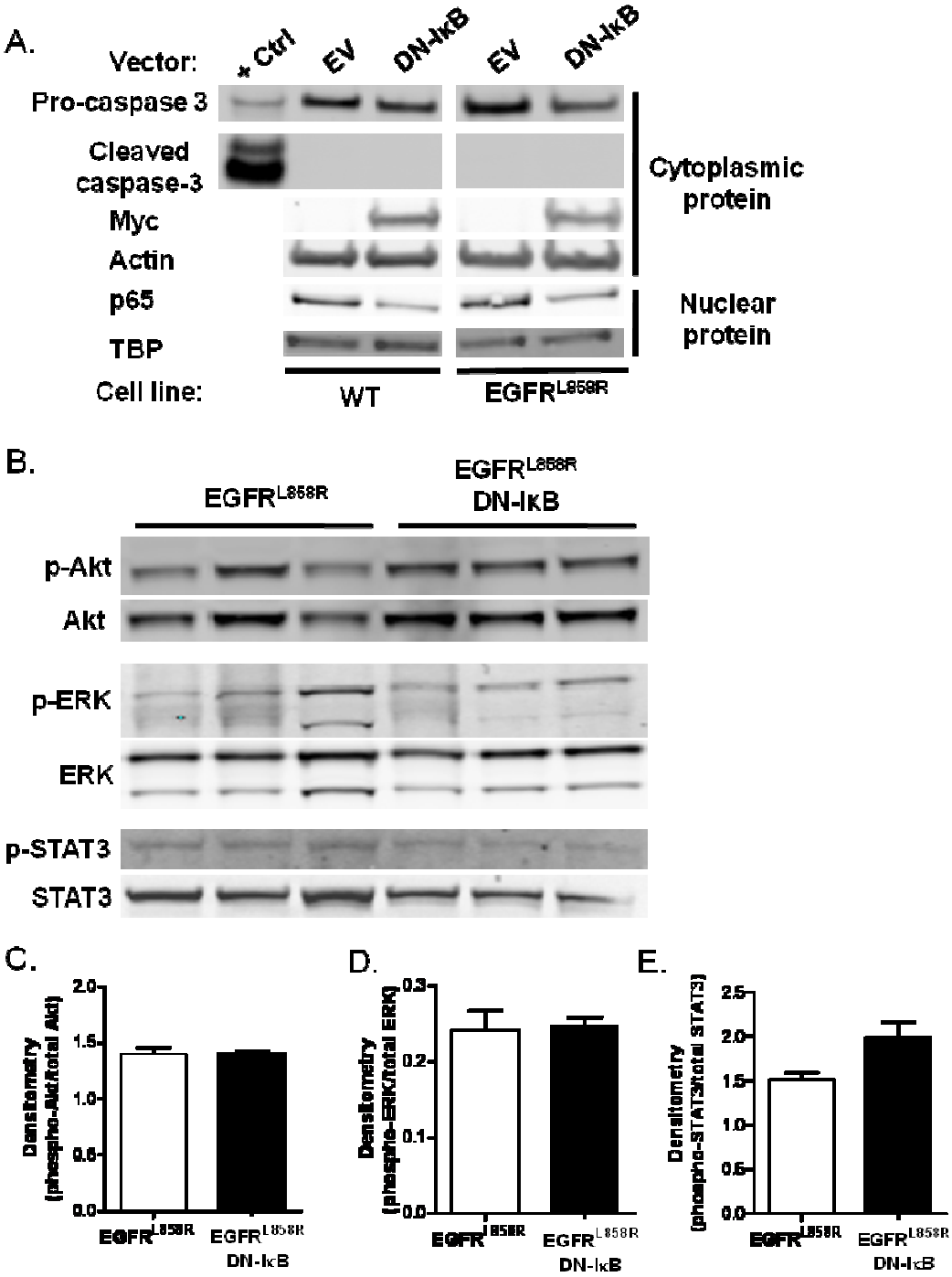

Figure 4: Canonical NF-κB inhibition in airway epithelial cells does not alter apoptosis or EGFR-regulated signaling pathways.

(A) Western blot of cytoplasmic and nuclear protein extracts from WT and $EGFR^{L858R}$-mutant immortalized human bronchial epithelial cells transfected with DN-IκB expression vector or control empty vector. β-actin and TATA-binding protein (TBP) were probed as cytoplasmic and nuclear loading controls, respectively. Western blot (B) and densitometry for phospho-Akt (C), phospho-ERK (D), and phospho-STAT3 (E) using lung lysates from $EGFR^{L858R}$ and $EGFR^{L858R}$ DN-IκB mice treated with dox for 2 weeks. For densitometry, phospho-proteins were normalized to total protein.

IκB mice (Figure 5A). When tumors were present at 5 weeks of dox treatment, a ≥10-fold increase in inflammatory cells was observed in $EGFR^{L858R}$ mice compared to control groups (Figure 5A). This dramatic increase was abrogated by inhibition of NF-κB in the epithelium. Together, these data indicate that epithelial canonical NF-κB signaling is important for recruiting inflammatory cells in this model, even prior to tumor formation.

To identify inflammatory cell subpopulations altered as a result of epithelial canonical NF-κB inhibition, we performed CD68 immunostaining and quantified CD68+ macrophages on lung sections from $EGFR^{L858R}$ and $EGFR^{L858R}$ DN-IκB mice treated with dox for 2 weeks or 5 weeks. At both time points, lungs from $EGFR^{L858R}$ DN-IκB mice contained fewer macrophages compared to $EGFR^{L858R}$ mice (Figure 5B, C). To analyze changes in other lung inflammatory cell populations, we performed flow cytometry on lung single cell suspensions generated from $EGFR^{L858R}$, $EGFR^{L858R}$ DN-IκB, DN-IκB, and WT mice. In mice administered dox for 5 weeks, NF-κB inhibition led to reduced neutrophils (CD45+CD11b+Ly6G+) in the lungs (Figure 5D) but no differences in T lymphocyte populations (Figure 5E). Together, these data demonstrate that canonical NF-κB inhibition results in reduced neutrophils when tumors are present and reduced macrophages throughout tumorigenesis.

Canonical NF-κB inhibition decreases lung tumors in mice expressing a TKI-resistant EGFR mutation

To assess whether epithelial canonical NF-κB inhibition affects lung tumor burden and inflammatory cell numbers in a TKI-resistant model of EGFR-mediated tumorigenesis, we used transgenic mice with dox-inducible expression of human $EGFR^{L858R+T790M}$ (CCSP-rtTA; tet-O-$EGFR^{L858R+T790M}$). Similar to the $EGFR^{L858R}$ model, these mice express $EGFR^{L858R+T790M}$ in the airway epithelium when given dox (designated $EGFR^{L/T}$ mice). However, the presence of the T790M mutation renders tumors in these mice insensitive to treatment with first generation TKIs erlotinib and gefitinib (Regales et al., 2007). To inhibit epithelial canonical NF-κB signaling in the lungs of these mice, $EGFR^{L/T}$ mice were mated to transgenic DN-IκB mice (designated $EGFR^{L/T}$ DN-IκB).

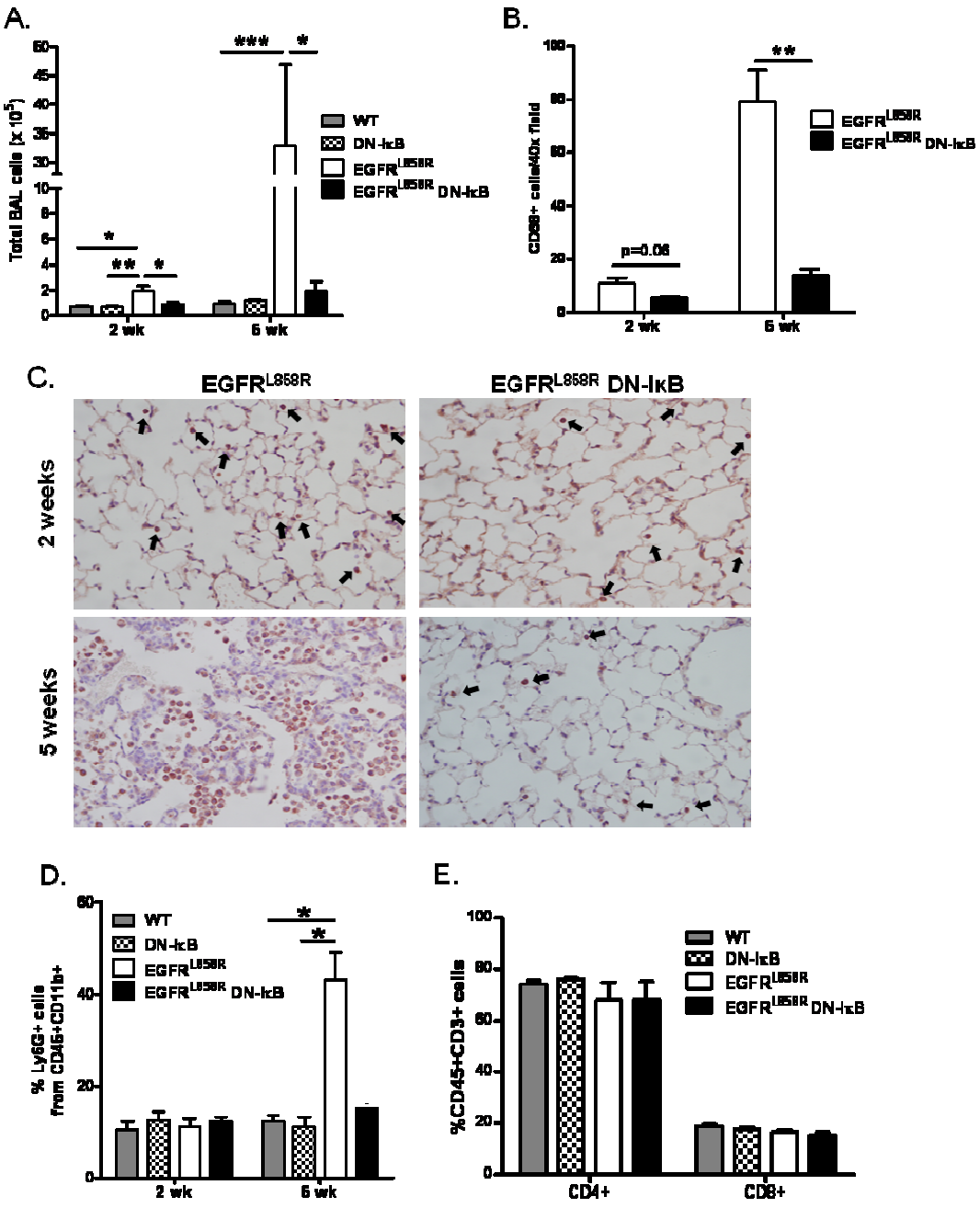

Figure 5: Inhibition of epithelial canonical NF-κB signaling decreases inflammatory cells in the lung during carcinogenesis.

(A) Total BAL inflammatory cell numbers from WT, DN-IκB, EGFR^{L858R}, and EGFR^{L858R} DN-IκB mice administered dox for 2 weeks or 5 weeks (for 2 week n=6-8/group, for 5 week n=6-14/group; *p<0.05, **p<0.01, ***p<0.001). Quantitation (B) and representative photomicrographs (40x magnification) (C) of CD68 macrophage immunostaining of lung sections from EGFR^{L858R} and EGFR^{L858R} DN-IκB mice administered dox for 2 weeks or 5 weeks (for 2 week n=4/group, for 5 week n=5/group; **p<0.01). D) Flow cytometry analysis of Ly6G+ cells from CD11b+CD45+ cells in lung single cell suspensions from WT, DN-IκB, EGFR^{L858R}, and EGFR^{L858R} DN-IκB mice administered dox for 2 weeks or 5 weeks (for 2 week n=3-4/group; for 5 week n=2-5/group; *p<0.05). (E) Flow cytometry analysis for CD4+ and CD8+ T cells using lung single cell suspensions from WT, DN-IκB, EGFR^{L858R} and EGFR^{L858R} DN-IκB mice administered dox for 2 weeks (n=3-4/group).

To determine the effect of epithelial canonical NF-κB inhibition on EGFR TKI-resistant $EGFR^{L/T}$ tumors, mice were treated with dox for 8 weeks, and tumor burden was assessed histologically. Similar to the $EGFR^{L858R}$ model, $EGFR^{L/T}$ DN-IκB mice demonstrated a dramatic reduction in lung tumor burden compared to $EGFR^{L/T}$ mice (Figure 6A, B). RT-PCR for EGFR transgene expression verified that $EGFR^{L/T}$ DN-IκB mice expressed the EGFR transgene after 8 weeks of dox administration (Figure 6C). In addition to decreased tumor burden, $EGFR^{L/T}$ DN-IκB mice had significantly fewer inflammatory cells in BAL (Figure 6D). Inflammatory cell subpopulations were analyzed on BAL cytospins as well as by CD68 staining for macrophages on lung sections from $EGFR^{L/T}$ and $EGFR^{L/T}$ DN-IκB mice, revealing a significant reduction in macrophages and neutrophils when canonical NF-κB signaling was inhibited (Figure 6E-G). These data were consistent with our findings in the $EGFR^{L858R}$ model and suggest that epithelial NF-κB signaling functions similarly in EGFR TKI-sensitive and TKI-resistant tumors.

Canonical NF-κB signaling promotes macrophage and neutrophil chemotaxis

To investigate whether epithelial canonical NF-κB inhibition affects macrophage and neutrophil recruitment to the lungs, we measured chemotaxis induced by BAL fluid or lung lysates using a modified Boyden chamber assay. Significantly more neutrophils migrated toward BAL fluid from $EGFR^{L858R}$ mice than BAL fluid from $EGFR^{L858R}$ DN-IκB mice (Figure 7A). To identify canonical NF-κB-regulated mediator(s) responsible for neutrophil chemotaxis in the setting of EGFR-mutant lung tumors, we measured mRNA expression of neutrophil chemokines by quantitative real-time PCR in lungs of mice treated with dox for 5 weeks, the time point at which we observed a significant difference in lung neutrophil numbers between $EGFR^{L858R}$ and $EGFR^{L858R}$ DN-IκB mice. KC and MIP-2 mRNA levels were reduced in $EGFR^{L858R}$ DN-IκB lungs compared to $EGFR^{L858R}$ (Figure 7B). KC and MIP-2 protein was also reduced in BAL from $EGFR^{L858R}$ DN-IκB mice (Figure 7C), suggesting that canonical NF-κB signaling promotes neutrophil migration to the lungs through regulation of CXC chemokines.

Similarly, more macrophages migrated toward lung lysates from $EGFR^{L858R}$ mice than from $EGFR^{L858R}$ DN-IκB mice (Figure 7D). By quantitative real-time PCR, we measured mRNA expression of

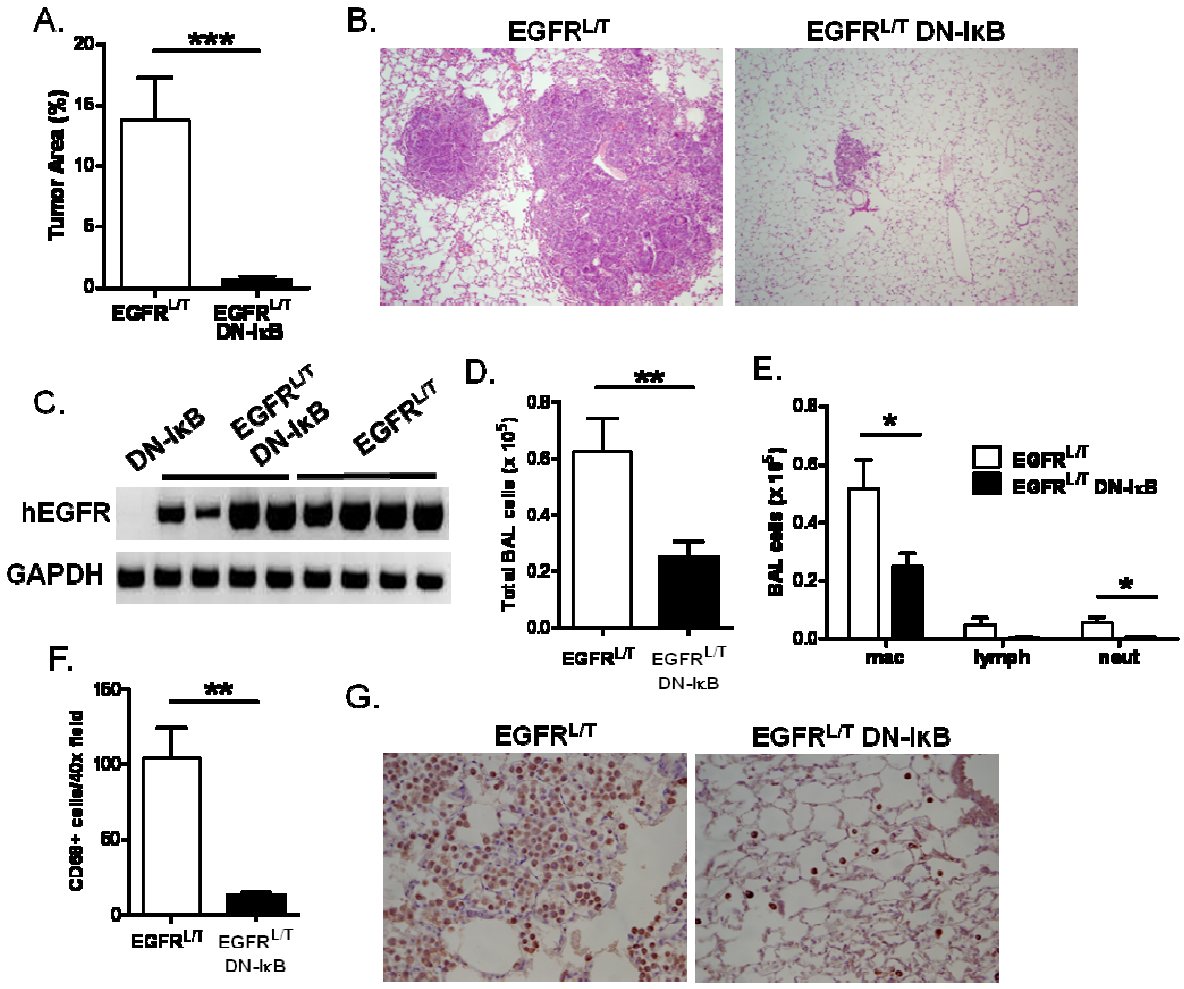

Figure 6: Canonical NF-κB inhibition reduces tumor burden and inflammatory cells in the TKI-resistant EGFR$^{L858R+T790M}$ lung carcinogenesis model.

Histological quantitation of lung tumor burden (A) and representative photomicrographs of H&E-stained lung sections (10x magnification) (B) from EGFR$^{L/T}$ and EGFR$^{L/T}$ DN-IκB mice treated with dox for 8 weeks (n=16 mice/group; ***p<0.001). (C) RT-PCR for EGFR$^{L/T}$ transgene (hEGFR) expression using mRNA isolated from lungs of EGFR$^{L/T}$ and EGFR$^{L/T}$ DN-IκB mice treated with dox for 8 weeks. Total BAL inflammatory cells (D) and BAL inflammatory cell differentials (E) for EGFR$^{L/T}$ and EGFR$^{L/T}$ DN-IκB mice treated with dox for 8 weeks (n=16 mice/group; **p<0.01, *p<0.05). Quantification (F) and representative photomicrographs (40x magnification) (G) of CD68 macrophage immunostaining of lung sections from EGFR$^{L/T}$ and EGFR$^{L/T}$ DN-IκB mice treated with dox for 8 weeks (n=6-8/group; **p<0.01).

the macrophage chemokine CCL2 and M-CSF, but neither of these factors was significantly reduced in lungs of $EGFR^{L858R}$ DN-IκB mice after 2 weeks of dox treatment (Figure 7E). To look more broadly for differences in potential macrophage chemotactic factors, we analyzed protein expression of a panel of inflammatory mediators (including known macrophage chemoattractants) in lung lysates from $EGFR^{L858R}$ and $EGFR^{L858R}$ DN-IκB mice treated with dox for 2 weeks or 5 weeks by protein array (Figure 7F and data not shown). However, we observed no significant reduction in any of these factors in $EGFR^{L858R}$ DN-IκB mice, suggesting that non-traditional or non-protein mediators may impact macrophage migration in this model.

Macrophages promote EGFR-mediated lung tumorigenesis

In both TKI-sensitive and TKI-resistant models of EGFR-mediated lung tumorigenesis, we identified increased neutrophils and macrophages in the lungs, and those inflammatory cell types were reduced in the setting of NF-κB inhibition, suggesting the importance of these cells for EGFR-driven lung cancer. Therefore, we next investigated whether neutrophils and/or macrophages contribute to EGFR-mediated tumorigenesis. To determine whether neutrophils play a role in tumorigenesis in $EGFR^{L858R}$ mice, we used Ly6G antibodies to deplete neutrophils throughout tumorigenesis. Ly6G depletion antibodies or IgG isotype control antibodies were administered by IP injection to $EGFR^{L858R}$ mice. Neutrophil depletion was verified by counting neutrophils in peripheral blood smears as well as by flow cytometry for neutrophils in lung single cell suspensions from mice on dox for 5 weeks (Figure 8A-B). Even though we observed successful neutrophil depletion, no difference in tumor burden was identified between $EGFR^{L858R}$ mice receiving Ly6G depletion antibodies and mice receiving isotype control antibodies (Figure 8C). These data indicate that neutrophils are not a critical cell type required for EGFR-mediated tumor formation in this model and suggest that neutrophils are not the primary cell type through which epithelial NF-κB signaling impacts tumorigenesis.

To test whether NF-κB–dependent recruitment of macrophages to the lungs is important for EGFR-mutant tumors, we depleted alveolar macrophages. Using a protocol that we previously developed

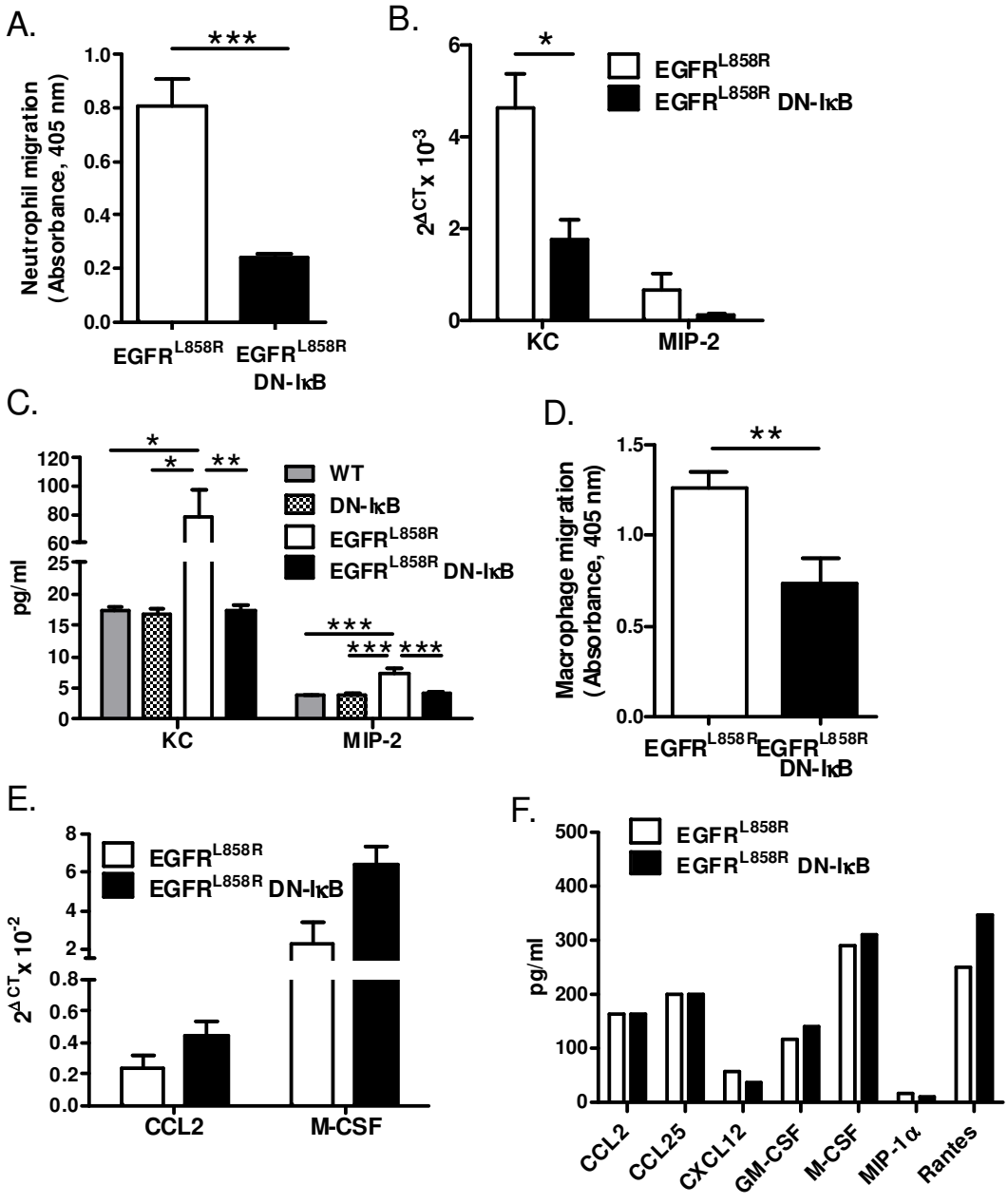

Figure 7: Epithelial canonical NF-κB signaling promotes macrophage and neutrophil migration.

(A) *In vitro* Boyden chamber chemotaxis assay for neutrophils using BAL fluid from EGFR^{L858R} and EGFR^{L858R} DN-IκB mice treated with dox for 5 weeks (n=8/group; ***p<0.001). B) Quantitative real-time PCR for KC and MIP-2 using mRNA from lungs of EGFR^{L858R} and EGFR^{L858R} DN-IκB mice administered dox for 5 weeks (n=5-9/group; *p<0.05; all EGFR^{L858R} DN-IκB MIP-2 measurements below threshold). C) KC and MIP-2 ELISA measurements using BAL fluid from WT, DN-IκB, EGFR^{L858R}, and EGFR^{L858R} DN-IκB mice treated with dox for 5 weeks (n=4-10 mice/group; *p<0.05, **p<0.01, ***p<0.001). (D) Boyden chamber chemotaxis assay for macrophages using lung lysates from EGFR^{L858R} and EGFR^{L858R} DN-IκB mice treated with dox for 5 weeks (n=5-8/group; **p<0.01). E) Quantitative real-time PCR for CCL2 and M-CSF using mRNA from lungs of EGFR^{L858R} and EGFR^{L858R} DN-IκB mice treated with dox for 2 weeks (n=4/group). (F) Select data from protein expression array for inflammatory mediators using whole lung lysates from EGFR^{L858R} and EGFR^{L858R} DN-IκB mice treated with dox for 2 weeks.

(Everhart et al., 2005; Zaynagetdinov et al., 2011a), macrophages were depleted by repeated dosing of liposomal clodronate, which causes selective macrophage apoptosis. Liposomal clodronate or control PBS liposomes were delivered IT to $EGFR^{L858R}$ mice weekly, beginning 3 days prior to starting dox treatment. CD68 immunostaining was performed on lung sections from mice treated with dox for 5 weeks, verifying macrophage depletion (Figure 8D). After 5 weeks of dox administration, tumor burden was significantly reduced in $EGFR^{L858R}$ mice administered IT liposomal clodronate when compared to mice receiving PBS liposomes (Figure 8E), indicating that recruitment of macrophages is important for EGFR-mediated tumor formation.

Discussion

These studies demonstrate that epithelial canonical NF-κB signaling promotes lung tumorigenesis, at least in part through recruitment of macrophages to the lungs. In transgenic mouse models of both EGFR TKI-sensitive and TKI-resistant lung tumorigenesis, epithelial canonical NF-κB inhibition reduced tumor burden. However, canonical NF-κB inhibition did not affect survival of EGFR-mutant airway epithelial cells or alter activation of known EGFR-mediated signaling pathways. Instead, in the settings of both TKI-sensitive and TKI-resistant lung tumors, epithelial canonical NF-κB signaling was important for recruiting inflammatory cells to the lung, namely macrophages and neutrophils. In additional studies, we observed that neutrophil depletion did not impact EGFR-mediated tumorigenesis, but macrophages contributed to tumor formation. Taken together, these data suggest that classical NF-κB signaling functions primarily in a non-cell autonomous manner to promote EGFR-mediated lung tumorigenesis.

In EGFR-mutant tumors, NF-κB signaling has been proposed as a common mechanism of TKI resistance (Bivona et al., 2011; Blakely et al., 2015; De et al., 2014; Galvani et al., 2015). De, et al. demonstrated that stimulation of NF-κB signaling *in vitro* enhanced resistance of lung cancer cells to erlotinib treatment (De et al., 2014). Furthermore, NF-κB inhibition in conjunction with erlotinib treatment has been shown to promote apoptosis of erlotinib-resistant lung cancer cells *in vitro* and reduce

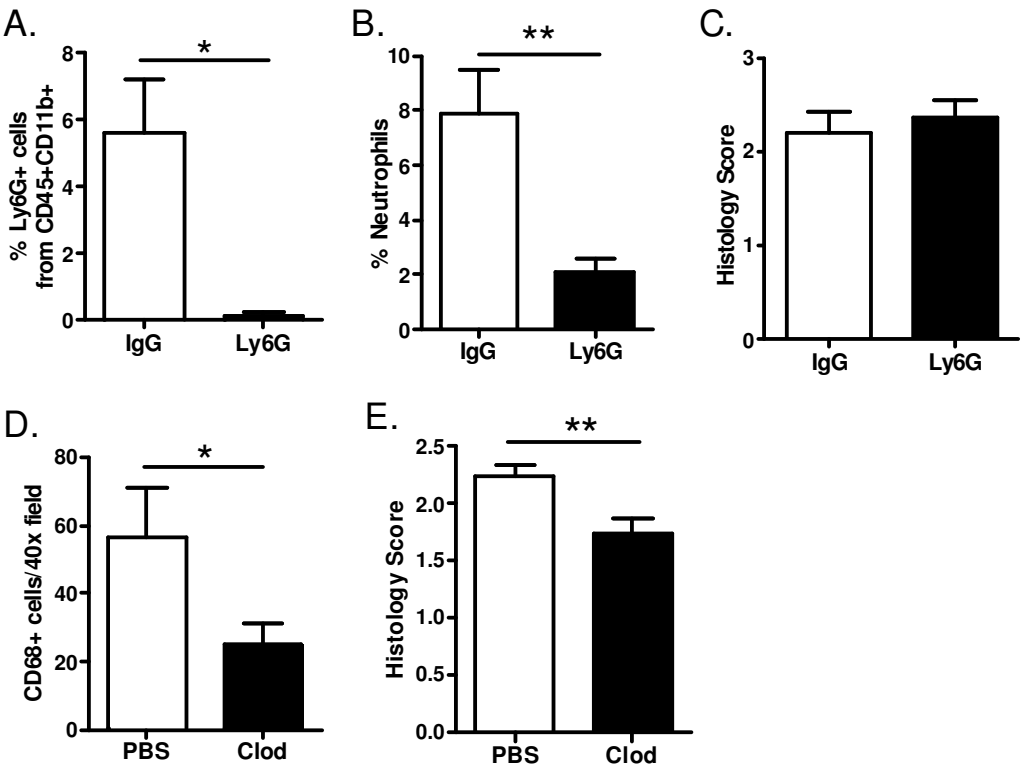

Figure 8: Macrophages promote EGFR-mediated lung tumorigenesis.
Flow cytometry analysis of lung single cell suspensions (A) (n=4/group; *p<0.05), quantification of neutrophils as a percentage of total white blood cells in peripheral blood smears (B) (n=7/group; **p<0.01), and histological analysis of tumors (C) (n=11-14/group) from $EGFR^{L858R}$ mice administered dox for 5 weeks and treated with Ly6G depletion or IgG isotype control antibodies. Quantification of CD68 macrophage immunostaining (D) (n=3-5/group; *p<0.05) and histological analysis of tumors (E) (n=12-14/group; **p<0.01) on lung sections from $EGFR^{L858R}$ mice administered dox for 5 weeks and treated with PBS or clodronate liposomes.

tumor growth in xenograft models (Bivona et al., 2011; Blakely et al., 2015). More recently, NF-κB activation was shown to drive resistance to an analog of the selective EGFR-T790M inhibitor CO-1686 in T790M mutant cells (Galvani et al., 2015). While these prior studies indicate that NF-κB signaling supports resistance of EGFR-mutant tumors to TKIs, our findings indicate that NF-κB signaling plays a broader role in EGFR-driven lung carcinogenesis.

Inflammation has been linked to cancer promotion through two pathways—the extrinsic pathway, characterized by a pre-existing inflammatory condition, and the intrinsic pathway, driven by oncogenic mutations that lead to an inflammatory response (Mantovani et al., 2008). In our transgenic mouse models, expression of oncogenic EGFR in the lungs led to a significant intrinsic inflammatory response that was dependent upon canonical NF-κB signaling. Similarly, transgenic mice with expression of oncogenic KRAS also exhibit an inflammatory influx, characterized by increased macrophages and neutrophils (Ji et al., 2006). Oncogenic KRAS has been shown to lead to activation of canonical NF-κB signaling (Bassères et al., 2010), and inhibition of canonical NF-κB signaling in KRAS-mutant tumors reduces tumor burden (Bassères et al., 2010; Meylan et al., 2009), suggesting that canonical NF-κB signaling may function similarly to promote intrinsic inflammation in both EGFR- and KRAS-mutant lung tumors.

Even though we observed no effect on tumorigenesis after neutrophil depletion, neutrophils have been shown to contribute to carcinogenesis in other contexts. Neutrophils can produce a variety of growth factors, ROS, and proteases that promote tumor angiogenesis, proliferation, and invasion (Gregory and Houghton, 2011), and NF-κB signaling in tumors has been shown to regulate expression of chemokines leading to neutrophil recruitment (Sparmann and Bar-Sagi, 2004). In human lung cancer, neutrophil influx is associated with a poor prognosis (Bellocq et al., 1998), and in a transgenic mouse model of KRAS-driven lung cancer, depletion of neutrophil elastase caused significantly fewer lung tumors due to reduced tumor cell proliferation (Houghton et al., 2010). While we saw enhanced neutrophil recruitment in our EGFR-driven lung cancer models, this increase in neutrophils was modest compared to the increase in macrophages and was only observed at later time points, suggesting that the contributions of the

neutrophils to lung tumorigenesis in this model may have been overshadowed by the pro-tumorigenic effect of the macrophage influx.

Our findings indicate that epithelial canonical NF-κB signaling recruits macrophages to promote lung carcinogenesis and suggest that therapeutic targeting of macrophages should be explored in EGFR-mutant lung cancer. Although NF-κB regulates a variety of chemokines that promote macrophage recruitment, we did not observe changes in known macrophage chemokines upon NF-κB inhibition. Although it is possible that novel protein mediators induce macrophage recruitment in our models, we speculate that non-protein mediators may account for the NF-κB-dependent influx of macrophages in mice expressing mutant EGFR. For example, eicosanoids can be potent macrophage chemoattractants, and a variety of factors involved in eicosanoid synthesis are regulated by NF-κB signaling (Haribabu et al., 2000; Osma-Garcia et al., 2015). Future studies to identify the NF-κB-regulated mechanism of macrophage recruitment in the $EGFR^{L858R}$ and $EGFR^{L/T}$ lung cancer models may reveal additional potential therapeutic targets for development of novel treatment strategies for patients with EGFR-mutant lung cancers.

CHAPTER III:

NON-CANONICAL NF-κB SIGNALING RESULTING FROM P52 EXPRESSION ENHANCES LUNG CANCER PROGRESSION THROUGH REGULATION OF CELL CYCLE GENES

Parts of this chapter were originally published in *The Journal of Immunology*. Saxon JA, Cheng D-S, Han W, Polosukhin V, McLoed AG, Richmond BW, Gleaves LA, Tanjore H, Sherrill TP, Barham W, Yull FE, Blackwell TS. 2016. p52 over-expression increases epithelial apoptosis, enhances lung injury, and reduces survival after LPS treatment. J. Immunol. 196(4) 1891-1899.

Rationale

Lung cancer is the leading cause of cancer-related death in the U.S. In 2015, an estimated 221,200 new lung cancer diagnoses are expected, representing 13 percent of all cancer diagnoses (Siegel et al., 2015). The five-year survival rate of a lung cancer diagnosis is less than 20 percent (Siegel et al., 2015), emphasizing the need for a better understanding of tumor biology in the development of new therapeutic approaches. In addition, identification of biomarkers that improve prediction of outcomes beyond the current staging system would be useful for developing new treatment strategies.

Numerous studies have demonstrated the critical role of epithelial NF-κB signaling in lung cancer (Bassères et al., 2010; Meylan et al., 2009; Stathopoulos et al., 2007). The NF-κB transcription factor family contains 5 members (p65/RelA, p52, p50, RelB, and c-Rel) and can be activated through either the canonical or non-canonical signaling pathways. Canonical pathway activation occurs when inhibitory IκBs are phosphorylated, releasing a p65/p50 heterodimer to translocate into the nucleus. Non-canonical NF-κB signaling hinges on proteolytic processing of p100 to p52, which removes an inhibitory C-terminal domain. p52 is then able to enter the nucleus, typically as a heterodimer bound to RelB. In lung tumors, increased expression of components of both the canonical and non-canonical NF-κB signaling pathways has been observed (Dimitrakopoulos et al., 2012; Tang et al., 2006). However, studies of NF-

κB in lung cancer have mainly focused on canonical pathway signaling, leaving the function of non-canonical pathway activation in lung tumors uninvestigated.

The majority of knowledge about the *in vivo* function of p100/p52 and non-canonical NF-κB signaling relates to its role in lymphoid development and hematopoietic disease. Mice with global knockout of the *Nfkb2* gene, which encodes p100, demonstrate defective dendritic cell function, B-cell maturation, T-cell responses, and secondary lymphoid organ development (Caamaño et al., 1998; Franzoso et al., 1998), presumably due to p52's role in regulating expression of chemokine genes important for normal lymphoid organogenesis (Dejardin et al., 2002). In several hematopoietic malignancies including multiple myeloma, chronic lymphocytic leukemia, and B- and T-cell cutaneous lymphomas, chromosomal translocations in the *Nfkb2* gene, which encodes p100, have been identified that truncate the C-terminus, removing the inhibitory domain (Migliazza et al., 1994; Neri et al., 1995, 1991). These truncated proteins localize in the nucleus, essentially leading to constitutively active p52 (Migliazza et al., 1994). Mice with global truncation of the *Nfkb2* gene develop enlarged lymph nodes and hyperactive T cell responses, providing some insight into the function of activated p52 in hematopoietic diseases (Ishikawa et al., 1997). However, these mice die prematurely due to significant gastric hyperplasia (Ishikawa et al., 1997), hinting that dysregulated p52 activation may play a role in epithelial cancers also.

Increased activation of p52 has been observed in lung (Dimitrakopoulos et al., 2012), breast (Cogswell et al., 2000), prostate (Lessard et al., 2005; Seo et al., 2009), and pancreatic cancer (Wharry et al., 2009). However, studies on the effects of p52 activation in cancers of epithelial origin have been limited due lack of appropriate *in vivo* models. Here, we generated a novel transgenic mouse model with inducible expression of p52 specifically in airway epithelial cells (designated CCSP-p52) to investigate a potential role for p52 in lung tumorigenesis. Together, these studies define a role for p52 in lung tumorigenesis and identify a p52-associated gene network that is highly correlated with patient prognosis.

Materials and Methods

Generation of CCSP-p52 mouse model

The p52 cFlag pcDNA3 plasmid containing C-terminal FLAG-tagged murine p52 was a gift from Stephen Smale (Addgene plasmid #20019). This plasmid was digested first with HindIII followed by SacI digestion to obtain a fragment containing the FLAG-p52. The ends of this fragment were filled in before ligation into the EcoRV site of a modified pBluescript II SK expression vector, which contains a $(tet\text{-}O)_7$-CMV promoter consisting of seven copies of the tet operator DNA-binding sequence linked to a minimal CMV promoter together with bovine growth hormone poly-adenylation sequences to ensure transcript termination. The final plasmid ($(tet\text{-}O)_7$-FLAG-p52-BGH.poly(A)) was verified by sequencing. To prevent basal leakiness, a construct expressing a tet-controlled transcriptional silencer (tTS) under control of the CCSP promoter (CCSP-tTS-hGH.poly(A)) was also included (Cheng et al., 2007; Zhu et al., 2001). The $(tet\text{-}O)_7$-FLAG-p52 microinjection fragment was excised from the plasmid by digesting with AscI, resulting in a 2.1 kb fragment. The 5 kb CCSP-tTs fragment was excised using XhoI and NotI. Both constructs were purified with the GELase Agarose Gel-Digesting Preparation kit (Epicentre) following the manufacturer's instructions. These constructs were co-injected at the Vanderbilt Transgenic Mouse/Embryonic Stem Cell Shared Resource to generate transgenic lines of FVB background mice with co-integration of both the CCSP-tTS and the $(tet\text{-}O)_7$-FLAG-p52 transgenes. Genotyping of the founder animals was performed by Southern blot, and all subsequent genotyping was performed by PCR analysis. Primers used for PCR of the $(tet\text{-}O)_7$-p52-FLAG are as follows: F: GACGCCATCCACGCTGTTTTG and R: AGGATAGGTCTTCCGGCCCTT. The product size is 322 bp. Primers used for PCR of the CCSP-tTS are as follows: F: GAGTTGGCAGCAGTTTCTCC and R: GAGCACAGCCACATCTTCAA. The product size is 472 bp. Four founder lines of CCSP-tTS/$(tet\text{-}O)_7$-FLAG-p52 mice were mated with CCSP-rtTA homozygous mice (gift from Dr. J.A. Whitsett, University of Cincinnati, Cincinnati, OH) (Tichelaar et al., 2000) to obtain triple transgenic mice, which were designated CCSP-p52. CCSP-p52

mice generated from two separate founder lines of CCSP-tTS/(tet-O)$_7$-FLAG-p52 mice were used for these studies.

Animal experiments

For urethane experiments, mice were placed on dox for 1 week prior to IP injection of urethane (1 g/kg body weight; Sigma-Aldrich) and remained on dox until euthanized. For 6 month tumor experiments, mice received weekly IP injections of urethane for 4 weeks. At sacrifice, lungs were lavaged, and total and differential BAL cell counts were determined as previously described (Stathopoulos et al., 2007; Zaynagetdinov et al., 2011b). The left lung was tied off and frozen, and the right lung was perfused and fixed by inflating with 10% neutral-buffered formalin. All animal studies were approved and conducted according to the guidelines of the Vanderbilt University Institutional Animal Care and Use Committee.

Generation of p52-overexpressing RLE-6TN cells

Rat type II alveolar epithelial cell line RLE-6TN (ATCC) was maintained at 37ºC 5% CO_2 in DMEM (Invitrogen) with 4.5 g/l glucose and 2mM L-glutamine, supplemented with 10% FBS, 100 units/ml penicillin, and 100 µg/ml streptomycin. p52 expression construct p52 cFLAG pcDNA3 and control EV cFLAG pcDNA3 were gifts from Stephen Smale (Addgene plasmids #20019 and #20011). RLE-6TN parental cells (RLE-WT) were stably transfected with p52 cFLAG pcDNA3 (RLE-p52) or empty vector cFLAG pcDNA3 (RLE-EV) using Effectene transfection reagents (Qiagen) according to the manufacturer's protocol, and G418-selected clones were pooled. To confirm transgene expression, the NE-PER Nuclear and Cytoplasmic Extraction Reagents (Thermo Scientific) were used to prepare nuclear protein from RLE-EV and RLE-p52 transfected cells that had undergone selection, and a western blot was performed and probed with antibodies as described for western blot analysis below.

Western blot analysis

Nuclear protein was prepared from lung tissue and RLE-6TN cells using the NE-PER Nuclear and Cytoplasmic Extraction Reagents (Thermo Scientific), separated by SDS-PAGE, transferred to nitrocellulose membranes, and probed using the following antibodies: FLAG (F3165, Sigma), p100/p52 (4882, Cell Signaling), p65 (C-20, Santa Cruz), p50 (C-19, Santa Cruz), RelB (C-19, Santa Cruz), cRel (C, Santa Cruz), and TBP (N-12, Santa Cruz). Immunodetection was performed using the corresponding AlexaFluor-conjugated antibodies and the Odyssey Infrared Imaging System (LI-COR Biosciences). All images were converted to grayscale.

Histology and immunostaining

After fixation, lungs were embedded in paraffin, sectioned (5 µm), and H&E-stained for histological analysis and quantification of tumor burden. Three sections were analyzed per mouse, and each section was separated by 50 µm. Tumor area was measured using Image-Pro Plus software (Media Cybernetics), and tumor number was enumerated on each section. AAH lesions and tumor histology were assessed by a pathologist blinded to the experimental groups. Tumors were classified as adenomas (clear border), MIAs (border mostly defined with one invasive edge), and adenocarcinomas (no defined border). To evaluate transgene expression in CCSP-p52 mice, 5 µm lung sections were stained with an anti-FLAG antibody (600-403-383, Rockland). To assess p100/p52 expression in human lung adenocarcinomas, immunostaining using a p100/p52 antibody (C-5, Santa Cruz) was performed on a lung adenocarcinoma tissue microarray (TMA) with 106 tumor samples (spots) from 34 patients. p100/p52 staining of tumor spots was scored by two independent readers, including a pathologist. Scoring was performed as follows: 0 = no staining; 1 = diffuse cytoplasmic staining, no nuclear staining; 2 = dark granular cytoplasmic staining, no nuclear; 3 = nuclear staining in <25% of tumor cells; 4 = nuclear staining in >25% of tumor cells. Each tumor had at least two spots on the TMA, and the mean score was calculated for each tumor based on the individual scores for each spot.

In vitro proliferation measurements

RLE-EV and RLE-p52 cells were plated in 96 well plates for viability and 5-bromo-2'-deoxyuridine (BrdU) incorporation measurements. 48 hours after plating, cells were incubated with BrdU for 4 hours, and BrdU incorporation was measured using the chemiluminescent BrdU Cell Proliferation ELISA (Roche). To ensure plating of equal numbers of cells, cell viability of RLE-EV and RLE-p52 cells was measured on the same day as a surrogate for cell number using the CellTiter-Glo Luminescent Cell Viability assay (Promega) according to the manufacturer's protocol.

Gene expression microarray analysis

The RNeasy Mini kit (Qiagen) was used to isolate whole lung mRNA from CCSP-p52 and WT mice on dox for 1 week and mice on dox for 1 week 48 hours after IT LPS administration. To minimize the effects of mouse-to-mouse-variability, RNA was pooled from 3 mice for each sample, resulting in a total of 8 samples (2 WT dox only, 2 WT with LPS, 2 CCSP-p52 dox only, 2 CCSP-p52 with LPS). RNA quality control, hybridization to the Affymetrix Mouse Gene 1.0 ST array, and array scanning were performed by the Vanderbilt Technologies for Advanced Genomics (VANTAGE) Core. Expression data have been deposited in Gene Expression Omnibus (Accession # GSE71648).

The Robust Multichip Average method (Bolstad et al., 2003) implemented in R package "oligo" (v1.28.3) (Carvalho and Irizarry, 2010) was employed to normalize imported raw data. Probe sets interrogating control, unmapped, or intron sequences were ignored, leaving 79% of probe sets for a differential expression analysis. Linear models and empirical Bayes methods implemented in R package "limma" (v3.20.8) (Smyth, 2005) were applied to estimate log fold changes (FCs) and p-values for the p52-vs-WT effect. Since samples with and without LPS stimulation were processed and microarray profiled at the same time, we assumed the random data variations were similar across all samples and built a linear model across the eight samples accounting for both p52 and LPS experimental factors (Smyth, 2004). The coefficient (estimated logFC) and p-value associated with the p52 factor were

retrieved for the selection of differentially expressed genes. When selecting top-ranking p52-induced genes, only probe sets mapping to known genes and having positive expression changes were considered.

Quantitative PCR

Quantitative real-time PCR was performed using Sybr Green PCR Master Mix (Applied Biosystems) and the following primer sets: Ccna2 F: AAGAGAATGTCAACCCCGAAAAA; R: ACCCGTCGAGTCTTGAGCTT (PrimerBank ID: 161353443c1), Top2a F: CAACTGGAACATATACTGCTCCG; R: GGGTCCCTTTGTTTGTTATCAGC (PrimerBank ID: 6755849a1), Ube2c F: CTCCGCCTTCCCTGAGTCA; R: GGTGCGTTGTAAGGGTAGCC (PrimerBank ID 21312888a1) and GAPDH (F: TGAGGACCAGGTTGTCTCCT R: CCCTGTTGCTGTAGCCGTAT) (Spandidos et al., 2010, 2008; Wang and Seed, 2003). Expression values were normalized to GAPDH using the ΔCT method.

Human lung cancer expression data analysis

Raw expression data for 513 lung adenocarcinoma patient samples, generated by The Cancer Genome Atlas (TCGA) project, were accessed from the ICGC data portal (https://dcc.icgc.org/; release 17). The raw RSEM values (Li and Dewey, 2011) were multiplied by 10^6 to normalized values of Transcripts Per Million. Of these 513 samples, matched tumor samples and paracancerous normal samples were available for 54 patients. A paired t-test was performed for each gene, and the resultant p-values were adjusted to false discovery rates (FDRs) using the Benjamini-Hochberg method (Benjamini and Hochberg, 1995).

Of the 513 lung adenocarcinoma samples, 437 primary lung adenocarcinoma samples had accompanying survival outcome data. In each survival analysis, samples were divided into two groups of equal sizes (termed high-expression and low-expression groups) by considering the collective expression of p52-associated genes. R package “survival” (v2.37-7) (Therneau and Grambsch, 2000) was employed

to conduct survival analyses. In survival analyses, survival time values were truncated to 5 years (1825 days) to reflect 5 year survival rates.

Gene functional analysis

Functions enriched within p52 associated genes were identified through a hypergeometric test with respect to Gene Ontology (GO) (Ashburner et al., 2000) terms, using R package GOstats (v1.7.4) (Falcon and Gentleman, 2007). For each GO term, genes from the reference set of whole human genome protein-coding genes and the concerned set of p52 associated genes were respectively identified, and a p-value indicative of enrichment significance was calculated and further adjusted to the FDR using the Benjamini-Hochberg method (Benjamini and Hochberg, 1995). Resultant GO terms were pruned to least common ancestors according to the Biological Process topology.

From Human Protein Reference Database (v9) (Keshava Prasad et al., 2009), a connected protein interaction network was derived that comprised 9,218 nodes and 36,728 edges. p52 associated genes were mapped to this Human Protein Reference Database network, and then the Steiner tree algorithm (Klein and Ravi, 1995) was implemented to retrieve the most parsimonious subnetwork that joined together the terminal genes.

Statistics

Unpaired student t-tests were performed for comparisons between two groups. Values are presented as the mean ± SEM, and $p<0.05$ was considered statistically significant. Data were analyzed using GraphPad Prism 5.0 software (GraphPad Software, Inc.).

Results

p100/p52 expression is prevalent in human lung adenocarcinoma tumors

To examine the distribution of p100/p52 expression in human lung adenocarcinoma tumors, we

performed p100/p52 immunostaining on a lung adenocarcinoma TMA (Figure 9A). After scoring each tumor sample on a 0 to 4 point scale based on the intensity and the localization of p100/p52 staining, we found p100/p52 expression in all lung adenocarcinomas tested (34/34) (Figure 9B). In addition, 47% (16/34) of tumors had mean scores >2, indicating some degree of nuclear staining for p52. In contrast, minimal p100/p52 expression was observed in normal lung parenchyma (Figure 9A). Together, these observations suggest that p100/p52 expression and p52 activation are frequent phenomena in lung adenocarcinoma tumors.

Construction of transgenic mice with inducible expression of p52 in airway epithelium

In order to investigate the role of p52 activation in lung cancer, we developed a novel mouse model of p52 expression in the airway epithelium using the tet-on system, placing a C-terminal FLAG-tagged p52 under the control of a $(tet\text{-}O)_7$-CMV promoter. Four founder lines were generated and mated to transgenic mice expressing rtTA under the control of the airway epithelial-specific CCSP promoter, generating mice designated CCSP-p52.

To test the induction of p52 expression, CCSP-p52 mice were administered dox in drinking water (2 g/l) for one week. High levels of FLAG-p52 expression were detected in two lines of CCSP-p52 mice by western blotting of lung nuclear protein (Figure 10A), demonstrating successful induction of FLAG-p52 expression and translocation of transgenic p52 into the nucleus. FLAG-p52 expression was also detectable in CCSP-p52 mice administered dox for one month (data not shown). No leaky FLAG-p52 expression was detected in other organs after dox treatment or in the lungs in the absence of dox (data not shown). Long term dox treatment for 6 months resulted in sustained transgene expression (Figure 10B). FLAG immunostaining demonstrated FLAG-p52 expression in airway epithelium (Figure 10C). Together, these data show that CCSP-p52 mice administered dox express p52 in airway epithelium and that transgene expression results in nuclear p52 accumulation.

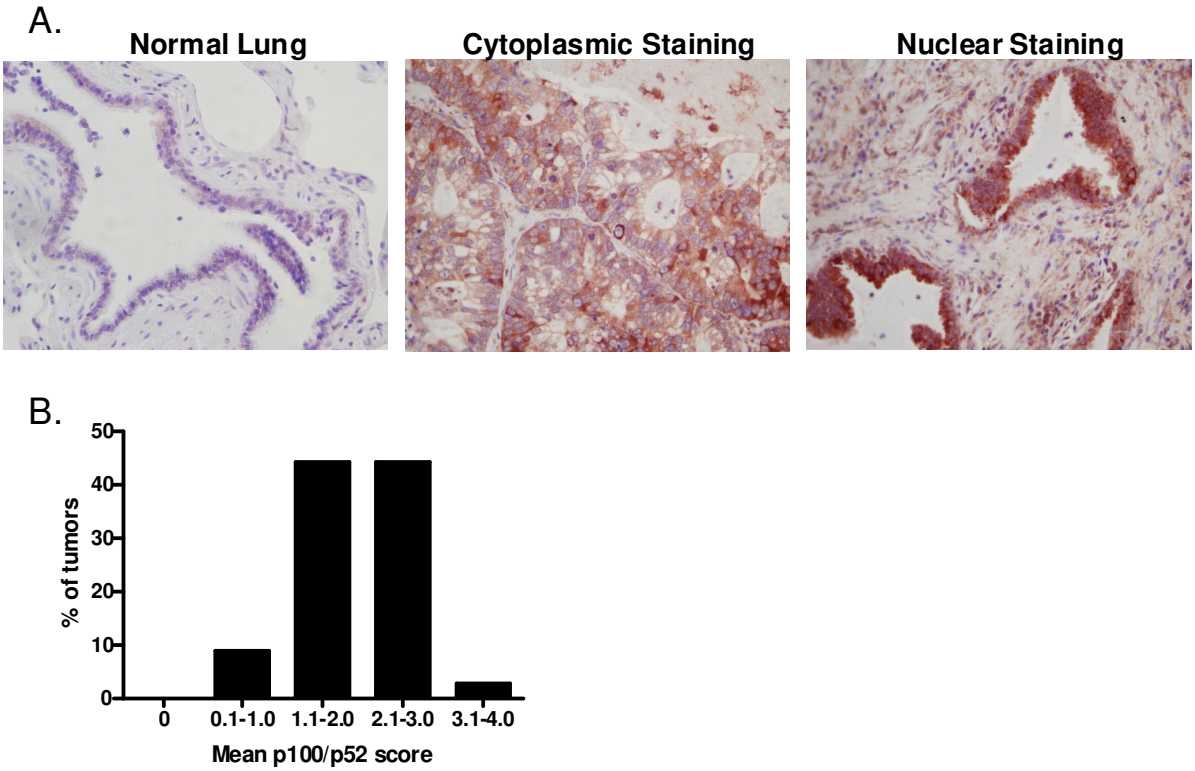

Figure 9: p100/p52 expression is present in human lung adenocarcinomas.
A) Representative images of p100/p52 immunostaining of lung adenocarcinoma and normal lung tissue (40x magnification). B) Distribution of p100/p52 immunostaining on a tumor tissue microarray (TMA) from 106 human lung adenocarcinoma samples obtained from 34 patients. Tumor spots were scored as follows: 0 = no staining; 1 = diffuse cytoplasmic staining, no nuclear staining; 2 = dark granular cytoplasmic staining, no nuclear; 3 = nuclear staining in <25% of tumor cells; 4 = nuclear staining in >25% of tumor cells. Each tumor had at least two spots on the TMA, and the mean score was calculated for each tumor based on the individual score for each spot.

p52 over-expression in airway epithelium does not significantly alter inflammatory signaling

We investigated whether p52 over-expression *in vivo* results in an inflammatory phenotype similar to canonical NF-κB pathway activation (Cheng et al., 2007). However, no significant difference in inflammatory cells was observed in lungs of CCSP-p52 mice compared to WT mice, and mice exhibited normal lung histology after dox treatment for 1 week, 1 month, or 6 months (Figure 10E, F). We also measured activation of other NF-κB family members by western blot using lung nuclear protein extracts from mice on dox for 1 week. As shown in Figure 10D, no difference was found in activation of other NF-κB family members. These data suggest that p52 over-expression in epithelial cells alone does not alter inflammatory signaling or inflammatory cell recruitment.

CCSP-p52 mice develop an increased tumor burden and more advanced lesions after urethane injection

In order to investigate the effect of p52 expression during lung tumorigenesis, we induced tumors in CCSP-p52 mice using the lung carcinogen urethane (ethyl carbamate), which causes tumors primarily through KRAS mutations (You et al., 1989) and, in FVB background mice, induces a mild inflammatory response (Stathopoulos et al., 2007). We first examined the effects of p52 over-expression on urethane-induced inflammation and AAH lesion formation. For these short-term experiments, CCSP-p52 and WT mice on dox for one week received a single IP injection of urethane (1 g/kg) and remained on dox until euthanized. Total inflammatory cell numbers in BAL were counted at 10 days, 21 days (3 weeks), and 42 days (6 weeks) after urethane injection. No differences were observed between CCSP-p52 and WT mice at any time point (Figure 11A). In addition, no differences in AAH lesion numbers were detected at 6 weeks post-urethane (Figure 11B).

To look at the later stages of tumor formation, CCSP-p52 and WT mice on dox for one week received a weekly IP urethane injection for 4 weeks and remained on dox until sacrifice 6 months after the first urethane injection. Lung tumor dimensions were measured, and lung tumors enumerated on lung sections, revealing a significant increase in tumor number and tumor size in CCSP-p52 lungs compared to

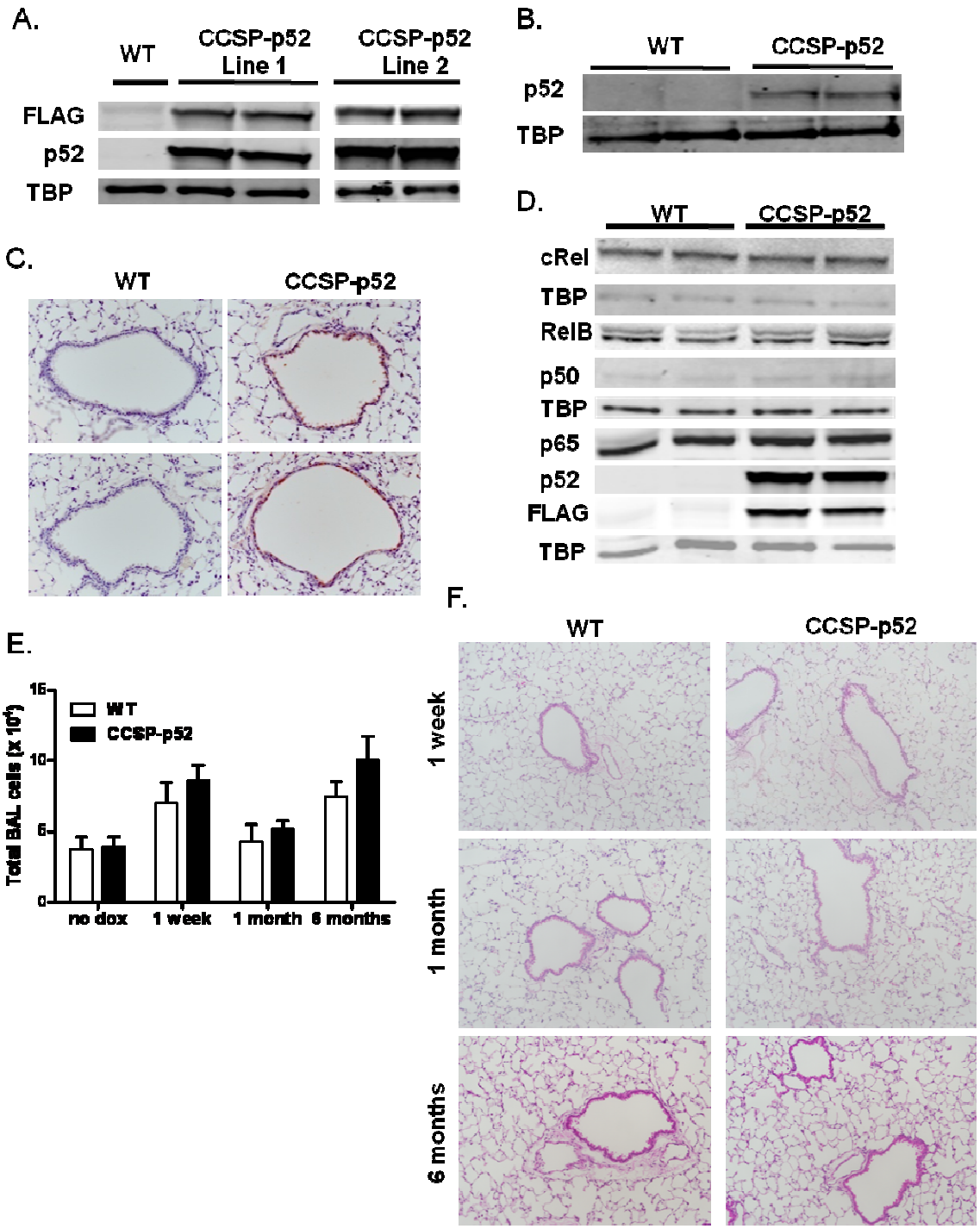

Figure 10: Characterization of a novel transgenic mouse model of lung epithelial p52 expression.

Western blot demonstrating FLAG-tagged p52 transgene expression in lung nuclear protein from WT and CCSP-p52 mice on dox for A) 1 week and B) 6 months. C) FLAG immunostaining of lung sections from WT and CCSP-p52 mice on dox for 1 week (20x magnification). D) Western blots for NF-κB family members using lung nuclear protein from mice on dox for 1 week. TBP was probed as a loading control for nuclear protein. E) Total BAL inflammatory cell numbers and F) representative photomicrographs of H&E-stained lung sections (40x magnification) from WT and CCSP-p52 mice (for no dox and 1 month n=3-7/group, for 1 week n=10-13/group, for 6 month n = 8/group).

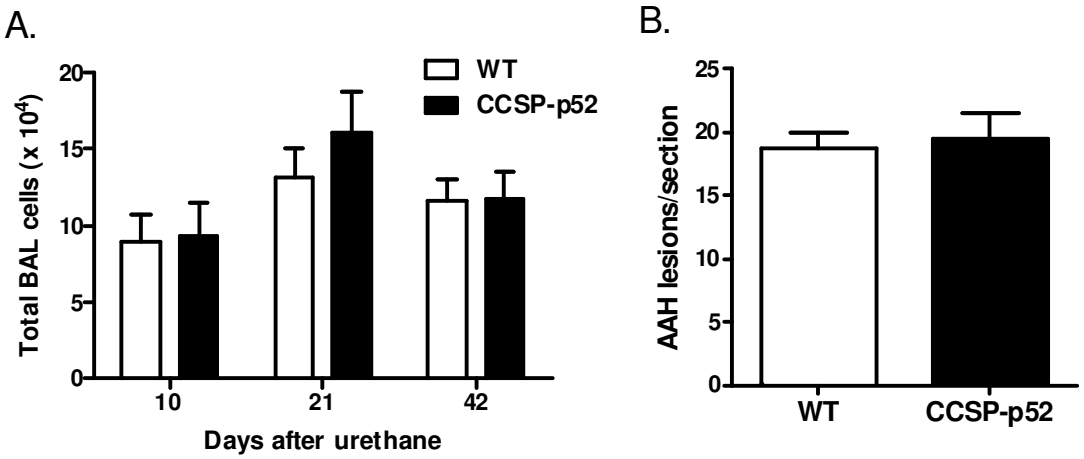

Figure 11: p52 expression does not affect urethane-induced inflammatory cell recruitment or formation of AAH lesions.

A) Total inflammatory cells in BALs from WT and CCSP-p52 mice 10 days, 21 days (3 weeks), and 42 days (6 weeks) after urethane injection (10 and 21 day n=7-8 mice/group; 42 day n=22-24 mice/group). B) Average number of AAH lesions counted on lung sections from WT and CCSP-p52 mice 6 weeks after urethane (n=13-16 mice/group).

WT (Figure 12A, B). We further analyzed these tumors by histology, classifying tumors as adenomas, MIAs, or adenocarcinomas. Compared to WT mice, CCSP-p52 mice had an increased proportion of more advanced lesions (MIAs and adenocarcinomas, $p<0.05$) (Figure 12C, D). Taken together, these studies demonstrate that p52 expression does play an important role in lung tumor formation and contributes directly to increased tumor burden and enhanced tumor progression.

p52 expression enhances proliferation through regulation of cell cycle genes

To understand the mechanism by which p52 expression augments tumorigenesis, we performed microarray gene expression analysis using mRNA isolated from lungs of CCSP-p52 and WT mice on dox for 1 week. Genes were ranked based on the log fold change (logFC) of expression between WT and CCSP-p52 mice using a cut off of 0.41 (approximately 30% increase in gene expression in CCSP-p52 mouse lungs) (Figure 13A). To evaluate the potential relevance of p52-regulated genes in human lung tumors, we focused only on genes that had known human homologs and were present in The Cancer Genome Atlas (TCGA) expression data from lung adenocarcinoma patients. Using these criteria, a total of 71 genes associated with increased p52 expression were identified (Figure 13A, B; Table 1). Quantitative PCR was performed to validate increased expression of selected genes from the 71 gene list in CCSP-p52 lungs (Figure 13C-E). To elucidate gene functions, we identified biological processes that were enriched in the p52-associated gene set using a Gene Ontology (GO) analysis. Applying a false discovery rate (FDR) of 0.001, we found that p52-associated genes were over-represented in processes related to cell cycle progression (Table 2), suggesting that p52 regulates expression of genes involved in proliferation.

To validate this finding, we generated lung epithelial cells with stable p52 over-expression using the RLE-6TN rat lung epithelial cell line (designated RLE-p52). p52 over-expression and nuclear localization in these cells was confirmed by western blotting of nuclear protein (Figure 14A). We found that BrdU incorporation was enhanced in RLE-p52 cells compared to empty vector (RLE-EV) cells (Figure 14B), indicating that p52 stimulates proliferation of lung epithelial cells, thus supporting our microarray findings.

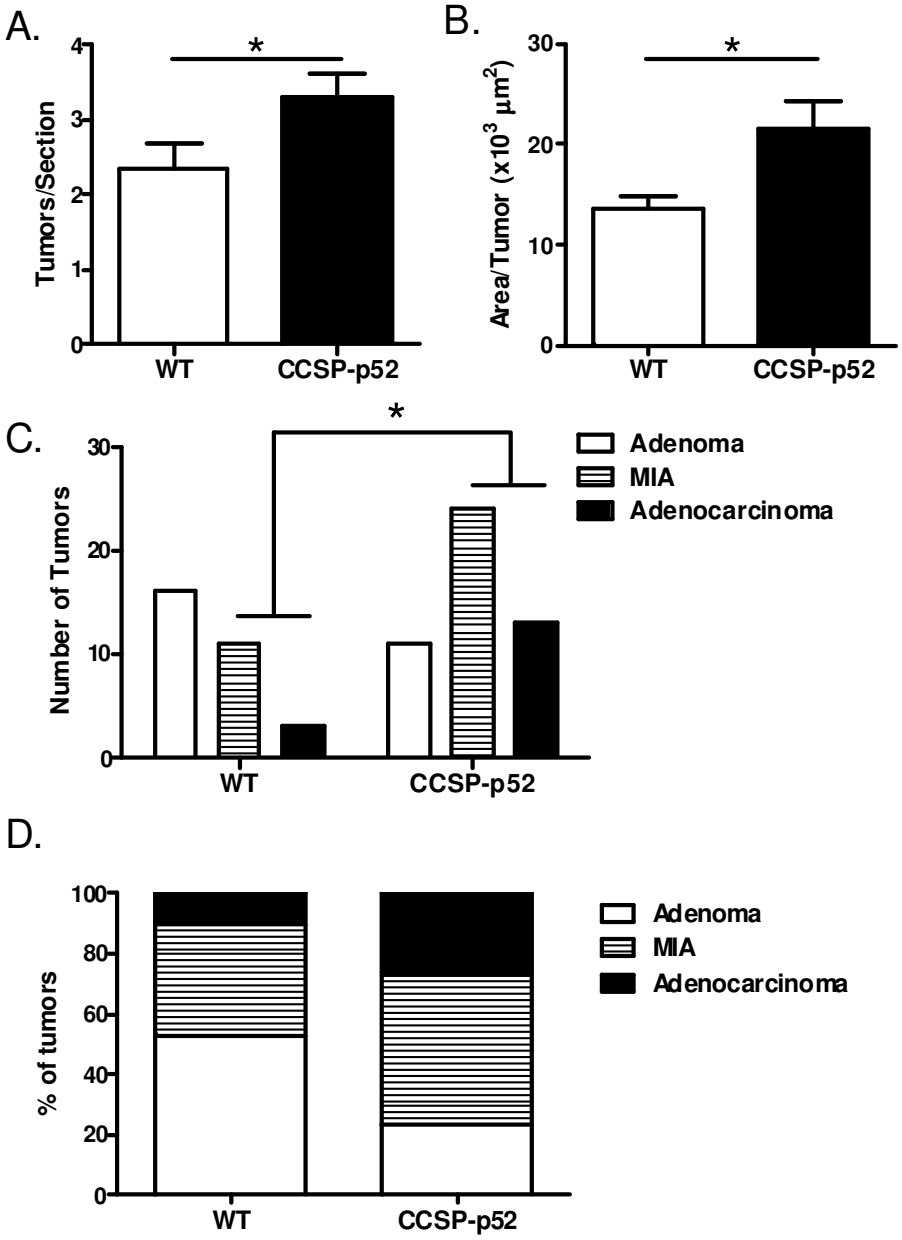

Figure 12: p52 over-expression results in increased tumor number, size, and progression.

A) Average tumor number per lung section and B) average tumor area from WT and CCSP-p52 mice 6 months after urethane injection (3 sections/mouse; n=13-14 mice/group;*p<0.05 compared to WT mice.). C) Number and D) proportion of lung tumors classified as adenomas, minimally invasive adenocarcinomas (MIA), or adenocarcinomas (n=13-14 mice/group; *p<0.05 comparing total number of advanced lesions [MIAs and adenocarcinomas] between CCSP-p52 and WT mice).

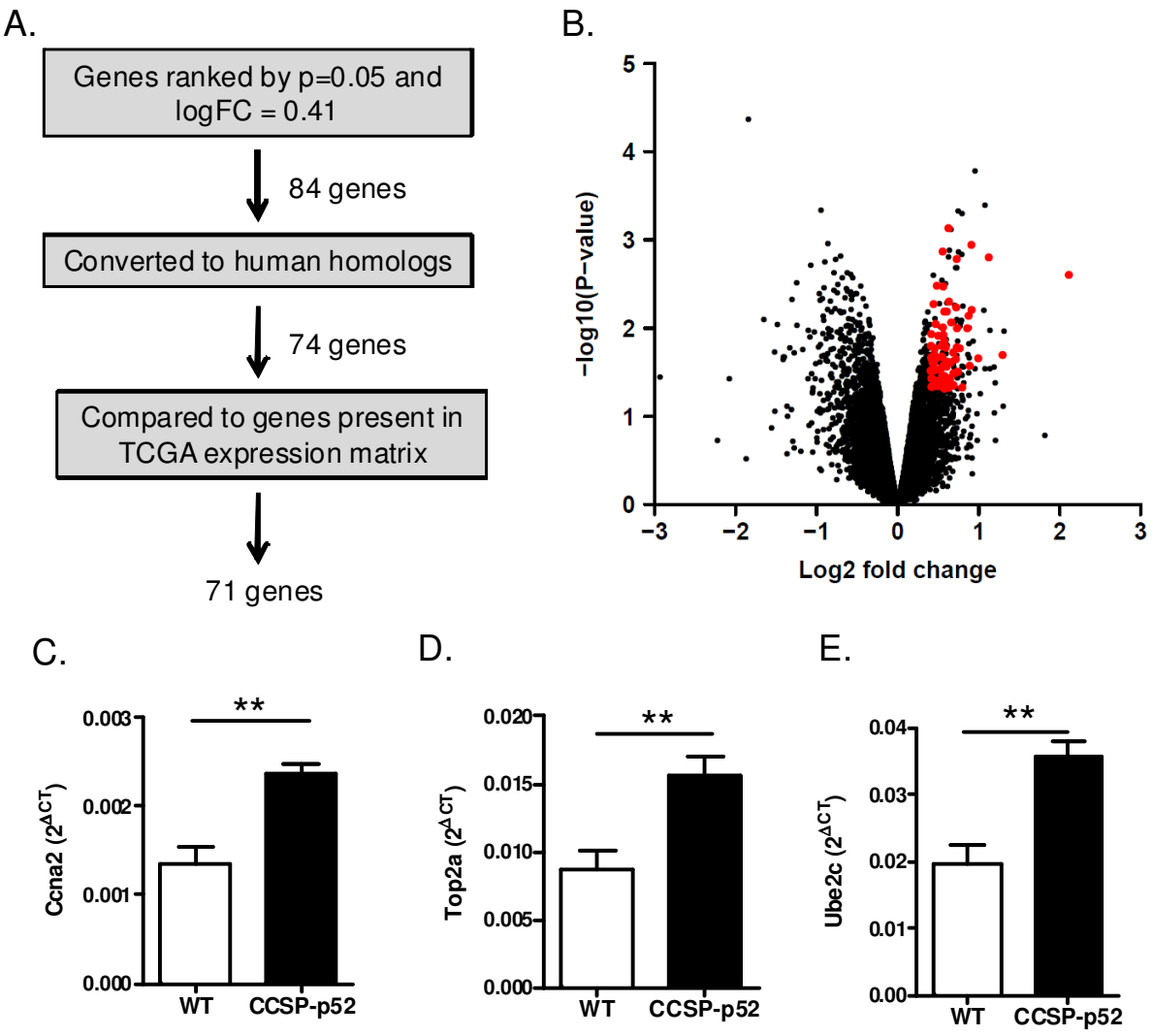

Figure 13: Identification of p52-regulated genes by microarray analysis.
A) Schematic of process used to identify p52-regulated genes from microarray data generated from pooled mRNA samples from lungs of WT and CCSP-p52 mice on dox for 1 week (n=4/group). B) Volcano plot of log fold changes and differential expression p-values comparing CCSP-p52 mice to WT. Black dots represent all genes in the expression data matrix. Red dots represent 71 genes identified for further analysis. C-E) Expression microarray data validation by quantitative PCR of identified p52-regulated genes *Ccna2* (C), *Top2a* (D), and *Ube2c* (E) measured in whole lung RNA from WT and CCSP-p52 mice on dox for 1 week (n=6 mice/group; *p<0.05 compared to WT).

Table 1: Log fold change and p-value of 71 p52-regulated genes in CCSP-p52 mice versus WT and log fold change and q-value in human paired lung adenocarcinoma versus normal samples.

Gene	CCSP-p52 vs. WT		tumor vs. normal	
(Human Homolog)	logFC	p-value	logFC	q-value
KIF20A	0.605	0.027	3.810	2.43E-18
EXO1	0.502	0.012	3.977	2.80E-18
UBE2C	0.912	0.001	3.995	2.89E-18
NUF2	0.730	0.017	4.153	9.18E-18
TOP2A	0.874	0.007	4.097	9.57E-18
IQGAP3	0.634	0.005	3.987	9.97E-18
KIF2C	0.577	0.044	4.027	2.80E-17
CEP55	0.652	0.025	3.444	7.76E-17
CDC20	0.574	0.014	4.057	9.43E-17
RRM2	0.572	0.041	3.409	1.30E-16
UHRF1	0.528	0.029	3.807	1.45E-16
HELLS	0.731	0.010	3.062	2.08E-16
SPAG5	0.621	0.040	3.267	2.85E-16
CDCA8	0.594	0.017	3.257	3.37E-16
CENPF	0.570	0.015	3.605	9.01E-16
KIF11	0.767	0.017	2.878	2.17E-15
CKAP2L	0.576	0.048	3.414	2.71E-15
ASPM	0.456	0.020	3.867	3.81E-15
ECT2	1.125	0.002	2.158	4.92E-15
ESCO2	0.647	0.037	2.914	6.14E-15
PBK	0.729	0.002	3.765	9.37E-15
AURKB	0.574	0.026	3.625	2.29E-14
CCNA2	0.860	0.010	3.049	2.37E-14
KIF18B	0.611	0.024	3.795	3.33E-14
CDCA2	0.517	0.045	3.213	8.41E-14
RAD51	0.560	0.010	2.374	7.14E-13
MCM6	0.577	0.006	1.623	4.45E-12
GEMIN6	0.443	0.005	1.032	7.74E-12
MCM2	0.469	0.022	2.027	2.04E-11
CCNE2	0.685	0.019	2.299	2.97E-11
SGOL2	0.480	0.046	1.676	1.04E-09
DTL	0.723	0.006	2.348	2.99E-08
PTGDS	0.627	0.001	-1.997	3.47E-08
RACGAP1	0.535	0.029	1.527	6.13E-08
MAL	0.564	0.003	-1.657	2.08E-05
BRCA1	0.447	0.028	1.248	4.48E-05
CFTR	0.914	0.006	-2.648	8.57E-05
KLF10	0.469	0.040	-0.864	1.31E-04
PSRC1	0.460	0.030	1.290	4.91E-04
HSPA1B	0.997	0.022	0.663	1.59E-03
ANGPTL4	0.660	0.009	1.466	0.012
POLE	0.542	0.021	0.808	0.028
GPX2	0.890	0.027	2.644	0.464

HSPA1A	0.997	0.022	0.473	1.00
MOXD1	0.418	0.047	0.671	1.00
CCDC18	0.411	0.016	0.712	1.00
CRYGN	0.421	0.037	282.976	1.00
MAGEB1	0.425	0.023	193.612	1.00
LCN2	0.585	0.036	1.387	1.00
HSPH1	0.689	0.033	0.379	1.00
PAPPA2	0.608	0.007	-176.187	1.00
CTNND2	0.547	0.035	-126.328	1.00
CDKN1A	0.432	0.025	-0.415	1.00
CYP2C8	0.417	0.022	-106.253	1.00
MAT1A	0.409	0.031	0.815	1.00
NFKB2	0.720	0.022	0.279	1.00
GRIN2A	0.416	0.012	-70.563	1.00
HIST1H2AA	0.545	0.016	52.794	1.00
TNIP3	2.112	0.003	-0.598	1.00
AREG	0.565	0.012	-0.599	1.00
DIAPH3	0.441	0.025	0.303	1.00
ADAMTS9	0.564	0.040	-0.261	1.00
YBX2	0.556	0.001	91.762	1.00
ATF7IP2	0.443	0.025	0.167	1.00
SLC26A4	1.295	0.020	0.262	1.00
GIF	0.485	0.003	35.537	1.00
EPHA7	0.573	0.035	-17.780	1.00
TNFSF9	0.796	0.047	0.093	1.00
ELOVL7	0.455	0.017	-0.075	1.00
RNASE2	0.742	0.031	1.143	1.00
OR4K1	0.471	0.009	0.070	1.00

Table 2: GO analysis of p52 regulated genes (FDR=0.001).

Gene Ontology term (Biological Process)	Reference set size	Expected Count	Observed count	Adjusted p-value[a]
Cell cycle checkpoint	230	0.98	9	2.59E-05
Mitotic cell cycle phase transition	443	1.88	11	8.83E-05
DNA unwinding involved in DNA replication	8	0.03	3	1.39E-04
Regulation of cell division	221	0.94	8	1.39E-04
Regulation of attachment of spindle microtubules to kinetochore	9	0.04	3	1.81E-04
DNA replication initiation	29	0.12	4	1.88E-04
Regulation of cell cycle process	435	1.85	10	3.68E-04
Chromosome organization	765	3.25	13	4.04E-04
Spindle assembly involved in mitosis	15	0.06	3	7.44E-04

[a]p-values have been adjusted using the Benjamini-Hochberg method.

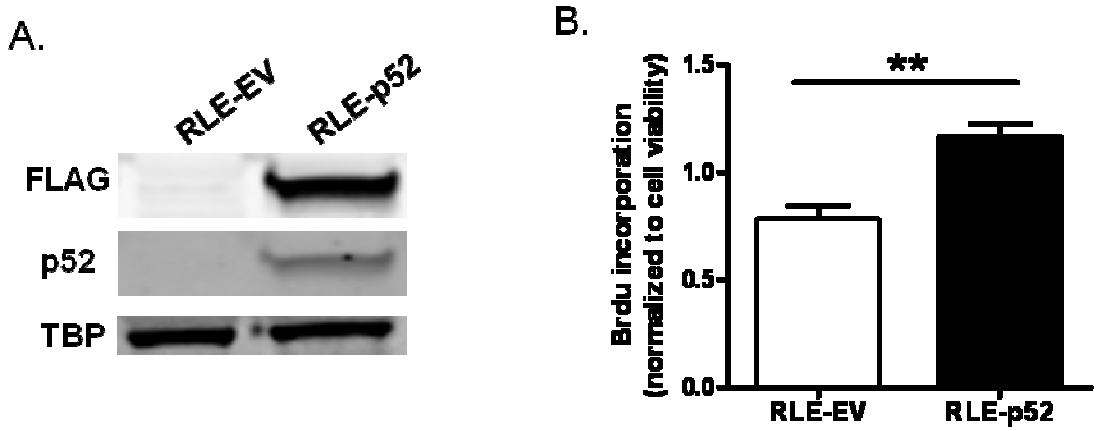

Figure 14: p52 promotes proliferation *in vitro*.
A) Western blot for p52 and FLAG using nuclear lysates from RLE-6TN cells stably transfected with a p52 expression vector (RLE-p52) or control empty vector (RLE-EV). TBP was used as a loading control. B) Quantification of BrdU incorporation of RLE-p52 and RLE-WT cells, normalized to total viable cells (**p<0.01 compared to RLE-EV).

Expression of p52-regulated genes predicts prognosis of lung cancer patients

To investigate the relevance of p52 expression in human lung cancer, we examined the expression of the 71 identified p52-regulated genes in matched tumor and normal samples. A differential expression test using a paired t-test was performed for each gene in paired tumor and normal samples from 54 lung adenocarcinoma patients available in the TCGA database. Up-regulated genes were defined as having both a logFC>1 and FDR<0.01. From the set of 20,501 genes, 1,274 up-regulated genes (6.2%) were identified in tumors compared to matched normal samples (Table 3). Of the 71 p52-regulated genes, 35 were up-regulated in tumors (49.3%), indicating a significant over-representation of p52-regulated genes in tumor samples compared to normal (hypergeometric test $p=6.0x10^{-25}$) (Table 1, Table 3, Figure 15) and suggesting that p52 is important in human lung tumors.

Since we observed more advanced tumors in urethane-treated CCSP-p52 mice, we wondered whether increased p52 expression would correlate with a worse prognosis in lung cancer patients. Therefore, we investigated the relationship between increased expression of p52-associated genes and patient outcomes using tumor expression data and clinical information from the TCGA dataset. 437 primary lung adenocarcinoma samples were divided into two equal groups based on the collective expression level of the 71 p52-associated genes by summing expression from all 71 genes (Table 4). Kaplan-Meier survival analysis revealed that patients with high expression of p52-associated genes had a significantly worse prognosis (log-rank test p=0.004) (Figure 16A). To validate this analysis, we divided patients by a second method into two equal groups. For the second method, sample division was based on summed "votes" from the 71 genes, where one gene counted as a vote for one sample if its expression in the sample was higher than the median expression level for this gene across samples (thus preventing a tumor sample with only a few highly-expressed genes from being placed in the "high expression group"). Using this method, Kaplan-Meier survival analysis again revealed that patients with high expression of p52-associated genes had significantly worse outcomes (log-rank test p=0.021) (Figure 16B). Furthermore, survival analysis of only Stage I patients revealed that patients with high expression of p52-associated genes still had a significantly worse prognosis (log-rank test p=0.036) (Figure 16C). Together,

Table 3: Over-representation of p52-associated genes in up-regulated genes identified in human lung adenocarcinomas tumor samples compared to matched normal controls.

	All genes	Significantly up-regulated genes[a]	p-value of over-representation
All genes (from TCGA)	20,501	1,274	6.0E-25
p52 genes	71	35	

[a]Up-regulated genes defined as logFC > 1 and FDR <0.01.

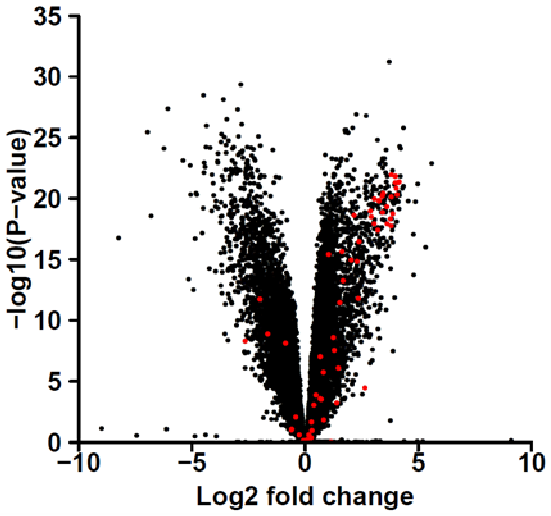

Figure 15: p52-associated genes are up-regulated in human lung adenocarcinoma tumor samples.
Volcano plot of log fold changes and differential expression p-values of tumor versus normal samples. Black dots represent all genes in the expression data matrix. Red dots represent p52-associated genes.

Table 4: Division of Stage I-IV lung adenocarcinoma patients based on summed expression of p52-associated genes.

	N	High expression group	Low expression group
Stage 1 patients	235	100	135
Stage 2 patients	103	63	40
Stage 3 patients	75	40	35
Stage 4 patients	23	14	9
Total	437	218[a]	219

[a]One sample in the high expression group had data for survival and expression but no stage information. This sample was included in overall analysis but not in stage-specific analysis.

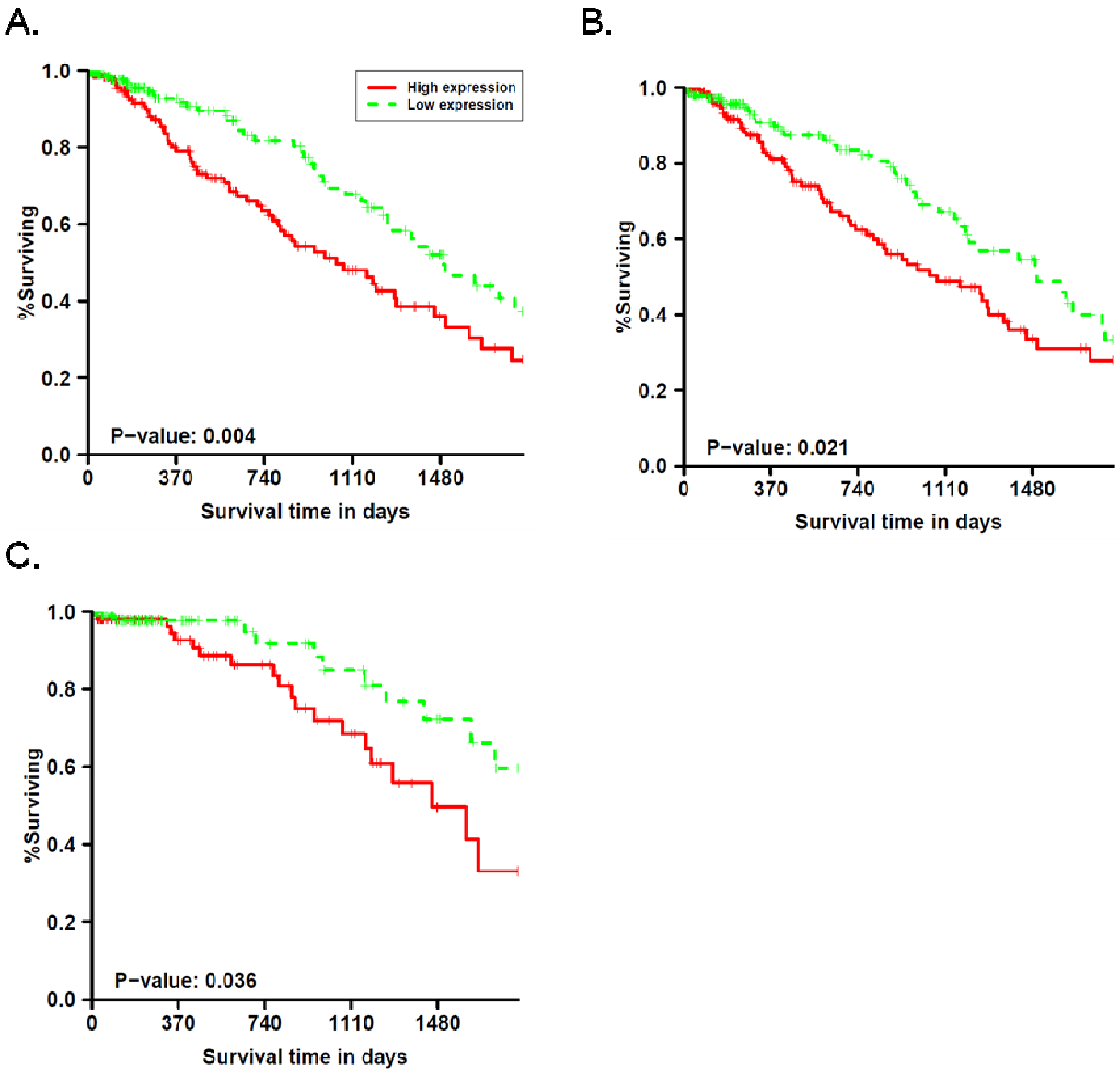

Figure 16: Expression of p52-associated genes correlates with prognosis of lung cancer patients.

Kaplan-Meier survival curves of overall patient survival data based on (A) summed expression or (B) on expression "votes"of p52-associated genes in tumors (log-rank test, p=0.004 for summed expression; p=0.021 for expression "votes"). C) Kaplan-Meier survival curve of Stage I patient survival data based on summed expression of p52-associated genes in tumors (log-rank test p=0.036).

these data suggest that expression of p52-associated genes in tumors of lung cancer patients leads to shorter survival and can be used to predict patient outcome in early stage lung cancer patients.

Since the GO analysis suggested that p52 regulates a number of genes that have highly related functions, we extracted a protein subnetwork connecting the p52-associated genes from a human protein-protein interaction network. The 35 p52-associated genes identified in tumor versus normal samples were used to generate a network consisting of genes from the p52-associated gene list as well as 13 imputed mediator genes (Figure 17A). To test the strength of this protein interaction network, a survival analysis was performed based only on expression of the 13 imputed mediator genes. High expression of the imputed genes also correlated with shorter survival (log-rank test p=0.047 by expression summation, p=0.097 by votes) (Figure 17B, C), supporting the strength of this p52-derived interaction network in predicting patient prognosis.

Discussion

These studies provide the first evidence of the involvement of p52 in lung cancer, identifying p52 as a novel mediator of lung cancer progression through regulation of cell cycle genes. For these studies, we generated a novel transgenic mouse model that enables expression of the NF-κB family member p52 in specific cell populations and characterized this model in airway epithelial cells. In CCSP-p52 mice, p52 over-expression did not induce activation of other NF-κB family members or inflammatory cell recruitment, even after injection with the lung carcinogen urethane. Still, p52 over-expression in the airway epithelium led to more tumors, larger tumors, and more advanced tumors after urethane injection. *In vitro* studies and gene expression microarray analysis revealed that p52 expression promotes proliferation of lung epithelial cells by increasing expression of a number of cell cycle-associated genes. Expression of these p52-associated genes was significantly associated with lung tumors compared to normal lung tissue in lung cancer patients. In addition, increased expression of p52-associated genes in lung tumors correlated with a significantly shorter survival, even for Stage I patients. Finally, we generated a protein-protein interaction network using the p52-associated genes found in tumors and

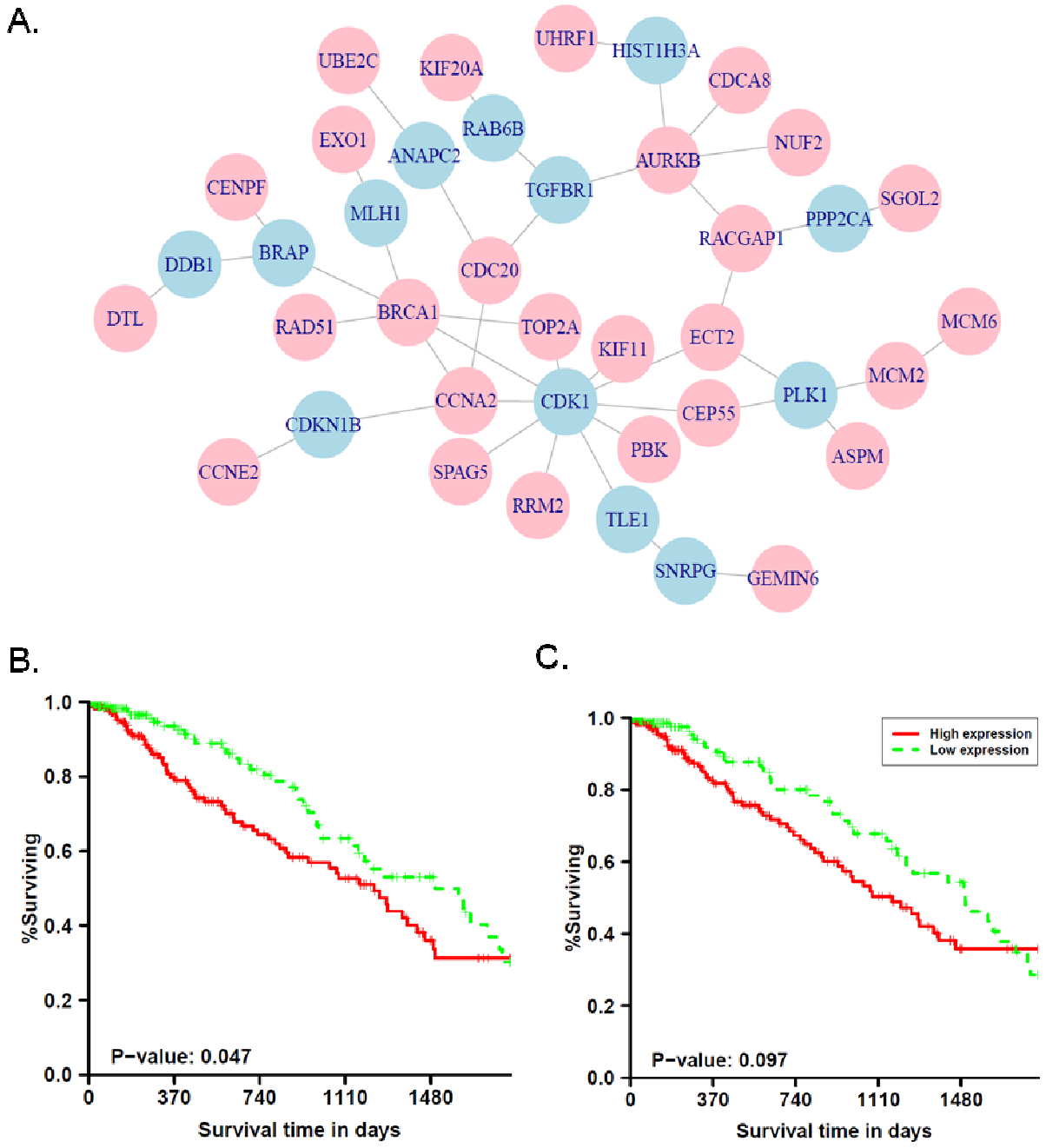

Figure 17: Expression of genes in p52-derived protein interaction correlate with poor prognosis of lung cancer patients.

A) Protein-protein interaction network generated using 35 p52-associated genes associated with tumors (see Table 1 and Table 3). Pink circles are genes identified as p52-regulated genes through microarray analysis, and blue circles are imputed genes. Kaplan-Meier survival curves of overall patient survival based on (B) summed expression or (C) expression "votes" of imputed mediator genes (log-rank test, p=0.047 for summed expression; p=0.097 for expression "votes").

examined patient survival based on expression of the imputed mediator genes, revealing poor prognosis with high expression of the imputed genes and demonstrating the strength of this p52-derived gene network in predicting patient prognosis. Taken together, these data suggest that p52 is an important contributor to lung tumorigenesis and that modulation of p52 activity or its downstream targets could potentially improve patient outcome.

Nuclear localization of p52 has been observed in a number of different tumor types, but the understanding of the function of p52 activation *in vivo* during carcinogenesis has remained limited due to the constraints of available models. In other studies using a mouse model with global truncation of the*Nfkb2* gene deleting the C-terminal inhibitory domain of p100, mice die from gastric hyperplasia (Ishikawa et al., 1997). However, unlike our studies, the individual contribution of inflammatory cells and surrounding stroma with dysregulated p52 activation was not separated from the effects of p52 activation in the epithelial cells of the stomach. Using a transgenic model with expression of the full *Nfkb2* gene under the control of the β-lactoglobulin milk protein promoter, Connelly et al. demonstrated ductal thickening and hyperplasia in the mammary gland after three pregnancies (Connelly et al., 2007), but in this model, expression was limited to the periods of milk production during the late stages of pregnancy and lactation. Studies described here improve upon these models by using an inducible p52-expressing mouse. The advantages of a mouse model with inducible p52 expression are many and include: p52 can be expressed with any cell type-specific promoter coupled to a reverse tetracycline transactivator, the duration of p52 expression can be manipulated, and p52 expression can be combined with other inducible mouse models, including oncogenic tumor models. Future studies using this p52-inducible model to modulate the duration of expression in the urethane model and to express p52 in other cell types and in combination with other inducible models will be valuable for developing a broader understanding of p52 activation in lung cancer and other contexts.

Like CCSP-p52 mice, activation of canonical NF-κB signaling in transgenic mice expressing constitutively active IKKβ in airway epithelium increases tumor burden following urethane treatment (Zaynagetdinov et al., 2011b). However, in contrast to non-canonical pathway activation, canonical NF-

κB activation causes a profound immune/inflammatory response, which promotes lung carcinogenesis through paracrine signaling (Cheng et al., 2007; Zaynagetdinov et al., 2011b). In the setting of lung epithelial canonical NF-κB activation, T-regulatory cell recruitment creates an immunosuppressive microenvironment that supports increased tumor formation (Zaynagetdinov et al., 2011b). In the context of non-canonical pathway activation, our studies indicate that non-canonical NF-κB signaling primarily regulates genes that function in a cell autonomous manner to promote carcinogenesis.

Among the NF-κB family members, p52 is structurally most similar to p50. Both undergo proteasomal processing of larger precursors to generate the active form, which can enter the nucleus to regulate gene transcription, and both have a Rel-homology domain enabling dimerization and DNA binding but lack a transactivation domain. Kravtsova-Ivantsiv et al. recently demonstrated that p50 over-expression suppressed *in vitro* colony formation of cancer cell lines as well as xenograft tumor growth (Kravtsova-Ivantsiv et al., 2015). In contrast, we observed increased proliferation of lung epithelial cells *in vitro* and increased tumor size and number *in vivo* as a result of p52 expression. In other contexts, p52 activation has also been shown to promote proliferation. Nadiminty et al. observed that p52 over-expression enhanced proliferation of prostate cancer cells in androgen-deprived conditions by stimulating cyclin D1 expression (Nadiminty et al., 2008). Similarly, increased p100 expression in mammary glands led to hyperplasia and increased cyclin D1 (Connelly et al., 2007). Although we did not identify cyclin D1 as an upregulated gene in our microarray analysis, both cyclin E2 and cyclin A2 were increased in CCSP-p52 lungs (Table 1). Despite the structural similarity between p50 and p52, these studies suggest that they function differently during tumorigenesis, which may be due to the differential affinities of each for specific promoter sequences or their propensity to interact with other NF-κB family members and transcriptional binding partners (Siggers et al., 2011; Zhao et al., 2014).

Although p100/p52 expression appears to be common in lung adenocarcinomas, how this pathway becomes activated remains unclear. Proteolytic processing of p100 to p52 can be activated by a number of stimuli, including lymphotoxin β (Dejardin et al., 2002), CD40 ligand (Coope et al., 2002), ROS (Iannetti et al., 2014), and STAT3 signaling (Nadiminty et al., 2006), suggesting that p52 activation

can occur in a tumor as a result of oncogenic signaling or microenvironmental stimuli. Additional evidence indicates that crosstalk occurs between the canonical and non-canonical NF-κB pathways, suggesting that factors leading to canonical pathway activation could also activate p52 (Liptay et al., 1994). Further investigations are necessary to identify the mechanisms behind p52 activation in tumors as well as the individual functional contributions of canonical and non-canonical NF-κB signaling during lung tumorigenesis.

In these studies, we took a gene list derived from p52 expression in a mouse model and demonstrated that these genes predict survival of early stage lung cancer patients. Since p52 was only over-expressed in a subset of cells in lungs of CCSP-p52 mice, the signal in our gene expression microarray analysis was likely diluted, explaining why we did not observe large expression differences between CCSP-p52 and WT lungs. However, we were still able to identify genes with significant expression changes as a result of p52 expression and these genes were highly related in function, indicating that p52 regulates expression of a network of related genes. Ianetti et al. also identified significant changes in many cell cycle-associated genes from microarray analysis of *Nfkb2* knockdown fibroblasts, and several of these genes overlap with our gene set (Iannetti et al., 2014). Because many of the genes in the gene list are known cell cycle regulators that have well-established roles in carcinogenesis, p52 modulation may be an attractive therapeutic target for drug development. In addition, inhibitors for several of the nodes in our p52-derived protein interaction network are being developed for clinical use, including aurora kinase B, CDK1, and polo-like kinase 1, suggesting that treatment with these drugs alone or in combination may be beneficial in patients with p52 activation in their tumors.

CHAPTER IV

P52 OVER-EXPRESSION INCREASES EPITHELIAL APOPTOSIS, ENHANCES LUNG INJURY, AND REDUCES SURVIVAL AFTER LPS TREATMENT

Parts of this chapter were originally published in *The Journal of Immunology*. Saxon JA, Cheng D-S, Han W, Polosukhin V, McLoed AG, Richmond BW, Gleaves LA, Tanjore H, Sherrill TP, Barham W, Yull FE, Blackwell TS. 2016. p52 over-expression increases epithelial apoptosis, enhances lung injury, and reduces survival after LPS treatment. J. Immunol. 196(4) 1891-1899.

Rationale

NF-κB regulates a number of key genes involved in cellular processes such as proliferation, apoptosis, and inflammation. The NF-κB transcription factor family contains 5 members (p65/RelA, p100/p52, p105/p50, RelB, and c-Rel). Traditionally, NF-κB signaling is associated with activation through either the canonical or non-canonical signaling pathways. In the non-canonical pathway, a heterodimer consisting of p100 and most commonly RelB remains sequestered in the cytoplasm due to the IκB-like inhibitory C-terminus of p100. Upon activation, p100 is phosphorylated and undergoes partial proteolytic processing to p52, enabling the p52-containing heterodimer to translocate into the nucleus. While many studies have identified crucial roles for canonical NF-κB signaling in inflammatory diseases, metabolic disorders, and cancer, few have investigated the involvement of non-canonical NF-κB signaling in these contexts. Global knockout of either *Relb* or *Nfkb2* (the genes for RelB and p100/p52) causes defects in secondary lymphoid organ development and impaired immune responses (Caamaño et al., 1998; Franzoso et al., 1998; Weih et al., 1995). Therefore, non-canonical NF-κB signaling has primarily been studied in hematopoietic cells, where it is an important pathway for regulating chemokine genes required for normal lymphoid organ development (Dejardin et al., 2002; Weih et al., 2001). However, little is known about the function of non-canonical NF-κB signaling in non-immune cell types.

Acute respiratory distress syndrome (ARDS) is a life-threatening form of hypoxemic respiratory failure that results in substantial morbidity and mortality. ARDS is characterized by an influx of

inflammatory cells, epithelial apoptosis, and vascular permeability. IT treatment of mice with *Escherichia coli* LPS is commonly used as a model of ARDS. We have previously shown that NF-κB signaling in the lung epithelium regulates the inflammatory response after LPS stimulation (Cheng et al., 2007), suggesting that epithelial NF-κB signaling is a critical component of ARDS pathogenesis. Although the role of the non-canonical NF-κB pathway in LPS-induced inflammation is unknown, studies with lung epithelial cells *in vitro* have shown that LPS stimulation induces non-canonical NF-κB activation with slower and more protracted kinetics compared to canonical NF-κB activation and that non-canonical NF-κB signaling may be important for regulation of pro-inflammatory cytokines (Tully et al., 2012).

We observed increased nuclear accumulation of the non-canonical NF-κB signaling component p52 in the airways of ARDS patients. To investigate the effect of p52 activation *in vivo* during acute inflammation, we used a transgenic mouse model with inducible expression of p52 specifically in airway epithelial cells. We found that p52 over-expression in conjunction with LPS stimulation led to increased mortality and exaggerated lung injury, along with increased epithelial cell apoptosis. Together, these studies demonstrate a novel role for non-canonical NF-κB signaling in cell survival/apoptosis during cellular stress and implicate p52 as a factor affecting the severity of ARDS pathogenesis.

Materials and Methods

Animal model

CCSP-tTS/(tet-O)$_7$-FLAG-p52 mice on an FVB background were mated to CCSP-rtTA homozygous mice (gift from Dr. J.A. Whitsett, University of Cincinnati, Cincinnati, OH) to generate CCSP-p52 mice, which inducibly express FLAG-tagged p52 in the airway epithelium as described in Chapter 3. CCSP-p52 mice generated from two separate CCSP-tTS/(tet-O)$_7$-FLAG-p52 founder lines were used for these studies. Age- and sex-matched transgenic mice along with genotype-negative littermate controls (called WT in our studies) were used in experiments. Transgene expression was activated by administering 2 g/l dox along with 2% sucrose in drinking water. Water was replaced twice

weekly. Mice were sacrificed at indicated time points, and lungs were lavaged as previously described (Zaynagetdinov et al., 2011b). The left lung was tied off and flash-frozen in liquid nitrogen, and the right lung was perfused and fixed by inflating with 10% neutral-buffered formalin. Total and differential BAL cell counts were determined as previously described (Stathopoulos et al., 2007). All animal care and experimental procedures were approved and conducted according to the guidelines of the Vanderbilt University Institutional Animal Care and Use Committee.

LPS, bleomycin, and RelB adenovirus administration

To establish transgene expression, mice were placed on dox for 1 week prior to IT LPS, bleomycin, or RelB adenovirus administration, and they remained on dox until sacrifice. For IT treatments, mice were anesthetized with isofluorane. *Escherichia coli* LPS (serotype 055:B5; Sigma-Aldrich) was diluted in sterile PBS and delivered IT at a dose of 3 µg/g body weight. Bleomycin (0.08 units) diluted in sterile saline was administered IT. 5 x 10^8 pfu of RelB-His adenovirus containing murine RelB with a His tag (Ad-RelB; ABM) or control luciferase adenovirus (Ad-Luc; gift from Dr. A. Powers, Vanderbilt University, Nashville, TN) was delivered IT. Inflammatory cell recruitment was assessed 96 hours after adenoviral administration. For experiments with LPS stimulation after adenovirus administration, LPS was given IT 96 hours after adenoviral delivery.

Lung histology

H&E staining was performed on 5 µm lung sections to assess lung histology. A pathologist scored lung fibrosis on H&E-stained sections as previously described using a 0 to 4 point scale (0 = normal lung architecture; 1 = increased thickness of ≤50% of interalveolar septa; 2 = thickening of >50% of interalveolar septa without fibrotic foci formation; 3 = thickening of the interalveolar septa with isolated fibrotic foci formation; 4 = formation of multiple fibrotic foci with distortion of parenchymal architecture) (Lawson et al., 2005).

Immunostaining

For TUNEL immunofluorescence staining, lung sections were stained using the fluorescein *In Situ* Cell Death Detection Kit (Roche), and TUNEL positive cells were counted in fifteen 60x fields using fluorescent confocal microscopy. Mean scores were calculated for each animal. For TUNEL co-immunofluorescence staining with CCSP or SPC, lung sections were first stained with anti-CCSP (S-20; Santa Cruz) or anti-SPC antibody (Millipore) followed by the TUNEL staining protocol. Using fluorescent confocal microscopy, SPC and TUNEL double-positive cells were enumerated in ten 20x fields, and total CCSP and TUNEL double-positive cells were counted on each lung section. To assess nuclear p52 in human lungs, immunostaining using an anti-p52 antibody (C-5, Santa Cruz) was performed on normal lung sections from 4 life-long non-smokers and on lung sections from 4 patients with ARDS. ARDS lung sections were a generous contribution from Dr. Lorraine Ware (Vanderbilt University, Nashville, TN). All patients had no known chronic lung disease.

Cell viability measurements

Rat type II alveolar epithelial cell line RLE-6TN (ATCC) were maintained at 37ºC 5% CO_2 in DMEM (Invitrogen) with 4.5 g/l glucose and 2mM L-glutamine, supplemented with 10% FBS, 100 units/ml penicillin, and 100 µg/ml streptomycin. Generation and validation of stable p52 over-expressing (RLE-p52) and control empty vector (RLE-EV) cells is described in Chapter 3. Viability of parental cells (RLE-WT), RLE-EV, and RLE-p52 RLE-6TN cells was assessed using the CellTiter-Glo Luminescent Cell Viability assay (Promega) according to the manufacturer's protocol. For serum starvation experiments, an equal number of RLE-WT, RLE-EV, and RLE-p52 cells were plated in 96 well plates in 10% serum medium as described above. Eight hours later, when cells had adhered to the wells, cells were switched to medium lacking serum, and cell viability was assessed after 12, 18, and 24 hours in medium without serum. Percent survival was determined by normalizing no serum viability measurements to viability measurements in 10% serum medium for each cell line at each time point. For H_2O_2 treatment experiments, an equal number of RLE-EV and RLE-p52 cells were plated in 96 well plates. After

overnight incubation, cells were treated with 100 μM H_2O_2, and cell viability was assessed at 24 hours. Percent survival was determined by normalizing H_2O_2-treated viability measurements to viability measurements in control (untreated) cells.

Western blot analysis

Nuclear protein was prepared from lung tissue using the NE-PER Nuclear and Cytoplasmic Extraction Reagents (Thermo Scientific), separated by SDS-PAGE, transferred to nitrocellulose membranes, and probed using the following antibodies: FLAG (F3165, Sigma), p100/p52 (4882, Cell Signaling), p65 (C-20, Santa Cruz), p50 (C-19, Santa Cruz), RelB (C-19, Santa Cruz), cRel (C, Santa Cruz), and TBP (N-12, Santa Cruz). Whole cell lysates were prepared from RLE-6TN cells using RIPA buffer (Invitrogen) and probed with antibodies for caspase-3 (9662, Cell Signaling) and β-actin (AC-74, Sigma). Immunodetection was performed using the corresponding AlexaFluor-conjugated antibodies and the Odyssey Infrared Imaging System (LI-COR Biosciences). All images were converted to grayscale.

Quantitative real-time PCR

Total mRNA was isolated using the RNeasy Mini kit (Qiagen) according to the manufacturer's instructions. Quantitative real-time PCR was performed using Sybr Green PCR Master Mix (Applied Biosystems) and the following primer sets: Cxcl12 (F: CCCATTCTCCTCATCCTCAT; R: ACTCTGCTCTGGTGGAAGGT) (Petty et al., 2007), Cxcl13 (F: AACTCCACCTCCAGGCAGAATG; R: TGTGTAATGGGCTTCCAGAATACC) (Hojgaard et al., 2006), Ccl19 (F: GGCCTGCCTCAGATTATCTGCCAT; R: GGAAGGCTTTCACGATGTTCC), Ccl21 (F: GGACCCAAGGCAGTGATGGAG; R: CTTCCTCAGGGTTTGCACATAG) (Proietto et al., 2008), RelB (F: GGGCATCCAGTGTGTTAGGAAGAA; R: GGAAGCAGATCCTGACGACATTCA), and GAPDH (F: TGAGGACCAGGTTGTCTCCT; R: CCCTGTTGCTGTAGCCGTAT). Expression values were normalized to GAPDH using the ΔCT method.

For the quantitative real-time PCR array analysis, RLE-WT, RLE-EV, and RLE-p52 cells plated in 10 cm plates underwent serum starvation for 18 hours as described for cell viability measurements. RNA was isolated from cells using the RNeasy Mini Kit (Qiagen) according to the manufacturer's protocol. RNA was converted to cDNA using the RT^2 First Strand Synthesis Kit (Qiagen). Apoptosis genes were assessed using the Rat Apoptosis RT^2 Profiler PCR array (Qiagen) according to the manufacturer's instructions. Four biological replicates were run for each cell type, and threshold cycle values greater than 32 were discarded from the analysis. Expression values for each sample were normalized to the mean of 5 measured housekeeping genes using the ΔCT method.

Multiplex Cytokine Bead Array

Levels of IFNγ, IL-1β, MCP-1, G-CSF, IL-6, KC, and MIP-1α were measured in BAL fluid and lung lysates as part of a multiplex mouse cytokine magnetic bead array panel (EMD Millipore, Darmstadt, Germany) using a Luminex 100 analyzer. Assays were performed according to the manufacturer's instructions with assistance from the VUMC Hormone Assay and Analytical Services Core. Other analytes in the panel that were below the limit of detection include GM-CSF, IL-4, IL-10, and IL-12p40.

ELISAs

Lung nuclear protein was isolated as described for western blot analysis, and p52 was detected using the TransAM NF-κB ELISA kit (Active Motif). Albumin was measured in cell-free BAL supernatants using the mouse albumin ELISA from GenWay Biotech, Inc. G-CSF, Mip-1α, KC, (R&D Systems) MCP-1, IL-1β, and IFNγ (Biolegend) were measured in whole lung lysates. All ELISAs were performed according to manufacturer's instructions.

Statistics

Data were analyzed using GraphPad Prism 5.0 software (GraphPad Software, Inc.), and all values

are presented as the mean ± SEM. Unpaired Student's t-tests were performed for comparisons between two groups. To analyze differences among more than two groups, one-way ANOVA followed by a Tukey's post-test was used. For the Kaplan-Meyer survival analysis, a log-rank test was employed. $p \leq 0.05$ was considered statistically significant.

Results

Increased nuclear p52 accumulation in lungs of ARDS patients

To investigate whether non-canonical NF- κB signaling is activated in the lungs of ARDS patients, we performed p100/p52 immunostaining on lung sections from patients with ARDS and control subjects. Faint cytoplasmic staining but no nuclear staining was observed in airways from normal lungs (Figure 18A, B). In contrast, ARDS airways and parenchyma had a marked increase in nuclear as well as cytoplasmic staining (Figure 18A, B). This finding of increased nuclear p52 staining in airways and lung parenchyma of ARDS patients suggests that p52 activation could influence ARDS pathogenesis.

CCSP-p52 mice exhibit exaggerated inflammation, lung injury, and mortality after IT LPS

In contrast to canonical NF-κB signaling, which is increased in the lungs within the first 24 hours following IT injection of *Escherichia coli* LPS (Blackwell et al., 1999), we found that treatment of WT mice with IT LPS (3 μg/g body weight) leads to increased nuclear p52 in the lungs that peaks at 48 hours (Figure 19). To investigate the function of p52 in the context of LPS stimulation *in vivo*, IT LPS was administered to dox-treated CCSP-p52 and WT mice. A significant increase in mortality was observed in CCSP-p52 mice compared to WT mice beginning 72 hours after LPS (Figure 20A). We measured albumin in BAL fluid as a marker of lung injury and found that albumin levels were significantly higher in BAL from CCSP-p52 mice 48 hours after LPS administration (Figure 20B). Total inflammatory cell numbers in BAL were also increased in CCSP-p52 mice compared to WT mice at 48 hours after LPS assessed by western blotting of lung nuclear protein from mice 24, 48, and 72 hours after LPS to

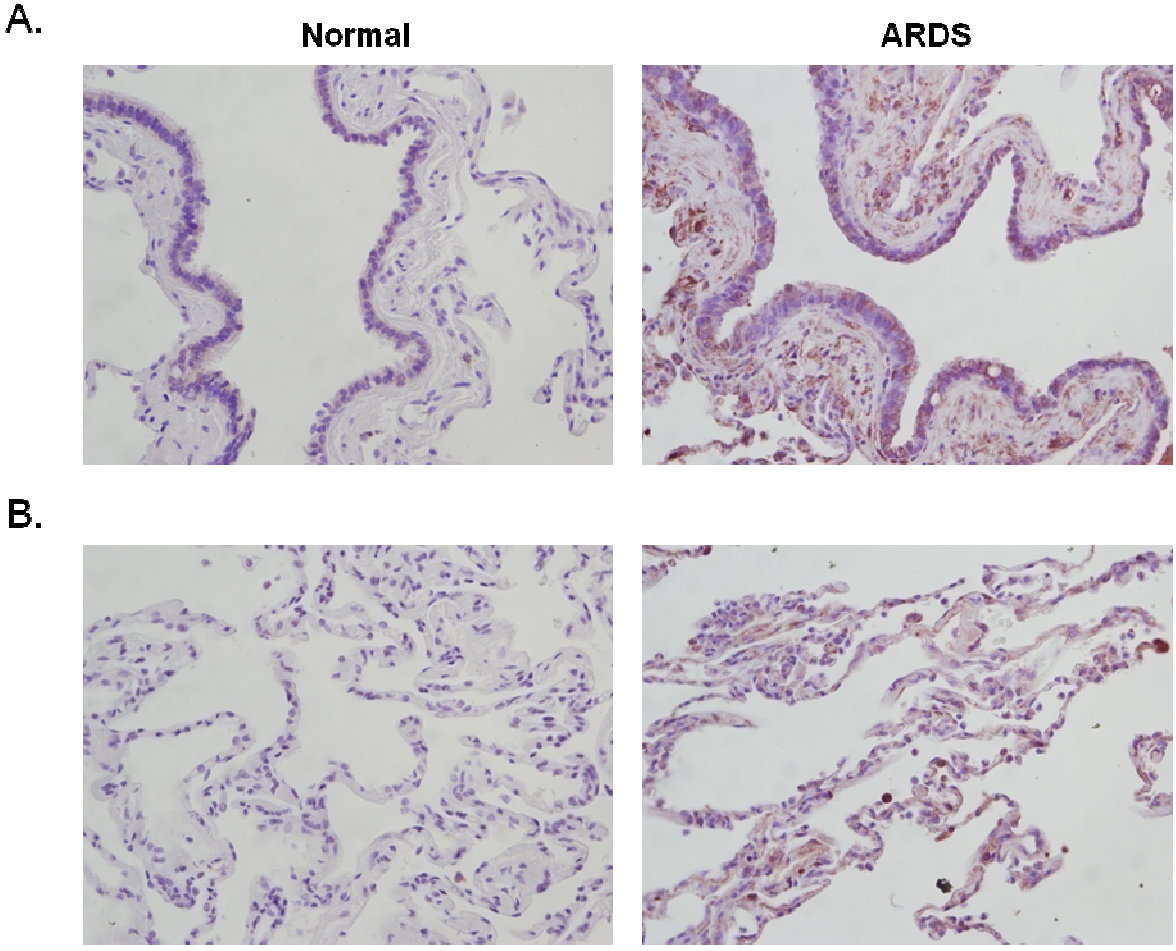

Figure 18: Increased nuclear p52 staining in airways of ARDS patients.
Photomicrographs of p52 immunostaining of airways (A) and lung parenchyma (B) from normal and ARDS human lung sections (40x magnification). Immunostaining is representative of lung sections from 4 individuals per group.

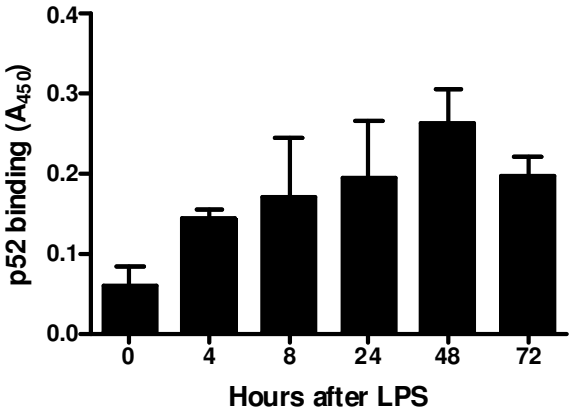

Figure 19: LPS stimulation leads to increased p52 activation *in vivo*.
p52 binding measured by ELISA in lung nuclear protein from WT mice at the indicated time points after LPS (n=3/time point).

determine whether altered activation of other NF-κB family members was associated with the enhanced inflammatory influx in CCSP-p52 mice. Compared to WT lungs, no differences in activation of other NF-κB family members in CCSP-p52 lungs were observed at any time point (Figure 20G, H and data not shown).

Since we observed increased inflammatory cells in BAL from CCSP-p52 mice following LPS treatment, we expected to find increased levels of cytokines/chemokines in the lungs. Therefore, we measured a panel of mediators in BAL fluid at 24 hours after LPS treatment and in lung lysates at 24, 48, and 72 hours after LPS. Surprisingly, no differences were found in levels of G-CSF, IL-1β, MCP-1, MIP-1α, IFNγ, IL-6, or KC at any time point (Figure 21A-D). We also measured expression of previously described non-canonical NF-κB signaling targets Cxcl12, Cxcl13, Ccl19, and Ccl21 (Dejardin et al., 2002) in lung lysates from CCSP-p52 and WT mice and found no differences between groups (Figure 21E). To determine whether inflammatory cells from CCSP-p52 mice produced more inflammatory cytokines, we isolated macrophage and neutrophil populations from the lungs of WT and CCSP-p52 mice 48 hours after LPS and measured expression of KC, TNF-α, IL-6, and IL-1β by quantitative real-time PCR. However, no increases in cytokine production by inflammatory cells from CCSP-p52 mice were observed (data not shown). Together, these data show that over-expression of p52 in the airway epithelium does not increase cytokine expression in this model.

The p52 precursor p100 preferentially binds to RelB in the cytoplasm, inhibiting its nuclear translocation (17). When non-canonical signaling is activated, processing of p100 to p52 induces translocation of RelB/p52 heterodimers into the nucleus (17, 18). To investigate the effect of RelB over-expression in combination with p52 over-expression on inflammatory cell recruitment, dox-treated WT and CCSP-p52 mice were administered adenoviral RelB (Ad-RelB) or control adenovirus (Ad-Luc) by IT injection. RelB over-expression in the lungs was confirmed by quantitative real-time PCR (Figure 22A), and inflammatory cell recruitment was assessed 96 hours after adenoviral administration. RelB over-expression caused a significant increase in inflammatory cell recruitment, characterized by increased macrophages, lymphocytes, and neutrophils in both WT and CCSP-p52 mice compared to mice treated

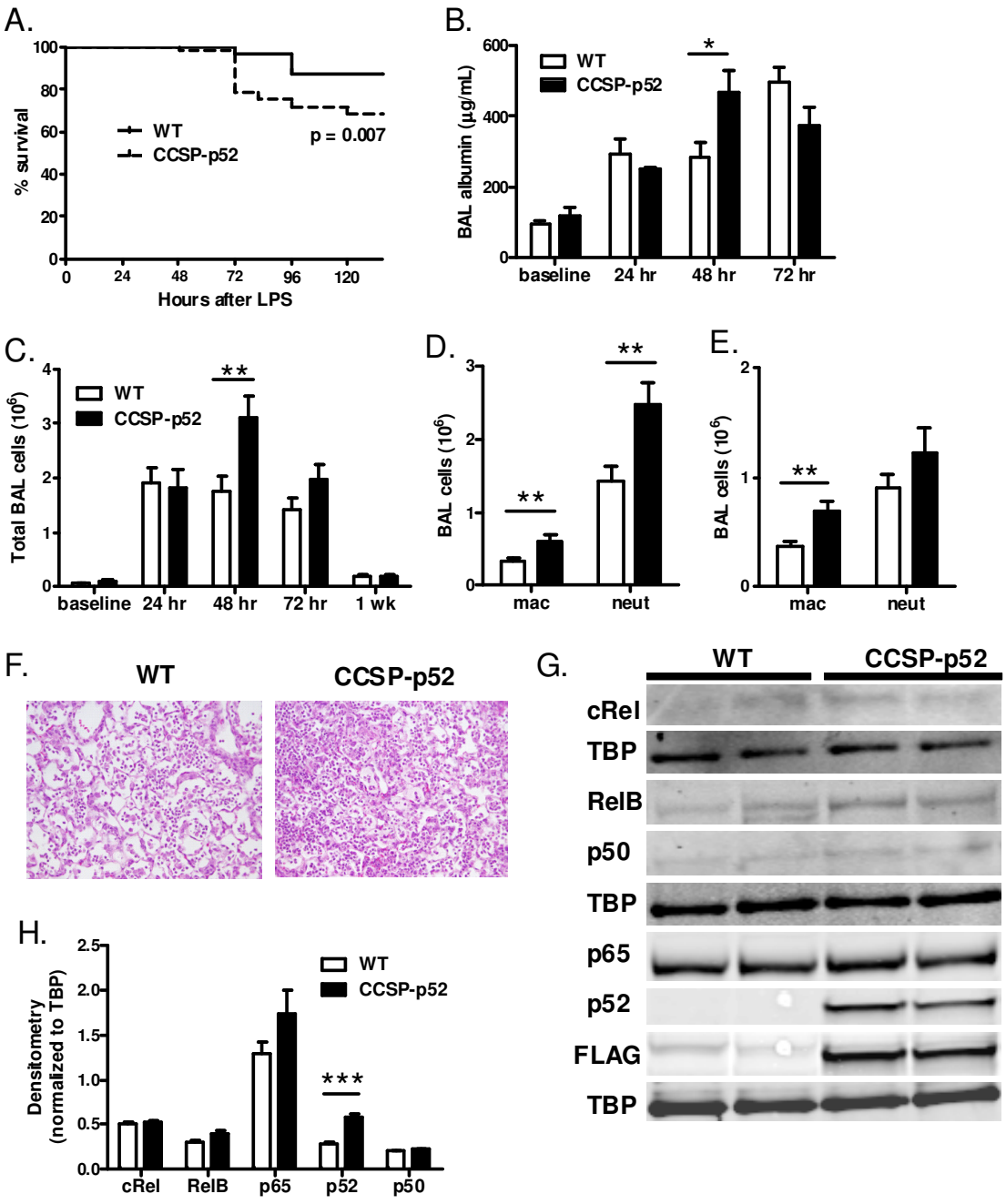

Figure 20: Treatment of CCSP-p52 mice with LPS results in increased inflammation, lung injury, and mortality.

A) Kaplan-Meier survival curve of WT and CCSP-p52 mice after LPS stimulation (n=57-60/group; log-rank test $p<0.01$). B) Albumin measured by ELISA in lavage fluid from WT and CCSP-p52 mice at baseline and after LPS stimulation (for baseline n=4/group, for 24 and 72 hour n=7-8/group, for 48 hour n=12-17/group;*$p<0.05$ compared to WT). C) Total BAL inflammatory cell numbers at baseline and after LPS stimulation (n=10-27/group, **$p<0.01$ compared to WT). BAL inflammatory cell differentials for CCSP-p52 and WT mice 48 hours (D) and 72 hours (E) after LPS (n=12-26/group; **$p<0.01$ compared to WT). F) Representative photomicrographs (40x magnification) from lungs of WT and CCSP-p52 mice at 48 hours after LPS. G) Western blot and H) densitometry for NF-κB family members using lung nuclear protein from mice at 48 hours after LPS stimulation. TBP was used as a loading control. H) (***$p<0.001$ compared to WT).

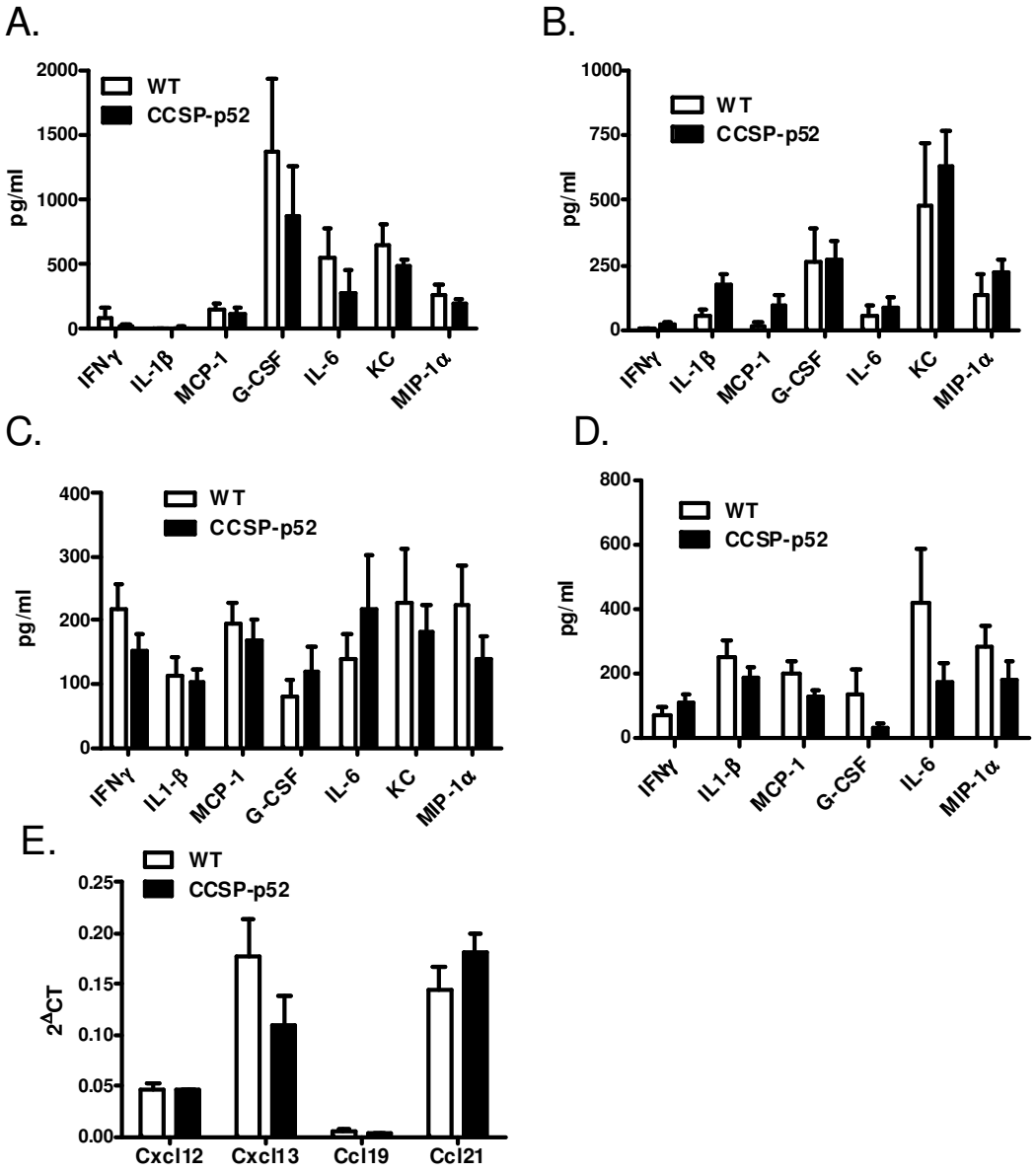

Figure 21: p52 over-expression does not affect chemokine production after LPS stimulation.

Levels of inflammatory mediators in (A) BAL fluid at 24 hours after LPS treatment and in lung lysates at (B) 24 hours, (C) 48 hours, and (D) 72 hours after LPS treatment in WT and CCSP-p52 mice (n=3-10 mice/group). E) Quantitative real-time PCR analysis of Cxcl12, Cxcl13, Ccl19, and Ccl21 expression in lungs of WT and CCSP-p52 mice 24 hours after LPS stimulation (n=4-5 mice/group).

with Ad-Luc (Figure 22B-E). However, in the context of LPS stimulation, RelB over-expression did not affect inflammatory cell influx into the lungs of CCSP-p52 mice after LPS treatment (Figure 22D, E). Together, these data indicate that RelB over-expression causes an inflammatory response independent of p52. However, RelB over-expression did not augment the effects of p52 over-expression in the context of LPS stimulation, indicating that p52 is the most important component of the non-canonical NF-κB signaling pathway responsible for altering the response to LPS.

To determine whether CCSP-p52 mice are more susceptible to lung injury, we tested their response to a different insult by administering IT bleomycin (0.08 units), a chemotherapeutic agent that causes lung inflammation, injury, and fibrosis in mice. Three weeks after bleomycin administration, no differences in BAL inflammatory cells or lung fibrosis were observed between dox-treated WT and CCSP-p52 mice (Figure 23), suggesting that p52-mediated exacerbation of lung injury may be dependent on the stimulus.

p52 over-expression causes apoptosis of airway epithelial cells after LPS

Since no differences in cytokine expression were observed between LPS-treated WT and CCSP-p52 mice, we wondered whether p52 over-expression could contribute to lung injury by altering epithelial cell survival. Therefore, we measured apoptosis by TUNEL staining in WT and CCSP-p52 lung sections at 24 and 48 hours after LPS. While no significant differences in apoptosis were observed at 24 hours after LPS, a trend toward increased apoptosis in CCSP-p52 lungs was present at 48 hours after LPS (Figure 24A). By co-immunofluorescence staining of TUNEL and CCSP, we looked more specifically at apoptosis in the CCSP+ airway epithelial cells where p52 is expressed. At 48 hours after LPS, a significant increase in the number of CCSP+TUNEL+ cells was detected in the airways of CCSP-p52 mice compared to WT mice (Figure 24B, C). In the absence of LPS stimulation, no significant difference in apoptotic CCSP+ cells was observed in CCSP-p52 mice compared to WT (Figure 24B). To determine whether apoptosis was restricted to the p52 transgene-expressing CCSP+ airway epithelial cells, we evaluated apoptosis of type II alveolar epithelial cells by co-immunofluorescence staining of TUNEL and

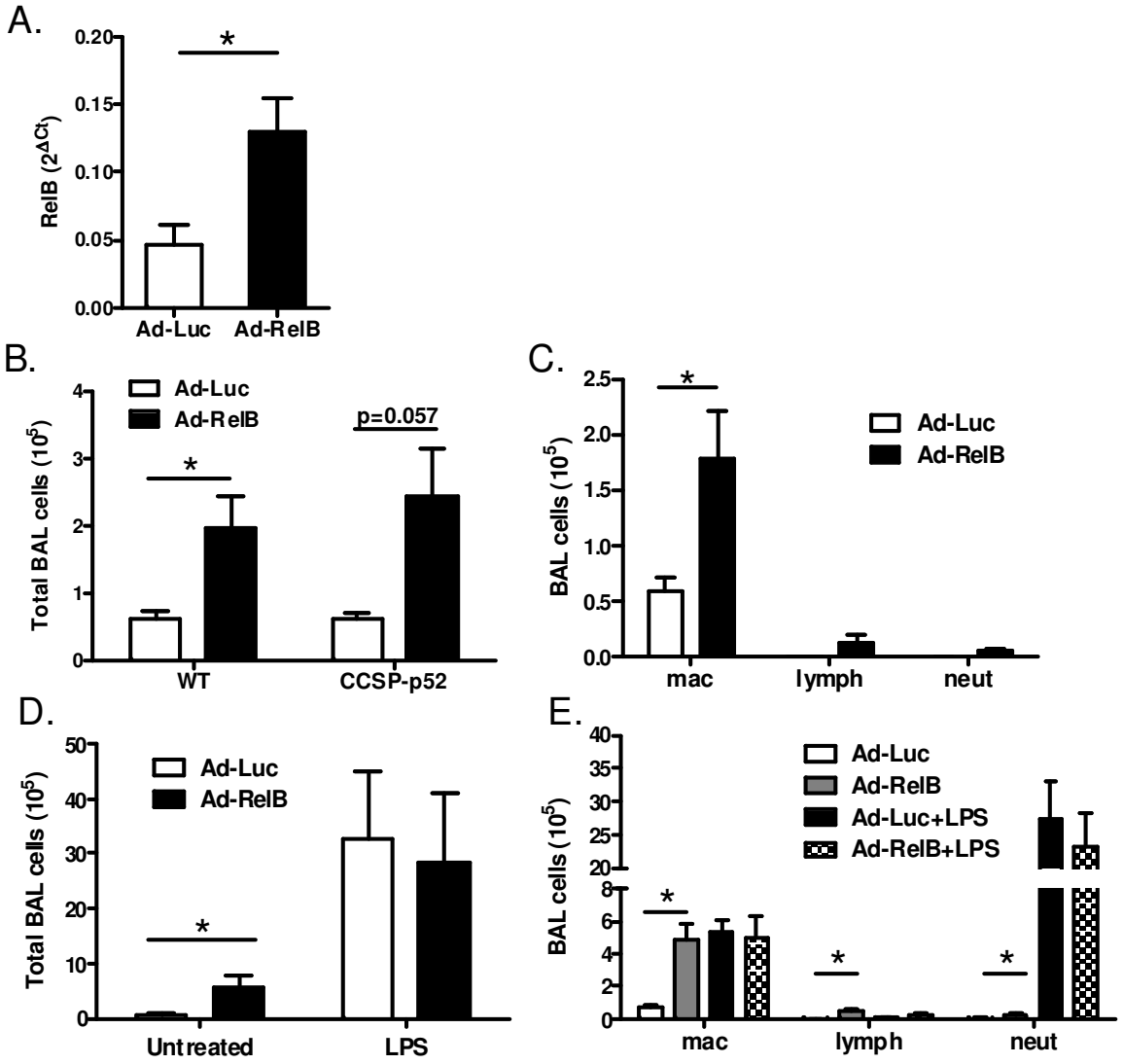

Figure 22: RelB expression does not augment effects of LPS stimulation in CCSP-p52 mice.

A) Quantitative real-time PCR for RelB expression in lungs of CCSP-p52 mice after control or RelB adenovirus delivery (n=3-4/group; $p<0.05$). B) Total BAL inflammatory cell numbers from WT and CCSP-p52 mice after IT administration of Ad-RelB or Ad-Luc (n=3-8/group; *$p<0.05$ compared to WT). C) BAL inflammatory cell differentials from WT mice after IT administration of Ad-RelB or Ad-Luc (n=7-8/group; *$p<0.05$). Total (D) and differential (E) BAL inflammatory cell numbers from CCSP-p52 mice after Ad-RelB or Ad-Luc delivery with and without LPS stimulation for 48 hours (n=4/group; *$p<0.05$).

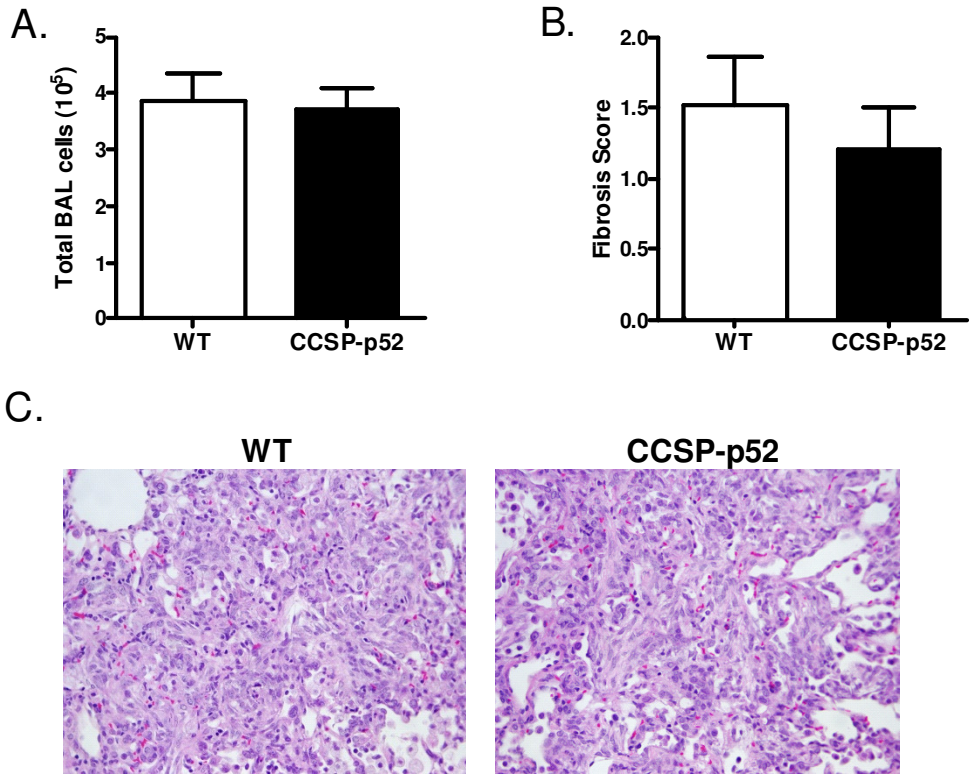

Figure 23: p52 over-expression does not affect inflammatory cell recruitment or fibrosis after bleomycin.

A) Total BAL inflammatory cell numbers, B) fibrosis scoring of lung sections, and C) representative lung photomicrographs (40x magnification) of fibrotic regions from WT and CCSP-p52 mice 3 weeks after bleomycin treatment (n=8-9 mice/group).

the type II cell-specific marker SPC. We found no differences in SPC+TUNEL+ type II cells between WT and CCSP-p52 mice after LPS (Figure 24D). Together, these data suggest that p52 directly regulates epithelial cell survival during conditions of inflammation or cellular stress.

p52 over-expression in stressed epithelial cells leads to enhanced expression of pro-apoptotic factors

To explore the mechanism by which p52 promotes apoptosis of epithelial cells, we used rat lung epithelial cells with stable p52 over-expression (designated RLE-p52), generated as described in Chapter 3. To investigate whether p52 over-expression resulted in differential apoptosis in RLE-6TN cells, we first tested inflammatory stimuli (LPS, TNF-α, and IL-1β), but none of these treatments resulted in substantial apoptosis in empty vector control (designated RLE-EV) or p52 over-expressing cells, indicating that these cells are resistant to apoptosis in response to inflammatory stimuli. Next we evaluated the effect of ROS stimulation by treating cells with H_2O_2 (100 μM). At 24 hours after H_2O_2 treatment, RLE-p52 cells demonstrated a significant decrease in cell viability compared to RLE-EV cells (Figure 25A). Increased apoptosis of RLE-p52 cells was supported by western blotting for cleaved caspase-3 at 18 hours of exposure to H_2O_2 (Figure 25B).

In another model of acute cellular stress, serum starvation, we found that RLE-p52 cells had significantly reduced cell viability compared to RLE-EV cells as well as the parental cell line (designated RLE-WT) (Figure 25C). Similar to H_2O_2 treatment, we observed increased apoptosis of RLE-p52 cells by western blotting for cleaved caspase-3 after 18 hours of serum starvation (Figure 25D).To identify specific mediators of apoptosis differentially upregulated in RLE-p52 cells, we measured apoptotic factors in RLE-p52, RLE-EV, and RLE-WT cells after 18 hours of serum starvation using a quantitative real-time PCR apoptosis array. Compared to RLE-EV and RLE-WT cells, ten pro-apoptotic factors were significantly upregulated in RLE-p52 cells, including Bcl10, Bid, Bcl2l11 (Bim), Bok, caspase-4, caspase-6, caspase-7, Fas, Gadd45α, and Pycard (Figure 26A-J), suggesting that p52 plays a role in regulating expression of these genes in stressed cells and that these genes in turn promote apoptosis.

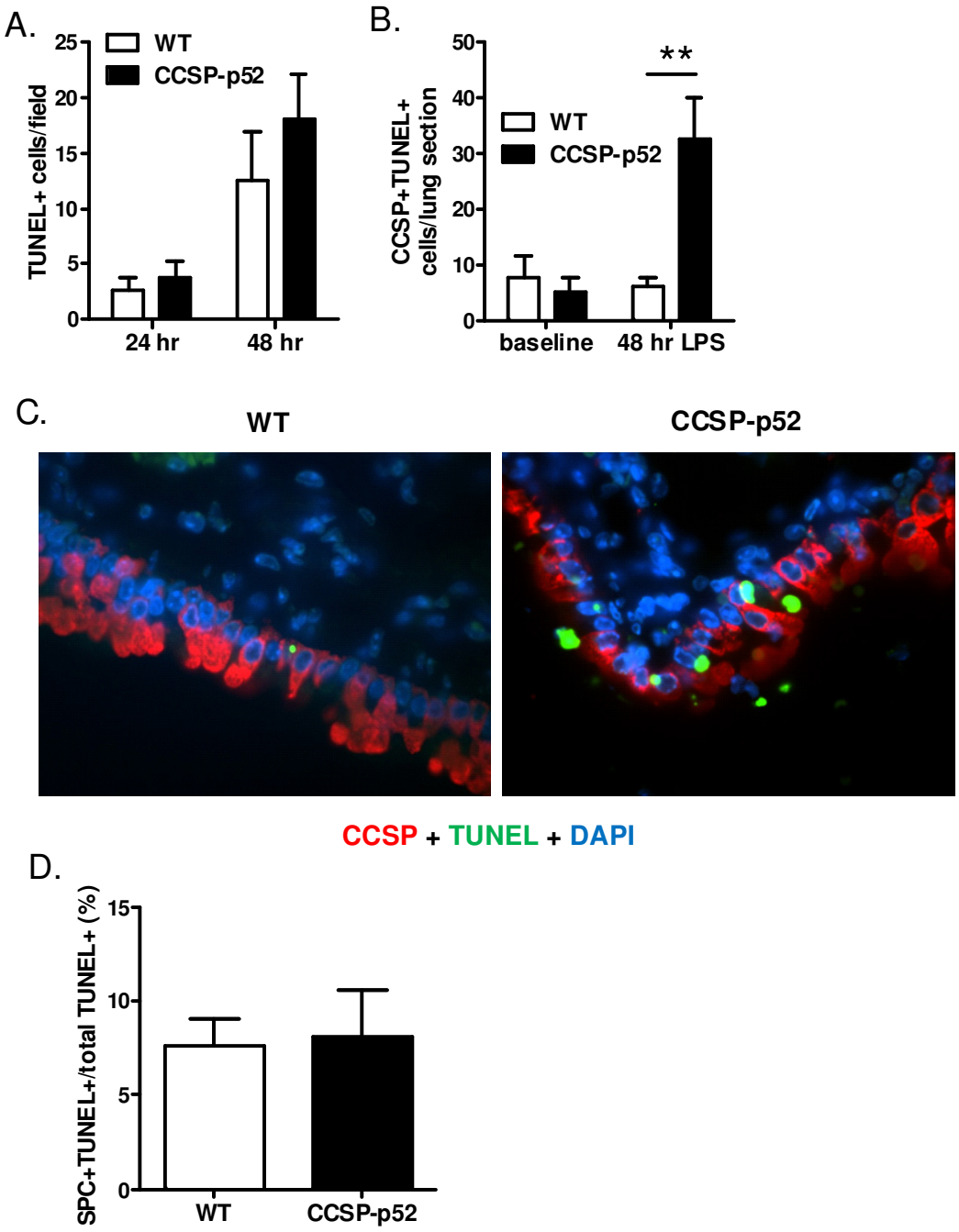

Figure 24: p52 over-expression causes increased apoptosis of CCSP+ cells after *in vivo* LPS treatment.

A) Quantification of TUNEL immunofluorescence staining (average number of TUNEL+ cells per high power field) performed on lung sections from WT and CCSP-p52 mice 24 and 48 hours after LPS (for 24 hours n=3/group, for 48 hours n=6/group). B) Quantification of CCSP+TUNEL+ cells on whole lung sections from WT and CCSP-p52 mice on dox for 1 week (baseline) or 48 hours after LPS (n=5-8/group; **p<0.01). C) Representative confocal images of CCSP and TUNEL co-immunofluorescence staining of WT and CCSP-p52 lungs 48 hours after LPS (red=CCSP, green=TUNEL, blue=DAPI; 60x magnification). D) Quantification of SPC+TUNEL+ cells as a percentage of total TUNEL+ cells counted in ten 20x fields on lung sections from WT and CCSP-p52 mice 48 hours after LPS (n=4/group).

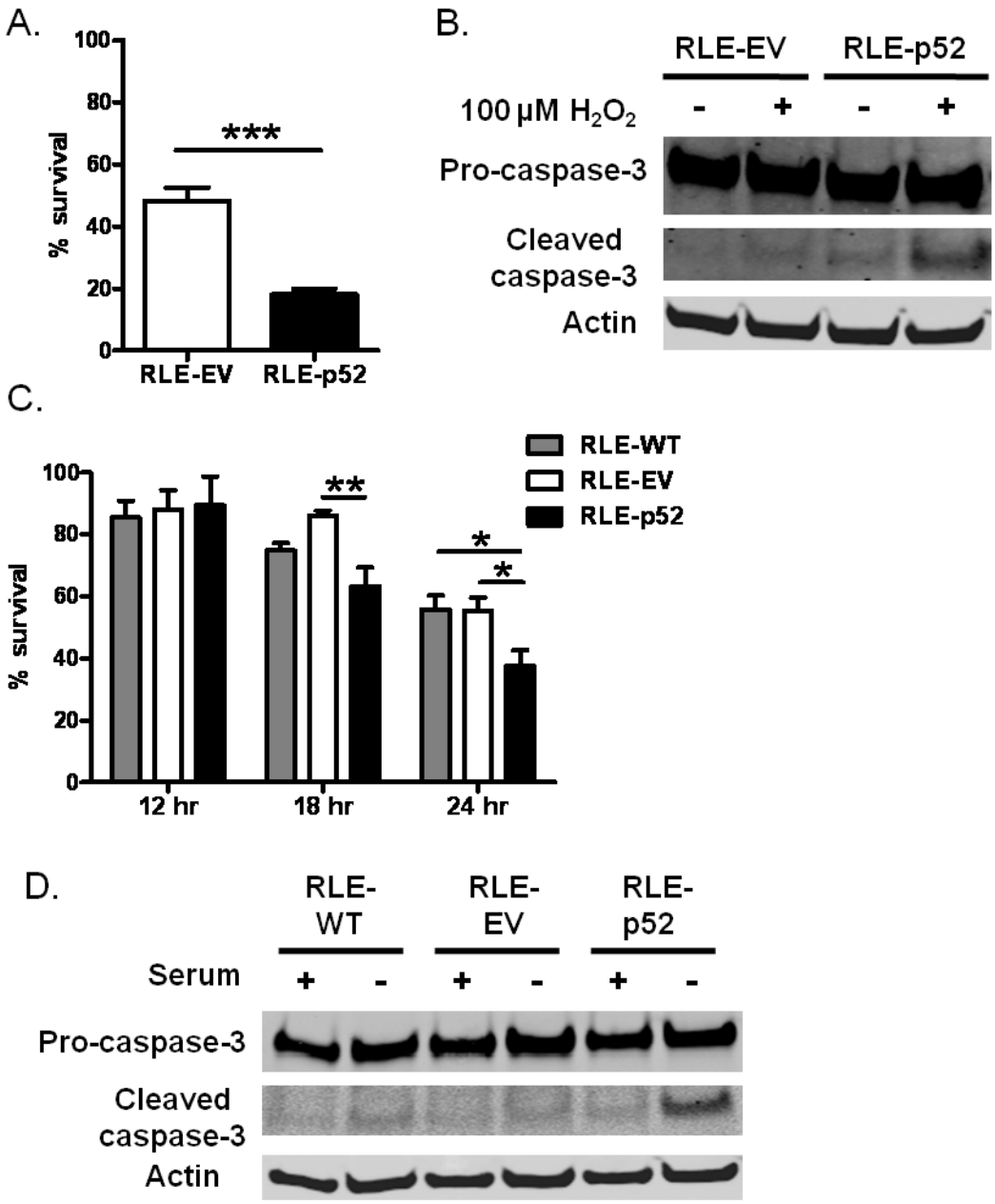

Figure 25: p52 enhances apoptosis of lung epithelial cells during cellular stress *in vitro*.

A) Survival of RLE-p52 and RLE-EV cells at 24 hours after H_2O_2 treatment (100 µM) measured by CellTiter-Glo (Promega). Percent survival was determined by normalizing values for each cell line treated with H_2O_2 to untreated values for each cell line (***$p<0.001$ comparing RLE-EV to RLE-p52). B) Pro-caspase-3 and cleaved caspase-3 measured by western blotting of whole cell lysates from RLE-EV and RLE-p52 with and without H_2O_2 stimulation. β-actin was used as a loading control. C) Survival of RLE-p52, RLE-EV, and parental cell line RLE-WT after 12, 18, and 24 hours of serum starvation. Percent survival was determined by normalizing values for each cell line in medium lacking serum to values for each cell line in 10% serum medium at each time point (18 hr **$p<0.01$ comparing RLE-EV to RLE-p52; 24 hr *$p<0.05$ comparing RLE-p52 to RLE-EV and RLE-p52 to RLE-WT). D) Pro-caspase-3 and cleaved caspase-3 measured by western blotting of whole cell lysates from RLE-WT, RLE-EV, and RLE-p52 cells grown in 10% serum medium or after 18 hours of serum starvation.

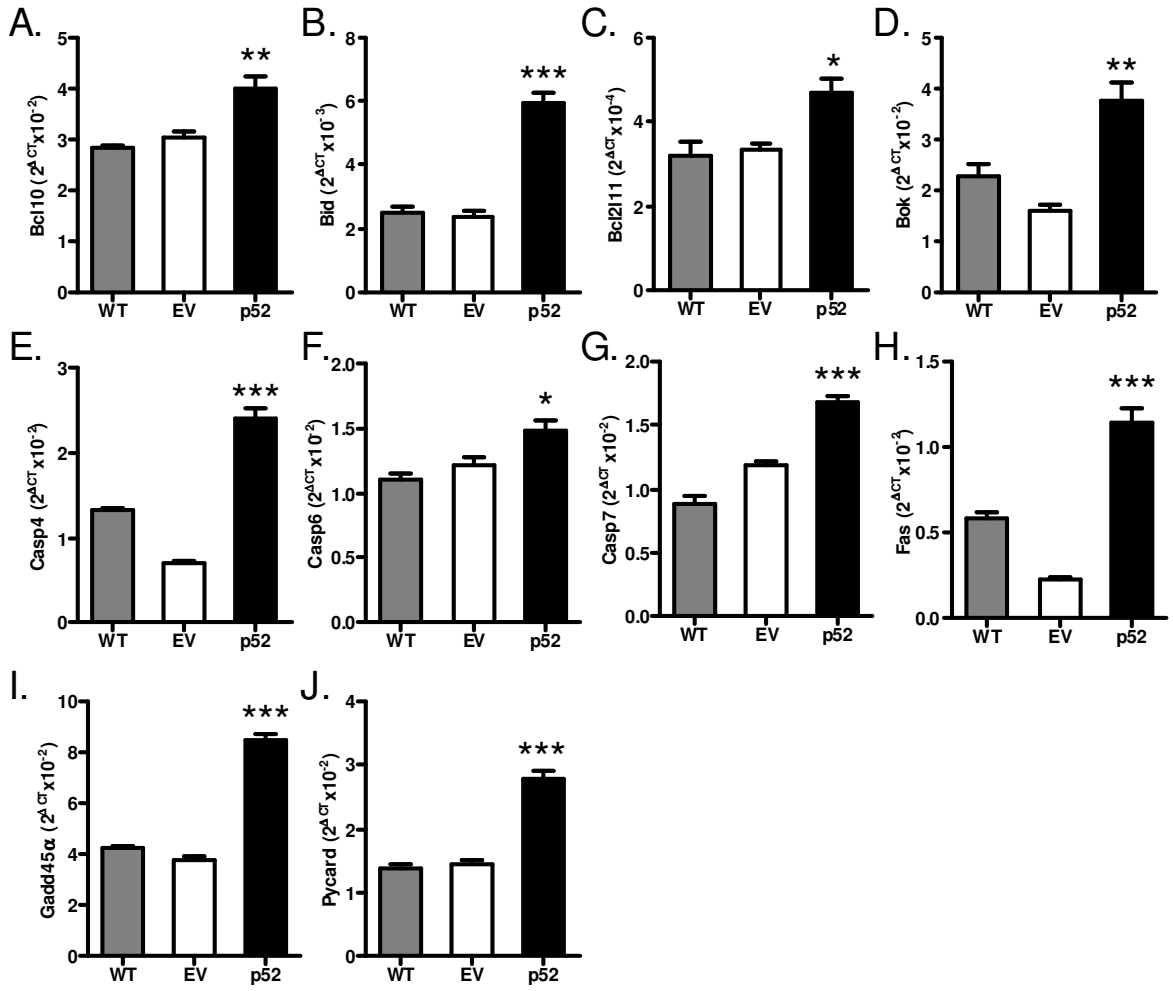

Figure 26: p52 regulates expression of apoptosis-associated genes during cellular stress.

Quantitative real-time PCR analysis of Bcl10 (A), Bid (B), Bcl2l11 (C), Bok (D), Casp4 (E), Casp6 (F), Casp7 (G), Fas (H), Gadd45α (I), and Pycard (J) expression in RLE-WT, RLE-EV, and RLE-p52 cells after 18 hours of serum starvation [n=4 biological replicates/group; *p<0.05, **p<0.01, ***p<0.001 p52 versus WT and EV].

Discussion

In these studies, we have identified an important and unexpected role for p52 in the airway epithelium in the setting of acute lung injury. In combination with LPS stimulation, p52 over-expression augmented epithelial apoptosis, enhanced lung inflammation without an increase in cytokine production, and enhanced lung injury and mortality. These effects appear to be driven directly by p52, since no changes in other NF-κB family members were observed after LPS stimulation and addition of RelB did not augment the phenotype. In addition, apoptosis of p52-expressing cells was specific to settings of acute cellular stress, since apoptosis was not observed in CCSP-p52 mice without LPS treatment or in RLE-p52 cells under normal culture conditions. In patients with ARDS, increased nuclear p52 staining was observed in the airways and lung parenchyma, suggesting that p52 could impact lung injury. Taken together, our studies implicate p52 as a potential factor in determining ARDS severity through regulation of epithelial survival/apoptosis.

Our findings, in conjunction with studies published by others, suggest that non-canonical and canonical NF-κB activation in the lung epithelium have different effects on inflammatory signaling and inflammatory cell recruitment. Over-expression of constitutively active IKKβ in the lung epithelium drives canonical NF-κB pathway activation causing a profound inflammatory response and elevated chemokine production (Cheng et al., 2007). In Chapter 3, we saw that over-expression of the non-canonical pathway effector p52 did not cause inflammation on its own. Here, in the setting of LPS treatment, p52 over-expression led to increased inflammatory cell influx into the lungs, although it is likely that the inflammatory cell infiltrate is an indirect effect of epithelial cell death and altered barrier function. While other studies have suggested that p52 cooperates in regulating inflammatory cytokines in airway epithelial cells (Tully et al., 2012), we observed no differences in inflammatory cytokine production. In contrast, RelB over-expression led to increased inflammatory cell recruitment, which was not enhanced further by p52 over-expression. However, in the setting of LPS stimulation, we found that RelB over-expression did not augment lung inflammation and injury, indicating that p52 is the functional effector of the non-canonical NF-κB pathway in this model. In a different inflammatory context, RelB has

been shown to limit cigarette smoke-induced inflammatory cell recruitment and cytokine production (McMillan et al., 2011). Collectively, these data imply that different NF-κB pathway components are uniquely involved in regulating lung epithelial inflammatory signaling, and their effects on inflammation may depend on the specific inflammatory signaling environment.

The discovery that p52 over-expression promotes apoptosis of airway epithelial cells after LPS stimulation was unexpected, as many studies have suggested that p52 is pro-survival/proliferative. In fibroblasts, p52 and RelB protect against ROS-induced senescence by regulating CDK4 and CDK6 expression and antagonizing p53 function (Iannetti et al., 2014), and in prostate cancer cells, p52 promotes proliferation through regulation of cyclin D1 (Nadiminty et al., 2008). *In vivo* studies have demonstrated that expression of p100 in the mammary gland leads to hyperplasia (Connelly et al., 2007) and global p52 expression caused by deletion of the C-terminal inhibitory domain causes hyperplasia of the gastric epithelium (Ishikawa et al., 1997). In our studies, we found that p52 promoted epithelial cell apoptosis only in the context of acute cellular stressors, including LPS treatment *in vivo*. In contrast, we observed no differences in bleomycin-induced fibrosis in CCSP-p52 mice. In this model bleomycin causes direct DNA damage leading to cell-cycle arrest and apoptosis of airway and alveolar epithelial cells, followed by inflammation and fibrosis. Although it is possible that apoptosis of CCSP-expressing cells does not impact the degree of bleomycin-induced inflammation and fibrosis, the lack of phenotypic differences between CCSP-p52 mice and WT mice suggests that p52 may have a different functional role in this direct epithelial injury model compared to LPS treatment, which can induce epithelial cell death through extrinsic and intrinsic apoptosis pathways as well as activation of effector cells, particularly neutrophils (Neff et al., 2006).

Interestingly, of the ten pro-apoptotic genes we identified with increased expression in p52 over-expressing cells during serum starvation, nine are known to be regulated by NF-κB signaling (Bcl2l11, Casp4, Fas, and Pycard) or contain NF-κB consensus sequence binding sites in their promoters (Bcl10, Bid, Bok, Casp7, and Gadd45α), indicating that p52 may preferentially bind these gene promoters under conditions of cellular stress. Structurally, p52 lacks a transactivation domain, suggesting that interactions

with other NF-κB family members or transcriptional co-factors are necessary for regulation of target genes. In the setting of cellular stress, the pool of available NF-κB binding partners may be altered or additional transcriptional co-factor(s) that cooperate with p52 may be activated, affecting p52 binding site preferences. Additionally, epigenetic changes may occur as a result of stress signals that alter accessibility of regulatory regions of pro-apoptotic genes. Future studies are necessary to identify factors that modulate the transcriptional outcome of p52 activation in different contexts.

Prior studies have demonstrated that LPS stimulation causes apoptosis of airway epithelial cells in murine models (Kawasaki et al., 2000; Vernooy et al., 2001), and our studies suggest that p52 augments this apoptotic response. Although we cannot conclude that enhanced epithelial cell apoptosis is directly responsible for increased mortality of CCSP-p52 mice following LPS treatment, epithelial cell apoptosis has been shown to impact the degree of lung injury and survival of rodents after LPS administration (Kawasaki et al., 2000). Similarly, epithelial cell apoptosis is a prominent feature in the lungs of humans with ARDS (Albertine et al., 2002; Bardales et al., 1996; Galani et al., 2010; Guinee et al., 1996; Lee et al., 2008), and the degree of epithelial injury is an important factor predicting patient outcome (Albertine et al., 2002; Matthay and Wiener-Kronish, 1990). The identification of increased nuclear p52 in lungs of ARDS patients combined with the effects of p52 expression in the LPS model of ARDS/acute lung injury indicate that non-canonical NF-κB signaling could be an important factor in regulating epithelial cell survival/apoptosis, barrier integrity, and disease severity in patients with ARDS. Although more investigation is required to better understand the function of p52 in the setting of ARDS, our studies indicate that p52 interactions and/or target genes may serve as potential therapeutic targets for patients with ARDS.

CHAPTER V:

CONCLUSIONS AND FUTURE DIRECTIONS

Summary

In vitro and xenograft models have indicated that canonical NF-κB signaling contributes to TKI-resistance of EGFR-mutant tumors (Bivona et al., 2011; Blakely et al., 2015; De et al., 2014; Galvani et al., 2015), but our studies reveal that canonical NF-κB activation promotes both TKI-sensitive and TKI-resistant EGFR-mediated lung cancer, suggesting a broader role for canonical NF-κB signaling in EGFR-mediated tumorigenesis. Canonical NF-κB inhibition had no measureable effect on apoptosis of EGFR-mutant cells. Instead, canonical pathway signaling was important for recruitment of inflammatory cells, namely tumor-promoting macrophages, suggesting that canonical NF-κB signaling contributes to lung carcinogenesis through paracrine signaling to the tumor microenvironment. These studies implicate canonical NF-κB as a key mediator of the intrinsic inflammatory response in EGFR-mutant tumors and suggest that therapeutic targeting of inflammatory cells, particularly macrophages, may be beneficial in patients with EGFR-mutant lung cancer.

Increased expression of non-canonical pathway components have been observed in lung cancer (Dimitrakopoulos et al., 2012). Our findings suggest that p52 activation is a common phenomenon in lung adenocarcinoma and provide the first evidence of the functional involvement of non-canonical NF-κB signaling in lung carcinogenesis. In contrast to the role of canonical NF-κB signaling in lung tumors described above, non-canonical NF-κB activation enhanced proliferation of lung epithelial cells, leading to increased tumor number, enhanced tumor size, and more malignant tumors. While others have suggested that non-canonical NF-κB signaling can contribute to regulation of pro-inflammatory cytokines (Tully et al., 2012), no changes in inflammatory cell recruitment or inflammatory cytokine and chemokine production were observed as a result of p52 over-expression alone. In the context of the inflammatory stimulus LPS, p52 over-expression led to apoptosis of airway epithelial cells. Increased

macrophages and neutrophils were observed in the setting of p52 over-expression with LPS stimulation. However, this inflammatory influx was likely an indirect effect of the increased lung injury and altered barrier permeability caused by p52 over-expression, since concomitant changes in chemokine production were not measured. Increased p100/p52 expression was observed in the lungs of ARDS patients, implicating p52 in the pathogenesis of this disease. Together, these data suggest that non-canonical NF-κB signaling functions primarily in a cell autonomous manner to regulate cell survival/apoptosis and proliferation.

Overall, these studies indicate that both non-canonical and canonical NF-κB signaling in the lung epithelium contribute to carcinogenesis, functioning through different but complementary methods to promote tumors. While these findings extend our understanding on the role of canonical and non-canonical NF-κB signaling in lung cancer, they also generate several important unanswered questions and suggest future experiments as discussed below.

Canonical NF-κB Signaling as a Regulator of Pro-Tumorigenic Inflammatory Cell Recruitment

In Chapter 2, we show that canonical NF-κB inhibition has no measureable effect on survival of EGFR-mutant tumor cells, yet in other models of lung cancer, canonical NF- κB signaling has been suggested to promote cell survival. In mouse models of urethane-induced and KRAS-driven lung cancers, inhibition of canonical NF-κB increased apoptosis or reduced proliferation (Bassères et al., 2010; Meylan et al., 2009; Stathopoulos et al., 2007; Xia et al., 2012), although whether these findings are a direct or indirect effect of NF-κB inhibition is unclear. Supporting our findings, others have reported that canonical NF-κB inhibition did not affect proliferation of human lung cancer cell lines (Hopewell et al., 2013). Our studies do not rule out a role for canonical NF-κB signaling in the survival and proliferation of EGFR-mutant lung tumors but suggest that cell-extrinsic signaling to recruit inflammatory cells may be a more important pro-tumor function of canonical NF-κB signaling in lung carcinogenesis.

Although our studies suggest that epithelial canonical NF-κB signaling generates a tumor-supportive inflammatory microenvironment, NF-κB-mediated paracrine signaling may not always

function in a pro-tumorigenic manner. Instead, canonical NF-κB signaling may be important for regulating the balance between a pro- and anti-tumor inflammatory microenvironment in lung cancer. Hopewell, et al. demonstrated that high levels of canonical NF-κB signaling in a murine lung cancer cell line led to recruitment of cytotoxic CD8+ T cells and reduced tumor burden (Hopewell et al., 2013), suggesting that canonical NF-κB activation could contribute to tumor rejection. In contrast, canonical NF-κB signaling in the lung epithelium has also been shown to prevent tumor elimination by recruiting T regulatory cells, promoting T cell-mediated immune suppression through inhibition of cytotoxic CD8+ T cell recruitment (Zaynagetdinov et al., 2011b). Interestingly, in murine and human lung cancer cell lines, canonical NF-κB activation increases expression of both pro-tumor chemokines as well as anti-tumor chemokines, and in human tumors, expression of these NF-κB-regulated anti-tumor and pro-tumor chemokine profiles are mutually exclusive (Hopewell et al., 2013). Furthermore, this same study demonstrated that pro-tumor chemokine expression was significantly associated with poor overall survival of lung cancer patients, while high expression of chemokine genes involved in anti-tumor responses was associated with significantly improved survival, suggesting that canonical NF-κB signaling can have differential effects on the inflammatory microenvironment of lung tumors that could affect patient outcome. Whether canonical NF-κB signaling promotes pro- or anti-tumor immunity could be dependent on the oncogenic driver, the level of NF-κB activation, or microenvironmental stimuli that cause selective induction of different chemokine subsets, and studies to identify these factors could yield novel therapeutic targets that take advantage of canonical NF-κB activation in tumors to modulate pro-tumor signaling to anti-tumor. Even though we did not observe differences in T cell numbers in our analysis, these studies also indicate that T cell recruitment is another important extrinsic function of canonical NF-κB signaling in lung tumors and suggest that the effect of T cell recruitment on tumors may depend on the ratio of the specific T cell populations in the tumor microenvironment.

Therapeutic Targeting of Macrophages in Lung Cancer

Our findings demonstrate that NF-κB-mediated inflammatory cell recruitment is important for

promoting EGFR-mutant lung tumors, suggesting that immunotherapeutic approaches, specifically those targeting macrophages, may be beneficial in patients with TKI-sensitive or TKI-resistant EGFR-mutant lung tumors. Because macrophages can promote tumors through a variety of mechanisms, a diverse array of strategies are being explored to therapeutically target them. The major approach has focused on preventing macrophage recruitment by inhibiting the MCP-1/CCL2 receptor or CSF1/M-CSF signaling (Noy and Pollard, 2014). However, in our studies, we did not measure significant differences in MCP-1/CCL2 or CSF1/M-CSF, suggesting a different mediator may be the dominant macrophage chemotactic factor in our model. Whether these inhibitors would reduce macrophage recruitment and consequently tumor burden in EGFR-driven pre-clinical models or in patients with EGFR-mutant lung cancer is unclear. Future studies to identify the NF-κB-regulated mechanism of macrophage recruitment in the $EGFR^{L858R}$ and $EGFR^{L/T}$ lung cancer models may identify novel therapeutic targets.

Therapies that target macrophage function or shift macrophage polarization, rather than their recruitment, could also be effective patients with EGFR-mutant lung cancers. Macrophages are an important producer of vascular endothelial growth factor (VEGF), which promotes high density angiogenesis and vessel leakiness in tumors. Depletion of alveolar macrophages reduces VEGF levels and therefore angiogenesis and tumor burden in a model of chemical carcinogen-induced lung tumorigenesis (Zaynagetdinov et al., 2011a), and bevacizumab, a VEGF monoclonal antibody, has been approved for treatment of NSCLC patients (Sandler et al., 2006). Macrophages can also directly suppress T cell proliferation and cytotoxic T cell function by expressing the PD-L1 or B7 ligands for the T cell receptors PD-1 or CTLA-4 receptors, respectively (Kuang et al., 2009; Linsley et al., 1994), and therapies targeting these interactions have already been approved for patients with NSCLC. IL-4 production by CD4+ T cells and tumor cells can induce an immunosuppressive, pro-tumor phenotype in macrophages (Coussens et al., 2013; DeNardo et al., 2009; Gocheva et al., 2010), and antagonist αIL-4 antibodies reprogram tumor-associated M2 macrophages, as well as other immunosuppressive immune cell types, toward an M1 phenotype in mammary cancer (DeNardo et al., 2009). Future studies to investigate the specific mechanism(s) by which macrophages promote EGFR-mediated lung tumorigenesis in our pre-clinical

models will provide valuable evidence regarding whether these therapies may benefit patients with EGFR mutations in their tumors.

Non-canonical NF-κB Signaling as a Regulator of Cell Survival/Proliferation and Apoptosis

A number of studies by others have suggested that non-canonical NF-κB signaling promotes cell survival/proliferation in a variety of cell types, including cancer cells (Connelly et al., 2007; Cormier et al., 2013; De Donatis et al., 2015; Iannetti et al., 2014; Ishikawa et al., 1997; Nadiminty et al., 2008), supporting our findings in urethane-induced lung cancer. However, our results extend the role of p52 to the promotion of apoptosis in certain contexts, suggesting that the net effect of non-canonical NF-κB activation may be dependent on the specific nature or level of cellular stress. The particular cell type may also influence the consequence of non-canonical NF-κB activation. Future studies employing SPC-rtTA mice (Perl et al., 2002) to drive p52 over-expression in type II pneumocytes would be useful for determining whether p52-induced proliferation after urethane and apoptosis after LPS are conserved mechanisms in lung epithelial cells. p52 likely promotes proliferation/apoptosis through changes in transcriptional regulation, since p52 over-expression led to increased mRNA levels of proliferative and apoptotic factors. Differential availability of other NF-κB family members or activation of transcriptional co-factors may modify p52 binding site preferences in different contexts. Additionally, epigenetic changes could occur that alter the availability of gene regulatory regions, thus affecting p52-mediated transcription. Studies to elucidate the contextual modifiers that affect p52 transcription could identify novel therapeutic targets, as modulation of these factors could potentially convert the pro-proliferative effect of p52 in the context of lung cancer to a pro-apoptotic effect.

One potential cofactor that could be involved in modifying p52 transcription is p53. The p53 transcription factor regulates transcriptional responses to cell cycle checkpoint engagement, DNA damage, and environmental stress, and in tumors, functions as a tumor suppressor. p53 can recruit p52 to promoters of p53 target genes to modulate their expression (Schumm et al., 2006), but the outcome of this p52-p53 crosstalk may depend on the relative levels of activation of each pathway. p52 cooperates with

p53 to promote expression of pro-apoptotic genes in cells with inducible p53 expression and in the context of UV-induced DNA damage, which strongly activates p53 (Schumm et al., 2006). In contrast, in a setting with lower levels of p53 activation, p52 has been shown to prevent ROS-induced senescence by antagonizing expression of p53-regulated genes (Iannetti et al., 2014). In the setting of an acute cellular stressor such as serum starvation or high-dose LPS, high levels of p53 activation may dominate the response and p52 may work together with p53 to promote apoptosis. Conversely, in lung cancer, high levels of p52 may enable p52 to overcome the effects of oncogene-mediated p53 activation, promoting proliferation of tumor cells. In addition to increased tumor burden, we observed enhanced malignant progression of lung tumors in CCSP-p52 mice. p53 is mutated in 50-70% of lung adenocarcinoma tumors (Herbst et al., 2008), and studies in genetic models of KRAS-induced lung tumorigenesis suggest that suppression of p53 activation is required for tumors to progress from adenomas to more malignant tumor stages (Feldser et al., 2010; Junttila et al., 2010). Our data suggest that non-canonical NF-κB and specifically p52 activation could be a mechanism enabling malignant progression of tumors retaining wild-type p53.

A second candidate cofactor that could affect p52 transcription is Bcl-3, an atypical member of the IκB family. Bcl-3 forms a complex with p52 homodimers to regulate gene transcription (Bours et al., 1993). Specifically, p52/Bcl-3 complexes have been shown to promote transcription of cyclin D1 (Rocha et al., 2003; Wang et al., 2010), but these complexes can also inhibit target gene transcription. Whether p52/Bcl-3 complexes cause transcriptional activation or repression may depend on the concentration and phosphorylation status of Bcl-3 (Bundy et al., 1997). Little is known about the role of Bcl-3 in epithelial cells during lung inflammation and carcinogenesis, so studies investigating Bcl-3 in these settings may provide further insight into p52 function and gene transcription.

Epigenetic factors could also modify the transcriptional landscape of the cell, affecting the transcriptional outcome of p52 activation in different contexts. p52 has been shown to recruit and, in some cases, directly interact with epigenetic modifiers, including histone acetyl transferases (HATs) p300 and cyclic-AMP response element binding protein (CBP) and histone deacetylase (HDAC) 1, HDAC2,

and HDAC4. Histone acetylation relaxes the interactions between the histone molecule and DNA, making DNA more accessible for transcription factor binding. In the placenta, binding of RelB and p52 enabled CBP recruitment and target gene transcription (Stefano et al., 2015). p52 can also recruit p300 to gene promoters, including the promoters of pro-apoptotic factors DR5 and PUMA, resulting in increased transcription (Nadiminty et al., 2010; Schumm et al., 2006). Conversely, histone deacetylation condenses the chromatin structure, repressing transcription. After UV stimulation, p52-HDAC1 complexes inhibit cyclin D1 transcription (Rocha et al., 2003). In multiple myeloma, a complex consisting of p52, RelB, and HDAC4 maintains repressive chromatin around pro-apoptotic genes *Bim* and *BMF*, and this complex was necessary for cell survival and tumor growth (Vallabhapurapu et al., 2015). In some instances both HAT and HDAC proteins are simultaneously recruited to promoters by p52 (Schumm et al., 2006; Stefano et al., 2015), suggesting that p52 may play a role in regulating the balance of histone acetylation and the activation state of chromatin. Adding another layer of complexity, HAT and HDAC proteins can also directly modify transcription factors such as p53 and NF-κB, although the effect of this modification on p52 remains unclear (Deng et al., 2006; Hu and Colburn, 2005). In lung cancer, increased expression of HDAC1 is associated with more advanced tumors and correlates with poor prognosis (Minamiya et al., 2011; Sasaki et al., 2004), and HDAC inhibitors have been proposed as therapies for patients with lung cancer (Neal and Sequist, 2012). Future studies to understand the interactions between non-canonical NF-κB signaling, HATs, and HDACs could identify novel therapeutic options for patients with p52 activation in their tumors.

Crosstalk between Canonical and Non-canonical NF-κB Signaling Pathways

While the paradigm of distinct canonical and non-canonical NF-κB signaling pathways is useful for thinking about NF-κB signaling, numerous studies suggest that extensive crosstalk occurs between these pathways, indicating that NF-κB signaling is likely much more complex physiologically. The canonical pathway can induce non-canonical pathway activation transcriptionally through regulation of the *Nfkb2* and *Relb* genes by p65/p50 heterodimers (Bren et al., 2001; Lombardi et al., 1995). The non-canonical pathway can also inhibit the canonical pathway through the C-terminal domain of p100, also

known as IκBδ (Shih et al., 2009), forming a negative feedback loop. Mice expressing a mutant form of p100 that is unable to undergo proteolytic processing show reduced activation of p65-containing dimers (Tucker et al., 2007), suggesting that IκBδ may sequester the canonical pathway heterodimer in the absence of IKKα activation (Shih et al., 2009). Activation of non-canonical pathway signaling can then lead to canonical pathway signaling through proteolytic processing of the C-terminal domain of p100, freeing bound p65/p50 (Basak et al., 2007).

Dimerization of NF-κB family members is more extensive than represented by the traditional p65/p50 and Relb/p52 heterodimers associated with canonical and non-canonical NF-κB signaling. In lymphoblastoid B cells, eleven different dimer combinations have been observed (Zhao et al., 2014). Different dimer combinations may have specific binding site affinities dictated by DNA sequence variations as small as a single nucleotide, affecting target gene transcription (Bonizzi et al., 2004; Fusco et al., 2009; Kunsch et al., 1992; Leung et al., 2004; Siggers et al., 2011), and dimers containing p52 may be recruited more frequently to atypical binding sites that lack a κB consensus sequence (Zhao et al., 2014). Many NF-κB target genes have multiple κB sites in their promoters, and gene expression analysis of lymphotoxin β-stimulated mouse embryonic fibroblasts revealed that the majority of induced genes require both p65- and RelB-containing dimers (Lovas et al., 2008), suggesting that transcriptional regulation may involve an interplay of different dimers at several sites in gene promoters. However, the differential specificity of NF-κB family members is not solely determined by DNA-protein interactions but may also be influenced by other transcription factors (Hoffmann et al., 2003; Wang et al., 2007; Zhao et al., 2014). Upon binding to specific κB sites, dimer pairs may adopt distinct DNA sequence-dependent conformations that are differentially recognized by other transcriptional cofactors (Chen-Park et al., 2002; Leung et al., 2004). In addition, chromatin configuration can control the steric accessibility of binding sites for different dimers (Saccani et al., 2001).

While the studies described here demonstrate that both canonical and non-canonical NF-κB signaling contribute to lung carcinogenesis, our understanding of how interactions between these pathways affect lung cancer is limited. The lack of therapeutic efficacy of canonical NF-κB inhibitors in

cancer patients, as discussed below, also suggests that a better understanding of crosstalk between these pathways may improve current treatment strategies. Using currently available mouse models, *in vivo* studies could be performed to explore the effect of p52 over-expression in the absence of canonical pathway activation by crossing DN-IκB mice to CCSP-p52 mice. CCSP-p52 mice could also be combined with p65 conditional knockout mice to determine the impact of p52 over-expression specifically in the absence of p65 (Steinbrecher et al., 2008). Additional *in vitro* studies knocking out combinations of NF-κB family members in cancer cell lines or in conjunction with inflammatory and cell stress stimuli would also enable a detailed analysis of the contributions of each family member in different contexts. Future studies using *in vivo* and *in vitro* models to examine the interactions between the canonical and non-canonical NF-κB signaling pathways in different contexts is necessary to fully understand how NF-κB influences cell survival/proliferation and apoptosis to impact tumorigenesis.

Therapeutic Targeting of NF-κB Signaling in Lung Cancer

A variety of studies have implicated canonical NF-κB signaling as a key regulator of human cancer and inflammatory disease. Consequently, much interest has centered on developing drugs to inhibit canonical NF-κB signaling. Global inhibition of canonical NF-κB signaling has shown therapeutic benefit in some pre-clinical models of lung cancer, with the major strategies focusing on IKKβ or proteasome inhibition, which prevents IκBα degradation. Treatment with the proteasome inhibitor bortezomib, BAY-117082 (a compound which prevents IκBα phosphorylation (Pierce et al., 1997)), and Compound A (a specific IKKβ inhibitor (Ziegelbauer et al., 2005)) have all reduced lung tumor burden in short term *in vivo* studies (Bassères et al., 2014; Karabela et al., 2012; Xue et al., 2011). However, despite evidence from *in vivo* models, including our own studies here, suggesting that canonical NF-κB inhibition inhibits lung carcinogenesis, no therapeutic benefit has been observed in clinical trials thus far (Besse et al., 2012; Fanucchi et al., 2006). Correspondingly, long term treatment with bortezomib in pre-clinical models of lung cancer led to resistance and, in one study, actually enhanced tumor formation (Karabela et al., 2012; Xue et al., 2011). *In vivo* studies also suggest that global IKKβ inhibition could have

undesirable and even detrimental side effects, since signaling through IKKβ is important for gut, skin, and liver homeostasis (Pasparakis, 2009) and inhibition of IKKβ can actually increase IL-1β secretion by myeloid cells (Greten et al., 2007), suggesting that global inhibition of canonical NF-κB signaling at least by these methods may not be the optimal therapeutic strategy for lung cancer patients.

Our findings provide a basis for investigations into targeting the non-canonical NF-κB pathway as a novel therapeutic approach in lung cancer. In Chapter 3, our *in vivo* studies suggested that non-canonical NF-κB activation can promote tumor growth and progression, and analysis of p100/p52 expression in human lung tumor samples suggested that this pathway is active in a large proportion of lung cancer patients. Non-canonical NF-κB signaling has also been shown to compensate for canonical pathway inhibition in diffuse large B cell lymphomas treated with IKKβ inhibitors, indicating that non-canonical pathway activation could limit the therapeutic efficacy of treatment with canonical pathway inhibitors (Lam et al., 2008).

Rational therapeutic strategies for targeting non-canonical NF-κB signaling include inhibition of NIK or IKKα, both key regulators of non-canonical NF-κB signaling. However, few specific inhibitors have been described for these kinases. Currently available IKK inhibitors either function as pan-IKK inhibitors or preferentially target IKKβ, but no selective IKKα inhibitors have been described. While selective NIK inhibitors have been identified, most are only effective *in vitro* due to their poor pharmacokinetic properties. Still, NIK-specific inhibitors induce apoptosis of multiple myeloma cell lines *in vitro* (Demchenko et al., 2014), suggesting that further development of these inhibitors to improve their functionality *in vivo* could be beneficial. Additionally, while non-canonical pathway inhibition could have a therapeutic effect on its own, specific inhibition of non-canonical NF-κB might also allow lower doses of IKKβ inhibitors to achieve comparable blockade of the canonical NF-κB pathway, potentially minimizing the undesirable side effects of IKKβ inhibition (Lam et al., 2008). Other strategies for inhibiting non-canonical NF-κB signaling include membrane-permeable peptides that inhibit nuclear translocation of RelB/p52 and targeting of upstream signaling mediators, such as TNFR-associated factors (TRAFs) and receptor interacting proteins (RIPs) (Storz, 2013; Xu et al., 2008).

The studies described here identify important functions of NF-κB signaling in lung tumors that could be exploited as indirect or downstream therapeutic targets, bypassing the unwanted side effects of and circumventing the need for specific NF-κB inhibitors. Our studies in Chapter 2 identified macrophage recruitment as a critical factor regulated by canonical NF-κB signaling that could be therapeutically targeted through a variety of mechanisms as discussed above. In Chapter 3, we identified a network of non-canonical pathway-associated genes that could potentially serve as indirect therapeutic targets in tumors with non-canonical pathway activation. In this network, several of the nodes (defined as having 4 or more connections) have targeted therapies currently in development for clinical use, including aurora kinase B (AURKB), CDK1, polo-like kinase 1 (PLK1) (Chopra et al., 2010; Kollareddy et al., 2012; Lapenna and Giordano, 2009), suggesting that these therapies may be beneficial for hindering the tumor-promoting effect of non-canonical pathway activation in lung cancer. As discussed above, studies to identify factors that can convert the pro-proliferative role of non-canonical NF-κB signaling in tumors to the pro-apoptotic effect observed in studies of acute cellular stress in Chapter 4 could also identify novel therapeutic targets to modulate non-canonical NF-κB signaling. Additionally, combined strategies targeting canonical and/or non-canonical signaling in conjunction with TKIs may be beneficial for patients with lung cancer, particularly since canonical NF-κB signaling has been proposed as a mechanism of therapeutic resistance to several EGFR inhibitors (Bivona et al., 2011; Galvani et al., 2015).

Concluding Remarks

The studies here demonstrate that both canonical and non-canonical NF-κB signaling can promote lung tumors and provide new insights into their mechanistic functions during carcinogenesis. Importantly, the complexities of canonical and non-canonical NF-κB signaling indicate that the consequences of pathway activation, as well as inhibition, can be dependent on the specific cell type and context. These studies advance our understanding of lung tumor development and progression as well as

NF-κB signaling in cancer and inflammation, while pointing toward new therapies for lung cancer patients that should be tested in preclinical models.

REFERENCES

Adamson, I., Bowden, D., 1974. The type 2 cell as progenitor of alveolar epithelial regeneration. A cytodynamic study in mice after exposure to oxygen. Lab. Investig. 30, 35–42.

Ahrendt, S.A., Decker, P.A., Alawi, E.A., Zhu Yr, Y.R., Sanchez-Cespedes, M., Yang, S.C., Haasler, G.B., Kajdacsy-Balla, A., Demeure, M.J., Sidransky, D., 2001. Cigarette smoking is strongly associated with mutation of the K-ras gene in patients with primary adenocarcinoma of the lung. Cancer 92, 1525–1530.

Alberti, C., Pinciroli, P., Valeri, B., Ferri, R., Ditto, A., Umezawa, K., Sensi, M., Canevari, S., Tomassetti, A., 2012. Ligand-dependent EGFR activation induces the co-expression of IL-6 and PAI-1 via the NFkB pathway in advanced-stage epithelial ovarian cancer. Oncogene 31, 4139–4149.

Albertine, K.H., Soulier, M.F., Wang, Z., Ishizaka, A., Hashimoto, S., Zimmerman, G.A., Matthay, M.A., Ware, L.B., 2002. Fas and fas ligand are up-regulated in pulmonary edema fluid and lung tissue of patients with acute lung injury and the acute respiratory distress syndrome. Am. J. Pathol. 161, 1783–1796.

Ancrile, B., Lim, K.-H., Counter, C.M., 2007. Oncogenic Ras-induced secretion of IL6 is required for tumorigenesis. Genes Dev. 21, 1714–1719.

Ashburner, M., Ball, C.A., Blake, J.A., Botstein, D., Butler, H., Cherry, J.M., Davis, A.P., Dolinski, K., Dwight, S.S., Eppig, J.T., Harris, M.A., Hill, D.P., Issel-Tarver, L., Kasarskis, A., Lewis, S., Matese, J.C., Richardson, J.E., Ringwald, M., Rubin, G.M., Sherlock, G., 2000. Gene ontology: tool for the unification of biology. The Gene Ontology Consortium. Nat. Genet. 25, 25–29.

Bardales, R.H., Xie, S.-S., Schaefer, R.F., Hsu, S.-M., 1996. Apoptosis is a major pathway responsible for the resolution of type II pneumocytes in acute lung injury. Am. J. Pathol. 149, 845–852.

Basak, S., Kim, H., Kearns, J., Tergaonkar, V., O'Dea, E., Werner, S., Benedict, C., Ware, C., Ghosh, G., Verma, I., Hoffmann, A., 2007. A fourth IκB protein within the NF-κB signaling module. Cell 128, 369–381.

Bassères, D.S., Ebbs, A., Cogswell, P.C., Baldwin, A.S., 2014. IKK is a therapeutic target in KRAS-induced lung cancer with disrupted p53 activity. Genes Cancer 5, 41–55.

Bassères, D.S., Ebbs, A., Levantini, E., Baldwin, A.S., 2010. Requirement of the NF-κB subunit p65/RelA for K-Ras-induced lung tumorigenesis. Cancer Res 70, 3537–3546.

Bellocq, A., Antoine, M., Flahault, A., Philippe, C., Crestani, B., Bernaudin, J.F., Mayaud, C., Milleron, B., Baud, L., Cadranel, J., 1998. Neutrophil alveolitis in bronchioloalveolar carcinoma: induction by tumor-derived interleukin-8 and relation to clinical outcome. Am. J. Pathol. 152, 83–92.

Benjamini, Y., Hochberg, Y., 1995. Controlling the false discovery rate: a practical and powerful approach to multiple testing. J. R. Stat. Soc. B 57, 289–300.

Besse, B., Planchard, D., Veillard, A.-S., Taillade, L., Khayat, D., Ducourtieux, M., Pignon, J.-P., Lumbroso, J., Lafontaine, C., Mathiot, C., Soria, J.-C., 2012. Phase 2 study of frontline bortezomib in patients with advanced non-small cell lung cancer. Lung Cancer 76, 78–83.

Bivona, T.G., Hieronymus, H., Parker, J., Chang, K., Taron, M., Rosell, R., Moonsamy, P., Dahlman, K., Miller, V.A., Costa, C., Hannon, G., Sawyers, C.L., 2011. FAS and NF-κB signalling modulate dependence of lung cancers on mutant EGFR. Nature 471, 523–526.

Blackwell, T.S., Lancaster, L.H., Blackwell, T.R., Venkatakrishnan, A., Christman, J.W., 1999. Differential NF-κB activation after intratracheal endotoxin. Am. J. Physiol. 277, L823–L830.

Blakely, C.M., Pazarentzos, E., Olivas, V., Asthana, S., Yan, J.J., Tan, I., Hrustanovic, G., Chan, E., Lin, L., Neel, D.S., Newton, W., Bobb, K.L., Fouts, T.R., Meshulam, J., Gubens, M.A., Jablons, D.M., Johnson, J.R., Bandyopadhyay, S., Krogan, N.J., Bivona, T.G., 2015. NF-κB-activating complex engaged in response to EGFR oncogene inhibition drives tumor cell survival and residual disease in lung cancer. Cell Rep. 11, 98–110.

Bolstad, B.M., Irizarry, R.A., Åstrand, M., Speed, T.P., 2003. A comparison of normalization methods for high density oligonucleotide array data based on variance and bias. Bioinformatics 19, 185–193.

Bonizzi, G., Bebien, M., Otero, D.C., Johnson-Vroom, K.E., Cao, Y., Vu, D., Jegga, A.G., Aronow, B.J., Ghosh, G., Rickert, R.C., Karin, M., 2004. Activation of IKKα target genes depends on recognition

of specific κB binding sites by RelB:p52 dimers. EMBO J 23, 4202–4210.

Borghaei, H., Paz-Ares, L., Horn, L., Spigel, D.R., Steins, M., Ready, N.E., Chow, L.Q., Vokes, E.E., Felip, E., Holgado, E., Barlesi, F., Kohlhäufl, M., Arrieta, O., Burgio, M.A., Fayette, J., Lena, H., Poddubskaya, E., Gerber, D.E., Gettinger, S.N., Rudin, C.M., Rizvi, N., Crinò, L., Blumenschein Jr., G.R., Antionia, S.J., Dorange, C., Harbison, C.T., Graf Finckenstein, F., Brahmer, J.R., 2015. Nivolumab versus docetaxel in advanced squamous-cell non-small-cell lung cancer. N. Engl. J. Med. 373, 1627–1639.

Bours, V., Franzoso, G., Azarenko, V., Park, S., Kanno, T., Brown, K., Siebenlist, U., 1993. The oncoprotein Bcl-3 directly transactivates through κB motifs via association with DNA-binding p50B homodimers. Cell 72, 729–739.

Boxio, R., Bossenmeyer-Pourie, C., Steinckwich, N., Dournon, C., Nu, O., 2004. Mouse bone marrow contains large numbers of functionally competent neutrophils. J. Leukoc. Biol. 75, 604–611.

Bray, F., Weiderpass, E., 2009. Lung cancer mortality trends in 36 European countries: secular trends and birth cohort patterns by sex and region 1970-2007. Int. J. Cancer 126, 1454–1466.

Bren, G.D., Solan, N.J., Miyoshi, H., Pennington, K.N., Pobst, L.J., Paya, C. V, 2001. Transcription of the RelB gene is regulated by NF-κB. Oncogene 20, 7722–7733.

Brown, K., Park, S., Kanno, T., Franzoso, G., Siebenlist, U., 1993. Mutual regulation of the transcriptional activator NF-κB and its inhibitor IκB-α. Proc. Natl. Acad. Sci. U. S. A. 90, 2532–2536.

Bundy, D.L., Mckeithan, T.W., Bundy, D.L., Mckeithan, T.W., 1997. Diverse effects of BCL3 phosphorylation on its modulation of NF- κB p52 homodimer binding to DNA. J. Biol. Chem. 272, 33132–33139.

Caamaño, J.H., Rizzo, C.A., Durham, S.K., Barton, D.S., Raventós-Suárez, C., Snapper, C.M., Bravo, R., 1998. Nuclear Factor (NF)-κB2 (p100/p52) is required for normal splenic microarchitecture and B cell-mediated immune responses. J. Exp. Med. 187, 185–196.

Carvalho, B.S., Irizarry, R.A., 2010. A framework for oligonucleotide microarray preprocessing.

Bioinformatics 26, 2363–2367.

Chen, Z., Parent, L., Maniatis, T., 1996. Site-specific phosphorylation of IκBα by a novel ubiquitination-dependent protein kinase activity. Cell 84, 853–862.

Cheng, D.-S., Han, W., Chen, S.M., Sherrill, T.P., Chont, M., Park, G.-Y., Sheller, J.R., Polosukhin, V. V, Christman, J.W., Yull, F.E., Blackwell, T.S., 2007. Airway epithelium controls lung inflammation and injury through the through the NF-κB pathway. J. Immunol. 178, 6504–6513.

Chen-Park, F.E., Huang, D.B., Noro, B., Thanos, D., Ghosh, G., 2002. The κB DNA sequence from the HIV long terminal repeat functions as an allosteric regulator of HIV transcription. J. Biol. Chem. 277, 24701–24708.

Cho, H.C., Lai, C.Y., Shao, L.E., Yu, J., 2011. Identification of tumorigenic cells in Kras G12D-induced lung adenocarcinoma. Cancer Res. 71, 7250–7258.

Chopra, P., Sethi, G., Dastidar, S., Ray, A., 2010. Polo-like kinase inhibitors: an emerging opportunity for cancer therapeutics. Expert Opin. Investig. Drugs 19, 27–43.

Cogswell, P.C., Guttridge, D.C., Funkhouser, W.K., Baldwin, A.S., 2000. Selective activation of NF-κB subunits in human breast cancer: potential roles for NF-κB2/p52 and for Bcl-3. Oncogene 19, 1123–1131.

Connelly, L., Robinson-Benion, C., Chont, M., Saint-Jean, L., Li, H., Polosukhin, V. V, Blackwell, T.S., Yull, F.E., 2007. A transgenic model reveals important roles for the NF-κB alternative pathway (p100/p52) in mammary development and links to tumorigenesis. J. Biol. Chem. 282, 10028–10035.

Coope, H.J., Atkinson, P.G.P., Huhse, B., Belich, M., Janzen, J., Holman, M.J., Klaus, G.G.B., Johnston, L.H., Ley, S.C., 2002. CD40 regulates the processing of NF-κB2 p100 to p52. EMBO J. 21, 5375–5385.

Cormier, F., Monjanel, H., Fabre, C., Billot, K., Sapharikas, E., Chereau, F., Bordereaux, D., Molina, T.J., Avet-Loiseau, H., Baud, V., 2013. Frequent engagement of RelB activation is critical for cell survival in multiple myeloma. PLoS One 8, e59127.

Coussens, L., Zitvogel, L., Palucka, A., 2013. Neutralizing tumor-promoting chronic inflammation: a

magic bullet? Science 339, 286–291.

Crusz, S.M., Balkwill, F.R., 2015. Inflammation and cancer: advances and new agents. Nat. Rev. Clin. Oncol. 12, 584–596.

Dallegri, F., Ottonello, L., Ballestrero, A., Dapino, P., Ferrando, F., Patrone, F., Sacchetti, C., 1991. Tumor cell lysis by activated human neutrophils: analysis of neutrophil-delivered oxidative attach and role of leukocyte function-associated antigen 1. Inflammation 15, 15–30.

Davidson, M., Gazdar, A., Clarke, B., 2013. The pivotal role of pathology in the management of lung cancer. J. Thorac. Dis. 5 Suppl 5, S463–S478.

De Donatis, G.M., Pape, E.L., Pierron, A., Cheli, Y., Hofman, V., Hofman, P., Allegra, M., Zahaf, K., Bahadoran, P., Rocchi, S., Bertolotto, C., Ballotti, R., Passeron, T., 2015. NF-kB2 induces senescence bypass in melanoma via a direct transcriptional activation of EZH2. Oncogene 1–11.

De, S., Dermawan, J.K.T., Stark, G.R., 2014. EGF receptor uses SOS1 to drive constitutive activation of NFκB in cancer cells. Proc. Natl. Acad. Sci. U. S. A. 111, 11721–11726.

Dejardin, E., Droin, N.M., Delhase, M., Haas, E., Cao, Y., Makris, C., Li, Z.-W., Karin, M., Ware, C.F., Green, D.R., 2002. The lymphotoxin-β receptor induces different patterns of gene expression via two NF-κB pathways. Immunity 17, 525–535.

Demchenko, Y., Brents, L., Li, Z., Bergsagel, L., McGee, L., Kuehl, M., 2014. Novel inhibitors are cytotoxic for myeloma cells with NFκB inducing kinase-dependent activaton of NFκB. Oncotarget 5, 4554–4566.

DeNardo, D., Barreto, J., Andreu, P., Vasquez, L., Tawfik, D., Kolhatkar, N., Coussens, L., 2009. CD4+ T cells regulate pulmonary metastasis of mammary carcinomas by enhancing protumor properties of macrophages. Cancer Cell 16, 91–102.

Deng, W.G., Tang, S.T., Tseng, H.P., Wu, K.K., 2006. Melatonin suppresses macrophage cyclooxygenase-2 and inducible nitric oxide synthase expression by inhibiting p52 acetylation and binding. Blood 108, 518–524.

Desai, T.J., Brownfield, D.G., Krasnow, M.A., 2014. Alveolar progenitor and stem cells in lung

development, renewal and cancer. Nature 507, 190–194.

Dimitrakopoulos, F.I.D., Antonacopoulou, A.G., Kottorou, A., Vlotinou, H., Panagopoulos, N.D., Dougenis, D., Scopa, C., Papadaki, H., Kalofonos, H.P., 2012. NSCLC and the alternative pathway of NF-κB: uncovering an unknown relation. Virchows Arch. 460, 515–523.

Evans, M., Cabral, L., Stephens, R., Freeman, G., 1975. Transformation of alveolar type 2 cells to type 1 cells following exposure to NO2. Exp. Mol. Pathol. 22, 142–150.

Everhart, M.B., Han, W., Parman, K.S., Polosukhin, V. V, Zeng, H., Sadikot, R.T., Li, B., Yull, F.E., Christman, J.W., Blackwell, T.S., 2005. Intratracheal administration of liposomal clodronate accelerates alveolar macrophage reconstitution following fetal liver transplantation. J. Leukoc. Biol. 77, 173–180.

Ezzati, M., Lopez, A., 2003. Estimates of global mortality attributable to smoking in 2000. Lancet 362, 847–852.

Falcon, S., Gentleman, R., 2007. Using GOstats to test gene lists for GO term association. Bioinformatics 23, 257–258.

Fanucchi, M.P., Fossella, F. V, Belt, R., Natale, R., Fidias, P., Carbone, D.P., Govindan, R., Raez, L.E., Robert, F., Ribeiro, M., Akerley, W., Kelly, K., Limentani, S. a, Crawford, J., Reimers, H.-J., Axelrod, R., Kashala, O., Sheng, S., Schiller, J.H., 2006. Randomized phase II study of bortezomib alone and bortezomib in combination with docetaxel in previously treated advanced non-small-cell lung cancer. J. Clin. Oncol. 24, 5025–5033.

Feldser, D.M., Kostova, K.K., Winslow, M.M., Taylor, S.E., Cashman, C., Whittaker, C.A., Sanchez-Rivera, F.J., Resnick, R., Bronson, R., Hemann, M.T., Jacks, T., 2010. Stage-specific sensitivity to p53 restoration during lung cancer progression. Nature 468, 572–575.

Franzoso, G., Carlson, L., Poljak, L., Shores, E.W., Epstein, S., Leonardi, A., Grinberg, A., Tran, T., Scharton-Kersten, T., Anver, M., Love, P., Brown, K., Siebenlist, U., 1998. Mice deficient in nuclear factor (NF)-κB/p52 present with defects in humoral responses, germinal center reactions, and splenic microarchitecture. J. Exp. Med. 187, 147–159.

Fridlender, Z.G., Kapoor, V., Buchlis, G., Cheng, G., Sun, J., Wang, L.-C.S., Singhal, S., Snyder, L.A., Albelda, S.M., 2011. Monocyte chemoattractant protein–1 blockade inhibits lung cancer tumor growth by altering macrophage phenotype and activating CD8+ cells. Am. J. Respir. Cell Mol. Biol. 44, 230–237.

Fridlender, Z.G., Sun, J., Kim, S., Kapoor, V., Cheng, G., Ling, L., Worthen, G.S., Albelda, S.M., 2009. Polarization of tumor-associated neutrophil phenotype by TGF-β: "N1" versus "N2" TAN. Cancer Cell 16, 183–194.

Fusco, A.J., Huang, D.-B., Miller, D., Wang, V.Y.-F., Vu, D., Ghosh, G., 2009. NF-κB p52:RelB heterodimer recognizes two classes of κB sites with two distinct modes. EMBO Rep. 10, 152–159.

Galani, V., Tatsaki, E., Bai, M., Kitsoulis, P., Lekka, M., Nakos, G., Kanavaros, P., 2010. The role of apoptosis in the pathophysiology of Acute Respiratory Distress Syndrome (ARDS): an up-to-date cell-specific review. Pathol. Res. Pract. 206, 145–150.

Galvani, E., Sun, J., Leon, L.G., Sciarrillo, R., Narayan, R.S., Tjin Tham Sjin, R., Lee, K., Ohashi, K., Heideman, D.A.M., Alfieri, R.R., Heynen, G.J., Bernards, R., Smit, E.F., Pao, W., Peters, G.J., Giovannetti, E., 2015. NF-κB drives acquired resistance to a novel mutant-selective EGFR inhibitor. Oncotarget 6, 42717–42732.

Garon, E.B., Rizvi, N.A., Hui, R., Leighl, N., Balmanoukian, A.S., Eder, J.P., Patnaik, A., Aggarwal, C., Gubens, M., Horn, L., Carcereny, E., Ahn, M., Felip, E., Lee, J., Hellmann, M.D., Hamid, O., Goldman, J.W., Soria, J., Dolled-Filhart, M., Rutledge, R.Z., Zhang, J., Lunceford, J.K., Rangwala, R., Lubiniecki, G.M., Roach, C., Emancipator, K., Gandhi, L., 2015. Pembrolizumab for the treatment of non-small-cell lung cancer. N. Engl. J. Med. 372, 2018–2028.

Germano, G., Frapolli, R., Belgiovine, C., Anselmo, A., Pesce, S., Liguori, M., Erba, E., Uboldi, S., Zucchetti, M., Pasqualini, F., Nebuloni, M., van Rooijen, N., Mortarini, R., Beltrame, L., Marchini, S., Fuso Nerini, I., Sanfilippo, R., Casali, P.G., Pilotti, S., Galmarini, C.M., Anichini, A., Mantovani, A., D'Incalci, M., Allavena, P., 2013. Role of macrophage targeting in the antitumor activity of trabectedin. Cancer Cell 23, 249–262.

Giangreco, A., Reynolds, S.D., Stripp, B.R., 2002. Terminal bronchioles harbor a unique airway stem cell population that localizes to the bronchoalveolar duct junction. Am. J. Pathol. 161, 173–182.

Gilmore, T., Gerondakis, S., 2011. The c-Rel transcription factor in development and disease. Genes Cancer 2, 695–711.

Gocheva, V., Wang, H., Gadea, B., Shree, T., Hunter, K., Garfall, A., Berman, T., Joyce, J., 2010. IL-4 induces cathepsin protease activity in tumor-associated macrophages to promote cancer growth and invasion. Genes Dev. 24, 241–255.

Gregory, A.D., Houghton, A.M., 2011. Tumor-associated neutrophils: new targets for cancer therapy. Cancer Res. 71, 2411–2416.

Greten, F.R., Arkan, M.C., Bollrath, J., Hsu, L.-C., Goode, J., Miething, C., Göktuna, S.I., Neuenhahn, M., Fierer, J., Paxian, S., Van Rooijen, N., Xu, Y., O'Cain, T., Jaffee, B.B., Busch, D.H., Duyster, J., Schmid, R.M., Eckmann, L., Karin, M., 2007. NF-κB is a negative regulator of IL-1β secretion as revealed by genetic and pharmacological inhibition of IKKβ. Cell 130, 918–931.

Grivennikov, S.I., Greten, F.R., Karin, M., 2010. Immunity, inflammation, and cancer. Cell 140, 883–899.

Guinee, D., Fleming, M., Hayashi, T., Woodward, M., Zhang, J., Walls, J., Koss, M., Ferrans, V., Travis, W., 1996. Association of p53 and WAF1 expression with apoptosis in diffuse alveolar damage. Am. J. Pathol. 149, 531–538.

Haribabu, B., Verghese, M., Steeber, D., Sellars, D., Bock, C., Snyderman, R., 2000. Targeted disruption of the leukotriene B4 receptor in mice reveals its role in inflammation and platelet-activating factor-induced anaphylaxis. J. Exp. Med. 192, 433–438.

Herbst, R.S., Heymach, J. V, Lippman, S.M., 2008. Lung cancer. N Engl J Med 359, 1367–80.

Hoffmann, A., 2006. Circuitry of nuclear factor κB signaling. Immunol. Rev. 210, 171–186.

Hoffmann, A., Leung, T., Baltimore, D., 2003. Genetic analysis of NF-κB/Rel transcription factors defines functional specificities. EMBO J. 22, 5530–5539.

Hojgaard, A., Close, R., Dunn, D., Weiss, R.B., Weis, J.J., Weis, J.H., 2006. Altered localization of

CXCL13 expressing cells in mice deficient in Pactolus following an inflammatory stimulus. Immunology 119, 212–223.

Hong, K.U., Reynolds, S.D., Giangreco, A., Hurley, C.M., Stripp, B.R., 2001. Clara cell secretory protein-expressing cells of the airway neuroepithelial body microenvironment include a label-retaining subset and are critical for epithelial renewal after progenitor cell depletion. Am. J. Respir. Cell Mol. Biol. 24, 671–681.

Hopewell, E.L., Zhao, W., Fulp, W.J., Bronk, C.C., Lopez, A.S., Massengill, M., Antonia, S., Celis, E., Haura, E.B., Enkemann, S.A., Chen, D.-T., Beg, A.A., 2013. Lung tumor NF-κB signaling promotes T cell-mediated immune surveillance. J. Clin. Invest. 123, 2509–2522.

Houghton, A.M., Rzymkiewicz, D.M., Ji, H., Gregory, A.D., Egea, E.E., Metz, H.E., Stolz, D.B., Land, S.R., Marconcini, L.A., Kliment, C.R., Jenkins, K.M., Beaulieu, K.A., Mouded, M., Frank, S.J., Wong, K.K., Shapiro, S.D., 2010. Neutrophil elastase-mediated degradation of IRS-1 accelerates lung tumor growth. Nat. Med. 16, 219–223.

Howlader, N., Noone, A., Krapcho, M., Garshell, J., Miller, D., Altekruse, S., Kosary, C., Yu, M., Ruhl, J., Tatalovich, Z., Mariotto, A., Lewis, D., Chen, H., Feuer, E., Cronin, K. (Eds.), 2015. SEER cancer statistics review, 1975-2012. http://seer.cancer.gov/csr/1975_2012/ based on November 2014 SEER data submission.

Hu, J., Colburn, N.H., 2005. Histone deacetylase inhibition down-regulates cyclin D1 transcription by inhibiting nuclear factor-kappaB/p65 DNA binding. Mol. Cancer Res. 3, 100–109.

Husgafvel-Pursiainen, K., Hackman, P., Ridanpää, M., Anttila, S., Karjalainen, A., Partanen, T., Taikina-Aho, O., Heikkilä, L., Vainio, H., 1993. K-ras mutations in human adenocarcinoma of the lung: association with smoking and occupational exposure to asbestos. Int. J. Cancer 53, 250–256.

Iannetti, A., Ledoux, A.C., Tudhope, S.J., Sellier, H., Zhao, B., Mowla, S., Moore, A., Hummerich, H., Gewurz, B.E., Cockell, S.J., Jat, P.S., Willmore, E., Perkins, N.D., 2014. Regulation of p53 and Rb links the alternative NF-κB pathway to EZH2 expression and cell senescence. PLoS Genet. 10, e1004642.

Imai, Y., Kubota, Y., Yamamoto, S., 2005. Neutrophils enhance invasion activity of human cholangiocellular carcinoma and hepatocellular carcinoma cells: an in vitro study. J. Gastroenterol. Hepatol. 20, 287–293.

Ishikawa, H., Carrasco, D., Claudio, E., Ryseck, R.-P., Bravo, R., 1997. Gastric hyperplasia and increased proliferative responses of lymphocytes in mice lacking the COOH-terminal ankyrin domain of NF-κB2. J. Exp. Med. 186, 999–1014.

Jackson, E.L., Willis, N., Mercer, K., Bronson, R.T., Crowley, D., Montoya, R., Jacks, T., Tuveson, D.A., 2001. Analysis of lung tumor initiation and progression using conditional expression of oncogenic K-ras. Genes Dev. 15, 3243–3248.

Jänne, P.A., Yang, J.C.-H., Kim, D.-W., Planchard, D., Ohe, Y., Ramalingam, S.S., Ahn, M.-J., Kim, S.-W., Su, W.-C., Horn, L., Haggstrom, D., Felip, E., Kim, J.-H., Frewer, P., Cantarini, M., Brown, K.H., Dickinson, P.A., Ghiorghiu, S., Ranson, M., 2015. AZD9291 in EGFR inhibitor-resistant non-small-cell lung cancer. N. Engl. J. Med. 372, 1689–1699.

Jemal, A., Bray, F., Center, M.M., Ferlay, J., Ward, E., Forman, D., 2011. Global cancer statistics. CA. Cancer J. Clin. 61, 69–90.

Jemal, A., Thun, M., Ries, L., Howe, H., Wier, H., Center, M., Ward, E., Wu, X.-C., Eheman, C., Anderson, R., Ajani, U., Kohler, B., Edwards, B., 2008. Annual report to the nation on the status of cancer, 1975-2005, featuring trends in lung cancer, tobacco use, and tobacco control. J. Natl. Cancer Inst. 100, 1672–1694.

Ji, H., Houghton, A.M., Mariani, T.J., Perera, S., Kim, C.B., Padera, R., Tonon, G., McNamara, K., Marconcini, L.A., Hezel, A., El-Bardeesy, N., Bronson, R.T., Sugarbaker, D., Maser, R.S., Shapiro, S.D., Wong, K.-K., 2006. K-ras activation generates an inflammatory response in lung tumors. Oncogene 25, 2105–2112.

Junttila, M.R., Karnezis, A.N., Garcia, D., Madriles, F., Kortlever, R.M., Rostker, F., Swigart, L.B., Pham, D.M., Seo, Y., Evan, G.I., Martins, C.P., 2010. Selective activation of p53-mediated tumour suppression in high-grade tumours. Nature 468, 567–571.

Kanarek, N., Ben-Neriah, Y., 2012. Regulation of NF-κB by ubiquitination and degradation of the IκBs. Immunol. Rev. 246, 77–94.

Karabela, S.P., Psallidas, I., Sherrill, T.P., Kairi, C.A., Zaynagetdinov, R., Cheng, D.-S., Vassiliou, S., McMahon, F., Gleaves, L.A., Han, W., Stathopoulos, I., Zakynthinos, S.G., Yull, F.E., Roussos, C., Kalomenidis, I., Blackwell, T.S., Stathopoulos, G.T., 2012. Opposing effects of bortezomib-induced nuclear factor-κB inhibition on chemical lung carcinogenesis. Carcinogenesis 33, 859–867.

Kawasaki, M., Kuwano, K., Hagimoto, N., Matsuba, T., Kunitake, R., Tanaka, T., Maeyama, T., Hara, N., 2000. Protection from lethal apoptosis in lipopolysaccharide-induced acute lung injury in mice by a caspase inhibitor. Am. J. Pathol. 157, 597–603.

Keshava Prasad, T.S., Goel, R., Kandasamy, K., Keerthikumar, S., Kumar, S., Mathivanan, S., Telikicherla, D., Raju, R., Shafreen, B., Venugopal, A., Balakrishnan, L., Marimuthu, A., Banerjee, S., Somanathan, D.S., Sebastian, A., Rani, S., Ray, S., Harrys Kishore, C.J., Kanth, S., Ahmed, M., Kashyap, M.K., Mohmood, R., Ramachandra, Y.I., Krishna, V., Rahiman, B.A., Mohan, S., Ranganathan, P., Ramabadran, S., Chaerkady, R., Pandey, A., 2009. Human Protein Reference Database - 2009 update. Nucleic Acids Res. 37, D767–772.

Kim, C.F.B., Jackson, E.L., Woolfenden, A.E., Lawrence, S., Babar, I., Vogel, S., Crowley, D., Bronson, R.T., Jacks, T., 2005. Identification of bronchioalveolar stem cells in normal lung and lung cancer. Cell 121, 823–835.

Kitamura, H., Kameda, Y., Ito, T., Hayashi, H., 1999. Atypical adenomatous hyperplasia of the lung. Implications for the pathogenesis of peripheral lung adenocarcinoma. Am. J. Clin. Pathol. 111, 610–622.

Klein, P., Ravi, R., 1995. A nearly best-possible approximation algorithm for node-weighted steiner trees. J. Algorithms 19, 104–115.

Kojima, M., Morisaki, T., Sasaki, N., Nakano, K., Mibu, R., Tanaka, M., Katano, M., 2004. Increased nuclear factor-kB activation in human colorectal carcinoma and its correlation with tumor progression. Anticancer Res. 24, 675–681.

Kollareddy, M., Zheleva, D., Dzubak, P., Brahmkshatriya, P., Lepsik, M., Hajduch, M., 2012. Aurora kinase inhibitors: progress towards the clinic. Invest. New Drugs 30, 2411–2432.

Kravtsova-Ivantsiv, Y., Shomer, I., Cohen-Kaplan, V., Snijder, B., Superti-Furga, G., Gonen, H., Sommer, T., Ziv, T., Admon, A., Naroditsky, I., Jbara, M., Brik, A., Pikarsky, E., Kwon, Y.T., Doweck, I., Ciechanover, A., 2015. KPC1-mediated ubiquitination and proteasomal processing of NF-κB1 p105 to p50 restricts tumor growth. Cell 161, 333–347.

Kuang, D.-M., Zhao, Q., Peng, C., Xu, J., Zhang, J.-P., Wu, C., Zheng, L., 2009. Activated monocytes in peritumoral stroma of hepatocellular carcinoma foster immune privilege and disease progression through PD-L1. J. Exp. Med. 206, 1327–1337.

Kunsch, C., Ruben, S., Rosen, C., 1992. Selection of optimal κB/Rel DNA-binding motifs: interaction of both subunits of NF-κB with DNA is required for transcriptional activation. Mol. Cell. Biol. 12, 4412–4421.

Lam, L., Davis, R., Ngo, V., Lenz, G., Wright, G., Xu, W., Zhao, H., Yu, X., Dang, L., Staudt, L., 2008. Compensatory IKKα activation of classical NF-κB signaling during IKKβ inhibition identified by an RNA interference sensitization screen. Proc. Natl. Acad. Sci. U. S. A. 105, 20798–20803.

Lapenna, S., Giordano, A., 2009. Cell cycle kinases as therpeutic targets for cancer. Nat. Rev. Drug Discov. 8, 547–566.

Lawson, W.E., Polosukhin, V. V, Stathopoulos, G.T., Zoia, O., Han, W., Lane, K.B., Li, B., Donnelly, E.F., Holburn, G.E., Lewis, K.G., Collins, R.D., Hull, W.M., Glasser, S.W., Whitsett, J.A., Blackwell, T.S., 2005. Increased and prolonged pulmonary fibrosis in surfactant protein C-deficient mice following intratracheal bleomycin. Am. J. Pathol. 167, 1267–1277.

Lee, K.S., Choi, Y.H., Kim, Y.S., Baik, S.H., Oh, Y.J., Sheen, S.S., Park, J.H., Hwang, S.C., Park, K.J., 2008. Evaluation of bronchoalveolar lavage fluid from ARDS patients with regard to apoptosis. Respir. Med. 102, 464–469.

Leek, R.D., Hunt, N.C., Landers, R.J., Lewis, C.E., Royds, J.A., Harris, A.L., 2000. Macrophage infiltration is associated with VEGF and EGFR expression in breast cancer. J. Pathol. 190, 430–436.

Lessard, L., Bégin, L.R., Gleave, M.E., Mes-Masson, A.-M., Saad, F., 2005. Nuclear localisation of nuclear factor-kappaB transcription factors in prostate cancer: an immunohistochemical study. Br. J. Cancer 93, 1019–1023.

Leung, T.H., Hoffmann, A., Baltimore, D., 2004. One nucleotide in a κB site can determine cofactor specificity for NF-κB dimers. Cell 118, 453–464.

Li, A.R., Chitale, D., Riely, G.J., Pao, W., Miller, V.A., Zakowski, M.F., Rusch, V., Kris, M.G., Ladanyi, M., 2008. EGFR mutations in lung adenocarcinomas: clinical testing experience and relationship to EGFR gene copy number and immunohistochemical expression. J. Mol. Diagnostics 10, 242–248.

Li, B., Dewey, C.N., 2011. RSEM: accurate transcript quantification from RNA-Seq data with or without a reference genome. BMC Bioinformatics 12, 323.

Lin, C., Song, H., Huang, C., Yao, E., Gacayan, R., Xu, S.-M., Chuang, P.-T., 2012. Alveolar type II cells possess the capability of initiating lung tumor development. PLoS One 7, e53817.

Linsley, P.S., Greene, J.L., Brady, W., Bajorath, J., Ledbetter, J.A., Peach, R., 1994. Human B7-1 (CD80) and B7-2 (CD86) bind with similar avidities but distinct kinetics to CD28 and CTLA-4 receptors. Immunity 1, 793–801.

Liptay, S., Schmid, R.M., Nabel, E.G., Nabel, G.J., 1994. Transcriptional regulation of NF-κB2: evidence for κB-mediated positive and negative autoregulation. Mol. Cell. Biol. 14, 7695–7703.

Lombardi, L., Ciana, P., Cappellini, C., Trecca, D., Guerrini, L., Migliazza, A., Maiolo, A., Neri, A., 1995. Structural and functional characterization of the promoter regions of the NFKB2 gene. Nucleic Acids Res. 23, 2328–2336.

Lovas, A., Radke, D., Albrecht, D., Yilmax, Z., Möller, U., Habenicht, A., Weih, F., 2008. Differential RelA- and RelB-dependent gene transcription in LTβR-stimulated mouse embryonic fibroblasts. BMC Genomics 9, 606.

Lynch, T.J., Bondarenko, I., Luft, A., Serwatowski, P., Barlesi, F., Chacko, R., Sebastian, M., Neal, J., Lu, H., Cuillerot, J.-M., Reck, M., 2012. Ipilimumab in combination with paclitaxel and carboplatin as first-line treatment in stage IIIB/IV non-small-cell lung cancer: results from a randomized,

double-blind, multicenter phase II study. J. Clin. Oncol. 30, 2046–2054.

Mainardi, S., Mijimolle, N., Francoz, S., Vicente-Dueñas, C., Sánchez-García, I., Barbacid, M., 2014. Identification of cancer initiating cells in K-Ras driven lung adenocarcinoma. Proc. Natl. Acad. Sci. U. S. A. 111, 255–260.

Mantovani, A., Allavena, P., Sica, A., Balkwill, F., 2008. Cancer-related inflammation. Nature 454, 436–444.

Martinez, F.O., Gordon, S., Locati, M., Mantovani, A., 2006. Transcriptional profiling of the human monocyte-to-macrophage differentiation and polarization: new molecules and patterns of gene expression. J. Immunol. 177, 7303–7311.

Matthay, M.A., Wiener-Kronish, J.P., 1990. Intact epithelial barrier function is critical for the resolution of alveolar edema in humans. Am. Rev. Respir. Dis. 142, 1250–1257.

McMillan, D.H., Baglole, C.J., Thatcher, T.H., Maggirwar, S., Sime, P.J., Phipps, R.P., 2011. Lung-targeted overexpression of the NF-κB member RelB inhibits cigarette smoke-induced inflammation. Am. J. Pathol. 179, 125–133.

Mercurio, F., Zhu, H., Murray, B., Shevchenko, A., Bennett, B., Li, J., Young, D., Barbosa, M., Mann, M., Manning, A., Rao, A., 1997. IKK-1 and IKK-2: cytokine-activated IκB kinases essential for NF-κB activation. Science 278, 860–866.

Meylan, E., Dooley, A.L., Feldser, D.M., Shen, L., Turk, E., Ouyang, C., Jacks, T., 2009. Requirement for NF-κB signalling in a mouse model of lung adenocarcinoma. Nature 462, 104–107.

Migliazza, A., Lombardi, L., Rocchi, M., Trecca, D., Chang, C.C., Antonacci, R., Fracchiolla, N.S., Ciana, P., Maiolo, A.T., Neri, A., 1994. Heterogeneous chromosomal aberrations generate 3' truncations of the NFKB2/lyt-10 gene in lymphoid malignancies. Blood 84, 3850–60.

Minamiya, Y., Ono, T., Saito, H., Takahashi, N., Ito, M., Mitsui, M., Motoyama, S., Ogawa, J., 2011. Expression of histone deacetylase 1 correlates with a poor prognosis in patients with adenocarcinoma of the lung. Lung Cancer 74, 300–304.

Mori, M., Rao, S., Popper, H., Cagle, P., Fraire, A., 2001. Atypical adenomatous hyperplasia of the lung:

a probably forerunner in the development of adenocarcinoma of the lung. Mod. Pathol. 14, 72–84.

Mu, C.-Y., Huang, J.-A., Chen, Y., Chen, C., Zhang, X.-G., 2011. High expression of PD-L1 in lung cancer may contribute to poor prognosis and tumor cells immune escape through suppressing tumor infiltrating dendritic cells maturation. Med. Oncol. 28, 682–688.

Munder, P., Modolell, M., Hoelzl Wallach, D., 1971. Cell propagation on films of polymeric fluorocarbon as a means to regulate pericellular pH and pO(2) in cultured monolayers. FEBS Lett. 15, 191–196.

Nadiminty, N., Chun, J.Y., Lou, W., Lin, X., Gao, A.C., 2008. NF-κB2/p52 enhances androgen-independent growth of human LNCaP cells via protection from apoptotic cell death and cell cycle arrest induced by androgen-deprivation. Prostate 68, 1725–1733.

Nadiminty, N., Lou, W., Lee, S.O., Lin, X., Trump, D.L., Gao, A.C., 2006. Stat3 activation of NF-κB p100 processing involves CBP/p300-mediated acetylation. Proc. Natl. Acad. Sci. U. S. A. 103, 7264–7269.

Nadiminty, N., Lou, W., Sun, M., Chen, J., Yue, J., Kung, H.-J., Evans, C.P., Zhou, Q., Gao, A.C., 2010. Aberrant activation of the androgen receptor by NF-kappaB2/p52 in prostate cancer cells. Cancer Res. 70, 3309–3319.

Neal, J.W., Sequist, L. V, 2012. Complex role of histone deacetylase inhibitors in the treatment of non-small-cell lung cancer. J. Clin. Oncol. 30, 2280–2282.

Neff, S.B., Z'graggen, B.R., Neff, T.A., Jamnicki-Abegg, M., Suter, D., Schimmer, R.C., Booy, C., Joch, H., Pasch, T., Ward, P.A., Beck-Schimmer, B., 2006. Inflammatory response of tracheobronchial epithelial cells to endotoxin. Am. J. Physiol. Lung Cell. Mol. Physiol. 290, L86–96.

Neri, A., Chang, C.C., Lombardi, L., Salina, M., Corradini, P., Maiolo, A.T., Chaganti, R.S., Dalla-Favera, R., 1991. B cell lymphoma-associated chromosomal translocation involves candidate oncogene lyt-10, homologous to NF-κB p50. Cell 67, 1075–1087.

Neri, A., Fracchiolla, N.S., Roscetti, E., Garatti, S., Trecca, D., Boletini, A., Perletti, L., Baldini, L., Maiolo, A.T., Berti, E., 1995. Molecular analysis of cutaneous B- and T-cell lymphomas. Blood 86,

3160–3172.

Noy, R., Pollard, J., 2014. Tumor-associated macrophages: from mechanisms to therapy. Immunity 41, 49–61.

Nozawa, H., Chiu, C., Hanahan, D., 2006. Infiltrating neutrophils mediate the initial angiogenic switch in a mouse model of multistage carcinogenesis. Proc. Natl. Acad. Sci. U. S. A. 103, 12493–12498.

Ondrey, F.G., Dong, G., Sunwoo, J., Chen, Z., Wolf, J.S., Crowl-Bancroft, C. V, Mukaida, N., Van Waes, C., 1999. Constitutive activation of transcription factors NF-κB, AP-1, and NF-IL6 in human head and neck squamous cell carcinoma cell lines that express pro-inflammatory and pro-angiogenic cytokines. Mol. Carcinog. 26, 119–129.

Osma-Garcia, I., Punzón, C., Fresno, M., Díaz-Muñoz, M., 2015. Dose-dependent effects of prostaglandin E2 in macrophage adhesion and migration. Eur. J. Immunol. Epub ahead of print.

Pao, W., Miller, V.A., Politi, K.A., Riely, G.J., Somwar, R., Zakowski, M.F., Kris, M.G., Varmus, H., 2005. Acquired resistance of lung adenocarcinomas to gefitinib or erlotinib is associated with a second mutation in the EGFR kinase domain. PLoS Med. 2, e73.

Pasparakis, M., 2009. Regulation of tissue homeostasis by NF-κB signalling: implications for inflammatory diseases. Nat. Rev. Immunol. 9, 778–788.

Perl, A.-K.T., Tichelaar, J., Whitsett, J., 2002. Conditional gene expression in the respiratory epithelium of the mouse. Transgenic Res. 11, 21–29.

Petty, J.M., Sueblinvong, V., Lenox, C.C., Jones, C.C., Cosgrove, G.P., Cool, C.D., Rai, P.R., Brown, K.K., Weiss, D.J., Poynter, M.E., Suratt, B.T., 2007. Pulmonary stromal-derived factor-1 expression and effect on neutrophil recruitment during acute lung injury. J. Immunol. 178, 8148–8157.

Pierce, J., Schoenleber, R., Jesmok, G., Best, J., Moore, S., Collins, T., Gerritsen, M., 1997. Novel inhibitors of cytokine-induced IκBα phosphorylation and endothelial cell adhesion molecule expression show anti-inflammatory effects in vivo. J. Biol. Chem. 272, 21096–21103.

Politi, K., Zakowski, M.F., Fan, P.-D., Schonfeld, E.A., Pao, W., Varmus, H.E., 2006. Lung adenocarcinomas induced in mice by mutant EGF receptors found in human lung cancers respond to

a tyrosine kinase inhibitor or to down-regulation of the receptors. Genes Dev. 20, 1496–1510.

Proietto, A.I., van Dommelen, S., Zhou, P., Rizzitelli, A., D'Amico, A., Steptoe, R.J., Naik, S.H., Lahoud, M.H., Liu, Y., Zheng, P., Shortman, K., Wu, L., 2008. Dendritic cells in the thymus contribute to T-regulatory cell induction. Proc. Natl. Acad. Sci. U. S. A. 105, 19869–19874.

Queen, M.M., Ryan, R.E., Holzer, R.G., Keller-Peck, C.R., 2005. Breast cancer cells stimulate neutrophils to produce oncostatin M: potential implications for tumor progression. Cancer Res. 65, 8896–8904.

Ramirez, R.D., Sheridan, S., Girard, L., Sato, M., Kim, Y., Pollack, J., Peyton, M., Zou, Y., Kurie, J.M., Dimaio, J.M., Milchgrub, S., Smith, A.L., Souza, R.F., Gilbey, L., Zhang, X., Gandia, K., Vaughan, M.B., Wright, W.E., Gazdar, A.F., Shay, J.W., Minna, J.D., 2004. Immortalization of human bronchial epithelial cells in the absence of viral oncoproteins. Cancer Res. 64, 9027–9034.

Redente, E.F., Orlicky, D.J., Bouchard, R.J., Malkinson, A.M., 2007. Tumor signaling to the bone marrow changes the phenotype of monocytes and pulmonary macrophages during urethane-induced primary lung tumorigenesis in A/J mice. Am. J. Pathol. 170, 693–708.

Regales, L., Balak, M.N., Gong, Y., Politi, K., Sawai, A., Le, C., Koutcher, J.A., Solit, D.B., Rosen, N., Zakowski, M.F., Pao, W., 2007. Development of new mouse lung tumor models expressing EGFR T790M mutants associated with clinical resistance to kinase inhibitors. PLoS One 2, e810.

Roca, H., Varsos, Z.S., Sud, S., Craig, M.J., Ying, C., Pienta, K.J., 2009. CCL2 and interleukin-6 promote survival of human CD11b+ peripheral blood mononuclear cells and induce M2-type macrophage polarization. J. Biol. Chem. 284, 34342–34354.

Rocha, S., Martin, A.M., Meek, D.W., Perkins, N.D., 2003. p53 represses cyclin D1 transcription through down regulation of Bcl-3 and inducing increased association of the p52 NF-κB subunit with histone deacetylase 1. Mol. Cell. Biol. 23, 4713–4727.

Rosell, R., Moran, T., Queralt, C., Porta, R., Cardenal, F., Camps, C., Majem, M., Lopez-Vivanco, G., Isla, D., Provencio, M., Insa, A., Massuti, B., Gonzalez-Larriba, J.L., Paz-Ares, L., Bover, I., Garcia-Campelo, R., Moreno, M.A., Catot, S., Rolfo, C., Reguart, N., Palmero, R., Sánchez, J.M.,

Bastus, R., Mayo, C., Bertran-Alamillo, J., Molina, M.A., Sanchez, J.J., Taron, M., 2009. Screening for epidermal growth factor receptor mutations in lung cancer. N. Engl. J. Med. 361, 958–967.

Rothwarf, D.M., Zandi, E., Natoli, G., Karin, M., 1998. IKK-γ is an essential regulatory subunit of the IκB kinase complex. Nature 395, 297–300.

Saccani, S., Pantano, S., Natoli, G., 2001. Two waves of nuclear factor κB recruitment to target promoters. J. Exp. Med. 193, 1351–1360.

Sai, J., Raman, D., Liu, Y., Wikswo, J., Richmond, A., 2008. Parallel phosphatidylinositol 3-kinase (PI3K)-dependent and Src-dependent pathways lead to CXCL8-mediated Rac2 activation and chemotaxis. J. Biol. Chem. 283, 26538–26547.

Samet, J., Avila-Tang, E., Boffetta, P., Hannan, L., Olivo-Marston, S., Thun, M., Rudin, C., 2009. Lung cancer in never smokers: clinical epidemiology and environmental risk factors. Clin. Cancer Res. 15, 5626–5645.

Sandhu, J.K., Privora, H.F., Wenckebach, G., Birnboim, H.C., 2000. Neutrophils, nitric oxide synthase, and mutations in the mutatect murine tumor model. Am. J. Pathol. 156, 509–518.

Sandler, A., Gray, R., Perry, M., Brahmer, J., Schiller, J., Dowlati, A., Lilenbaum, R., Johnson, D., 2006. Paclitaxel-carboplatin alone or with bevacizumab for non-small-cell lung cancer. N. Engl. J. Med. 355, 2542–2550.

Sasaki, H., Moriyama, S., Nakashima, Y., Kobayashi, Y., Kiriyama, M., Fukai, I., Yamakawa, Y., Fujii, Y., 2004. Histone deacetylase 1 mRNA expression in lung cancer. Lung Cancer 46, 171–178.

Sato, M., Vaughan, M.B., Girard, L., Peyton, M., Lee, W., Shames, D.S., Ramirez, R.D., Sunaga, N., Gazdar, A.F., Shay, J.W., Minna, J.D., 2006. Multiple oncogenic changes (K-RAS(V12), p53 knockdown, mutant EGFRs, p16 bypass, telomerase) are not sufficient to confer a full malignant phenotype on human bronchial epithelial cells. Cancer Res. 66, 2116–2128.

Schreiber, R., Old, L., Smyth, M., 2011. Cancer immunoediting: integrating immunity's roles in cancer suppression and promotion. Science 331, 1565–1570.

Schumm, K., Rocha, S., Caamano, J., Perkins, N.D., 2006. Regulation of p53 tumour suppressor target

gene expression by the p52 NF-κB subunit. EMBO J. 25, 4820–4832.

Senftleben, U., Cao, Y., Xiao, G., Greten, F.R., Krähn, G., Bonizzi, G., Chen, Y., Hu, Y., Fong, A., Sun, S.C., Karin, M., 2001. Activation by IKKα of a second, evolutionary conserved, NF-κB signaling pathway. Science 293, 1495–1499.

Seo, S.I., Song, S.Y., Kang, M.R., Kim, M.S., Oh, J.E., Kim, Y.R., Lee, J.Y., Yoo, N.J., Lee, S.H., 2009. Immunohistochemical analysis of NF-κB signaling proteins IKKε, p50/p105, p52/p100 and RelA in prostate cancers. APMIS 117, 623–628.

Sequist, L. V, Soria, J.-C., Goldman, J.W., Wakelee, H.A., Gadgeel, S.M., Varga, A., Papadimitrakopoulou, V., Solomon, B.J., Oxnard, G.R., Dziadziuszko, R., Aisner, D.L., Doebele, R.C., Galasso, C., Garon, E.B., Heist, R.S., Logan, J., Neal, J.W., Mendenhall, M.A., Nichols, S., Piotrowska, Z., Wozniak, A.J., Raponi, M., Karlovich, C.A., Jaw-Tsai, S., Isaacson, J., Despain, D., Matheny, S.L., Rolfe, L., Allen, A.R., Camidge, D.R., 2015. Rociletinib in EGFR-mutated non-small-cell lung cancer. N. Engl. J. Med. 372, 1700–1709.

Shi, Y., Au, J.S.-K., Thongprasert, S., Srinivasan, S., Tsai, C.-M., Khoa, M.T., Heeroma, K., Itoh, Y., Cornelio, G., Yang, P.-C., 2014. A prospective, molecular epidemiology study of EGFR mutations in Asian patients with advanced non-small-cell lung cancer of adenocarcinoma histology (PIONEER). J. Thorac. Oncol. 9, 154–162.

Shih, V.F.-S., Kearns, J., Basak, S., Savinova, O., Ghosh, G., Hoffmann, A., 2009. Kinetic control of negative feedback regulators of NF-κB/RelA determines their pathogen- and cytokine-receptor signaling specificity. Proc. Natl. Acad. Sci. U. S. A. 106, 9619–9624.

Sica, A., Mantovani, A., 2012. Macrophage plasticity and polarization: in vivo veritas. J. Clin. Invest. 122, 787–795.

Siegel, R.L., Miller, K.D., Jemal, A., 2015. Cancer Statistics, 2015. CA. Cancer J. Clin. 65, 5–29.

Siggers, T., Chang, A.B., Teixeira, A., Wong, D., Williams, K.J., Ahmed, B., Ragoussis, J., Udalova, I.A., Smale, S.T., Bulyk, M.L., 2011. Principles of dimer-specific gene regulation revealed by a comprehensive characterization of NF-κB family DNA binding. Nat. Immunol. 13, 95–102.

Smyth, G., 2005. Limma: linear models for microarray data, in: Gentleman, R., Carey, V., Dudoit, R., Irizarry, W. (Eds.), Bioinformatics and Computational Biology Solutions Using R and Bioconductor. Springer, New York, pp. 397–420.

Smyth, G.K., 2004. Linear models and empirical bayes methods for assessing differential expression in microarray experiments. Stat. Appl. Genet. Mol. Biol. 3, Article3.

Sovak, M.A., Bellas, R.E., Kim, D.W., Zanieski, G.J., Rogers, A.E., Traish, A.M., Sonenshein, G.E., 1997. Aberrant nuclear factor-κB/Rel expression and the pathogenesis of breast cancer. J. Clin. Invest. 100, 2952–2960.

Spandidos, A., Wang, X., Wang, H., Dragnev, S., Thurber, T., Seed, B., 2008. A comprehensive collection of experimentally validated primers for polymerase chain reaction quantitation of murine transcript abundance. BMC Genomics 9, 633.

Spandidos, A., Wang, X., Wang, H., Seed, B., 2010. PrimerBank: a resource of human and mouse PCR primer pairs for gene expression detection and quantification. Nucleic Acids Res. 38, D792–799.

Sparmann, A., Bar-Sagi, D., 2004. Ras-induced interleukin-8 expression plays a critical role in tumor growth and angiogenesis. Cancer Cell 6, 447–458.

Stathopoulos, G.T., Sherrill, T.P., Cheng, D.-S., Scoggins, R.M., Han, W., Polosukhin, V. V, Connelly, L., Yull, F.E., Fingleton, B., Blackwell, T.S., 2007. Epithelial NF-κB activation promotes urethane-induced lung carcinogenesis. Proc. Natl. Acad. Sci. U. S. A. 104, 18514–18519.

Stayner, L., Bena, J., Sasco, A., Smith, R., Steenland, K., Kreuzer, M., Straif, K., 2007. Lung cancer risk and workplace exposure to environmental tobacco smoke. Am. J. Public Health 97, 545–551.

Stefano, V. Di, Wang, B., Parobchak, N., Roche, N., Rosen, T., 2015. RelB/p52-mediated NF- κB signaling alters histone acetylation to increase the abundance of corticotropin-releasing hormone in human placenta. Sci. Signal. 8, ra85.

Steinbrecher, K., Harmel-Laws, E., Sitcheran, R., Baldwin, A., 2008. Loss of epithelial RelA results in deregulated intestinal proliferative/apoptotic homeostasis and susceptibility to inflammation. J. Immunol. 180, 2588–2599.

Storz, P., 2013. Targeting the alternative NF-κB pathway in pancreatic cancer: a new direction for therapy? Expert Rev. Anticancer Ther. 13, 501–504.

Sun, L., Carpenter, G., 1998. Epidermal growth factor activation of NF-κB is mediated through IκBα degradation and intracellular free calcium. Oncogene 16, 2095–2102.

Sutherland, K.D., Song, J.-Y., Kwon, M.C., Proost, N., Zevenhoven, J., Berns, A., 2014. Multiple cells-of-origin of mutant K-Ras-induced mouse lung adenocarcinoma. Proc. Natl. Acad. Sci. U. S. A. 111, 4952–4957.

Sweeney, C., Li, L., Shanmugam, R., Bhat-Nakshatri, P., Jayaprakasan, V., Baldridge, L.A., Gardner, T., Smith, M., Nakshatri, H., Cheng, L., 2004. Nuclear factor-κB is constitutively activated in prostate cancer in vitro and is overexpressed in prostatic intraepithelial neoplasia and adenocarcinoma of the prostate. Clin. Cancer Res. 10, 5501–5507.

Tang, X., Liu, D., Shishodia, S., Ozburn, N., Behrens, C., Lee, J.J., Hong, W.K., Aggarwal, B.B., Wistuba, I.I., 2006. Nuclear factor-κB (NF-κB) is frequently expressed in lung cancer and preneoplastic lesions. Cancer 107, 2637–46.

Taylor, R., Najafi, F., Dobson, A., 2007. Meta-analysis of studies of passive smoking and lung cancer: effects of study type and continent. Int. J. Epidemiol. 36, 1048–1059.

The National Lung Screening Trial Research Team, 2011. Reduced lung-cancer mortality with low-dose computed tomographic screening. N. Engl. J. Med. 365, 395–409.

Therneau, T., Grambsch, P., 2000. Modeling survival data: extending the cox model. Springer, New York.

Tichelaar, J.W., Lu, W., Whitsett, J.A., 2000. Conditional expression of fibroblast growth factor-7 in the developing and mature lung. J. Biol. Chem. 275, 11858–11864.

Tichelaar, J.W., Zhang, Y., LeRiche, J.C., Biddinger, P.W., Lam, S., Anderson, M.W., 2005. Increased staining for phospho-Akt, p65/RELA and cIAP-2 in pre-neoplastic human bronchial biopsies. BMC Cancer 5, 155.

Trahey, M., McCormick, F., 1987. A cytoplasmic protein stimulates normal N-ras p21 GTPase, but does

not affect oncogenic mutants. Science 238, 542–545.

Travis, W., Brambilla, E., Noguchi, M., Nicholson, A., Geisinger, K., Yatabe, Y., Beer, D., Powell, C., Riely, G., Van Schil, P., Garg, K., Austin, J., Asamura, H., VW, R., Hirsch, F., Scagliotti, G., Mitsudomi, T., Huber, R., Ishikawa, Y., Jett, J., Sanchez-Cespedes, M., Sculier, J., Takahashi, T., Tsuboi, M., Vansteenkiste, J., Wistuba, I., Yang, P., Aberle, D., Brambilla, C., Flieder, D., Franklin, W., Gazdar, A., Gould, M., Hasleton, P., Henderson, D., Johnson, B., Johnson, D., Kerr, K., Kuriyama, K., Lee, J., Miller, V., Petersen, I., Roggli, V., Rosell, R., Saijo, N., Thunnissen, E., Tsao, M., Yankelewitz, D., 2011. International association for the study of lung cancer/american thoracic society/european respiratory society international multidisciplinary classification of lung adenocarcinoma. J. Thorac. Oncol. 6, 244–285.

Tucker, E., O'Donnell, K., Fuchsberger, M., Hilton, A., Metcalf, D., Greig, K., Sims, N., Quinn, J., Alexander, W., Hilton, D., Kile, B., Tarlinton, D., Starr, R., 2007. A novel mutation in the Nfkb2 gene generates an NF-κB2 "super repressor." J. Immunol. 179, 7514–7522.

Tully, J.E., Nolin, J.D., Guala, A.S., Hoffman, S.M., Roberson, E.C., Lahue, K.G., van der Velden, J., Anathy, V., Blackwell, T.S., Janssen-Heininger, Y.M.W., 2012. Cooperation between classical and alternative NF-κB pathways regulates proinflammatory responses in epithelial cells. Am. J. Respir. Cell Mol. Biol. 47, 497–508.

Vallabhapurapu, S.D., Noothi, S.K., Pullum, D.A., Lawrie, C.H., Pallapati, R., Potluri, V., Kuntzen, C., Khan, S., Plas, D.R., Orlowski, R.Z., Chesi, M., Kuehl, W.M., Bergsagel, P.L., Karin, M., Vallabhapurapu, S., 2015. Transcriptional repression by the HDAC4–RelB–p52 complex regulates multiple myeloma survival and growth. Nat. Commun. 6, 8428.

Vernooy, J.H., Dentener, M.A., van Suylen, R.J., Buurman, W.A., Wouters, E.F., 2001. Intratracheal instillation of lipopolysaccharide in mice induces apoptosis in bronchial epithelial cells: no role for tumor necrosis factor-alpha and infiltrating neutrophils. Am. J. Respir. Cell Mol. Biol. 24, 569–576.

Wang, F., Shi, Y., Yadav, S., Wang, H., 2010. p52-Bcl3 complex promotes cyclin D1 expression in BEAS-2B cels in response to low concentration arsenite. Toxicology 273, 12–18.

Wang, J., Wang, X., Hussain, S., Zheng, Y., Sanjabi, S., Ouaaz, F., Beg, A., 2007. Distinct roles of different NF-κB subunits in regulating inflammatory and T cell stimulatory gene expression in dendritic cells. J. Immunol. 178, 6777–6788.

Wang, W., Abbruzzese, J.L., Evans, D.B., Larry, L., Cleary, K.R., Chiao, P.J., 1999. The nuclear factor-κB RelA transcription factor is constitutively activated in human pancreatic adenocarcinoma cells. Clin. Cancer Res. 5, 119–127.

Wang, X., Seed, B., 2003. A PCR primer bank for quantitative gene expression analysis. Nucleic Acids Res. 31, e154.

Weih, D.S., Yilmaz, Z.B., Weih, F., 2001. Essential role of RelB in germinal center and marginal zone formation and proper expression of homing chemokines. J. Immunol. 167, 1909–1919.

Weih, F., Carrasco, D., Durham, S.K., Barton, D.S., Rizzo, C.A., Ryseck, R.-P., Lira, S.A., Bravo, R., 1995. Multiorgan inflammation and hematopoietic abnormalities in mice with a targeted disruption of RelB, a member of the NF-κB/Rel family. Cell 80, 331–340.

Wharry, C.E., Haines, K.M., Carroll, R.G., May, M.J., 2009. Constitutive non-canonical NFκB signaling in pancreatic cancer cells. Cancer Biol. Ther. 8, 1567–1576.

Wislez, M., Fujimoto, N., Izzo, J.G., Hanna, A.E., Cody, D.D., Langley, R.R., Tang, H., Burdick, M.D., Sato, M., Minna, J.D., Mao, L., Wistuba, I., Strieter, R.M., Kurie, J.M., 2006. High expression of ligands for chemokine receptor CXCR2 in alveolar epithelial neoplasia induced by oncogenic Kras. Cancer Res. 66, 4198–4207.

Wislez, M., Spencer, M.L., Izzo, J.G., Juroske, D.M., Balhara, K., Cody, D.D., Price, R.E., Hittelman, W.N., Wistuba, I.I., Kurie, J.M., 2005. Inhibition of mammalian target of rapamycin reverses alveolar epithelial neoplasia induced by oncogenic K-ras. Cancer Res. 65, 3226–3235.

Wong, D., Teixeira, A., Oikonomopoulos, S., Humburg, P., Lone, I.N., Saliba, D., Siggers, T., Bulyk, M., Angelov, D., Dimitrov, S., Udalova, I., Ragoussis, J., 2011. Extensive characterization of NF-κB binding uncovers non-canonical motifs and advances the interpretation of genetic functional traits. Genome Biol. 12, R70.

Woo, E.Y., Chu, C.S., Goletz, T.J., Schlienger, K., Yeh, H., Coukos, G., Rubin, S.C., Kaiser, L.R., June, C.H., 2001. Regulatory CD4+ CD25+ T cells in tumors from patients with early-stage non-small cell lung cancer and late-stage ovarian cancer. Cancer Res. 61, 4766–4772.

Woo, E.Y., Yeh, H., Chu, C.S., Schlienger, K., Carroll, R.G., Riley, J.L., Kaiser, L.R., June, C.H., 2002. Regulatory T cells from lung cancer patients directly inhibit autologous T cell proliferation. J. Immunol. 168, 4272–4276.

Woronicz, J., Gao, X., Cao, Z., Rothe, M., Goeddel, D., 1997. IκB kinase-β: NF-κB activation and complex formation with IκB kinase-α and NIK. Science 278, 866–869.

Xia, Y., Yeddula, N., Leblanc, M., Ke, E., Zhang, Y., Oldfield, E., Shaw, R.J., Verma, I.M., 2012. Reduced cell proliferation by IKK2 depletion in a mouse lung-cancer model. Nat. Cell Biol. 14, 257–265.

Xiao, G., Fong, A., Sun, S.C., 2004. Induction of p100 processing by NF-κB-inducing kinase involves docking IκB kinase α (IKKα) to p100 and IKKα-mediated phosphorylation. J. Biol. Chem. 279, 30099–30105.

Xiao, G., Harhaj, E.W., Sun, S.C., 2001. NF-κB-inducing kinase regulates the processing of NF-κB2 p100. Mol. Cell 7, 401–409.

Xu, X., Rock, J.R., Lu, Y., Futtner, C., Schwab, B., Guinney, J., Hogan, B.L.M., Onaitis, M.W., 2012. Evidence for type II cells as cells of origin of K-Ras-induced distal lung adenocarcinoma. Proc. Natl. Acad. Sci. U. S. A. 109, 4910–4915.

Xu, Y., Fang, F., St. Clair, D., Sompol, P., Josson, S., St. Clair, W., 2008. SN52, a novel nuclear factor-κB inhibitor, blocks nuclear import of RelB:p52 dimer and sensitizes prostate cancer cells to ionizing radiation. Mol. Cancer Ther. 7, 2367–2376.

Xue, W., Meylan, E., Oliver, T.G., Feldser, D.M., Winslow, M.M., Bronson, R., Jacks, T., 2011. Response and resistance to NF-κB inhibitors in mouse models of lung adenocarcinoma. Cancer Discov. 1, 236–247.

Yamaoka, S., Courtois, G., Bessia, C., Whiteside, S., Weil, R., Agou, F., Kirk, H., Kay, R., Israël, A.,

1998. Complementation cloning of NEMO, a component of the IκB kinase complex essential for NF-κB activation. Cell 93, 1231–1240.

You, M., Candrian, U., Maronpot, R.R., Stoner, G.D., Anderson, M.W., 1989. Activation of the Ki-ras protooncogene in spontaneously occurring and chemically induced lung tumors of the strain A mouse. Proc. Natl. Acad. Sci. U. S. A. 86, 3070–3074.

Yun, C.-H., Boggon, T.J., Li, Y., Woo, M.S., Greulich, H., Meyerson, M., Eck, M.J., 2007. Structures of lung cancer-derived EGFR mutants and inhibitor complexes: mechanism of activation and insights into differential inhibitor sensitivity. Cancer Cell 11, 217–227.

Yun, C.-H., Mengwasser, K.E., Toms, A. V, Woo, M.S., Greulich, H., Wong, K.-K., Meyerson, M., Eck, M.J., 2008. The T790M mutation in EGFR kinase causes drug resistance by increasing the affinity for ATP. Proc. Natl. Acad. Sci. U. S. A. 105, 2070–2075.

Zarbock, A., Allegretti, M., Ley, K., 2008. Therapeutic inhibition of CXCR2 by Reparixin attenuates acute lung injury in mice. Br. J. Pharmacol. 155, 357–364.

Zaynagetdinov, R., Sherrill, T.P., Polosukhin, V. V, Han, W., Ausborn, J.A., McLoed, A.G., McMahon, F.B., Gleaves, L.A., Degryse, A.L., Stathopoulos, G.T., Yull, F.E., Blackwell, T.S., 2011a. A critical role for macrophages in promotion of urethane-induced lung carcinogenesis. J. Immunol. 187, 5703–5711.

Zaynagetdinov, R., Stathopoulos, G.T., Sherrill, T.P., Cheng, D.-S., McLoed, A.G., Ausborn, J.A., Polosukhin, V. V, Connelly, L., Zhou, W., Fingleton, B., Peebles, R.S., Prince, L.S., Yull, F.E., Blackwell, T.S., 2011b. Epithelial nuclear factor-κB signaling promotes lung carcinogenesis via recruitment of regulatory T lymphocytes. Oncogene 31, 3164–3176.

Zhang, Y., Huang, S., Gong, D., Qin, Y., Shen, Q., 2010. Programmed death-1 upregulation is correlated with dysfunction of tumor-infiltrating CD8+ T lymphocytes in human non-small cell lung cancer. Cell. Mol. Immunol. 7, 389–395.

Zhang, Z., Ma, J., Li, N., Sun, N., Wang, C., 2006. Expression of nuclear factor-κB and its clinical significance in nonsmall-cell lung cancer. Ann. Thorac. Surg. 82, 243–248.

Zhao, B., Barrera, L.A., Ersing, I., Willox, B., Schmidt, S.C.S., Greenfeld, H., Zhou, H., Mollo, S.B., Shi, T.T., Takasaki, K., Jiang, S., Cahir-McFarland, E., Kellis, M., Bulyk, M.L., Kieff, E., Gewurz, B.E., 2014. The NF-κB genomic landscape in lymphoblastoid B cells. Cell Rep. 8, 1595–1606.

Zhu, Z., Ma, B., Homer, R.J., Zheng, T., Elias, J.A., 2001. Use of the tetracycline-controlled transcriptional silencer (tTS) to eliminate transgene leak in inducible overexpression transgenic mice. J. Biol. Chem. 276, 25222–25229.

Ziegelbauer, K., Gantner, F., Lukacs, N., Berlin, A., Fuchikami, K., Niki, T., Sakai, K., Inbe, H., Takeshita, K., Ishimori, M., Komura, H., Murata, T., Lowinger, T., Bacon, K., 2005. A selective novel low-molecular-weight inhibitor of IκB kinase-β (IKK-β) prevents pulmonary inflammation and shows broad anti-inflammatory activity. Br. J. Pharmacol. 145, 178–192.